DIVISION OF CANCER AND STEM CELLS

Project Title: Role of tumour microenvironment in the development of lymphovascular invasion in breast cancer

Name: Pavan Lakshmi Narasimha

Word Count: 21693

DECLARATIONS

The work presented in this dissertation by: Pavan Lakshmi Narasimha

is his/her own work except where stated in the text.

Technical assistance with the project has been acknowledged where appropriate.

Name of Supervisor: Professor Emad Rakha and Dr Chitra Joseph

Signature of Supervisor: 

This work was part of a Group Project ~~Yes~~/No

and my contribution was - Identifying potential Breast cancer markers.

I understand the nature of plagiarism and that it is a serious academic offence. I confirm that no material in this project has been plagiarized.

Name of Student: Pavan Lakshmi Narasimha

Signature of Student:

Title: Role of tumour microenvironment in the development of lymphovascular invasion in breast cancer

Author: Pavan Lakshmi Narasimha
Date: January 2020

Abstract:

Lymphovascular invasion (LVI) refers to tumour cells invasion through the lymphatic space, blood vessel. Although the LVI mechanism has not been clearly demonstrated, LVI may reflect a surrounding tumour microenvironment that predicts aggressive tumour underlying thus worse prognosis. Therefore, intreaction of LVI with Tumour micro-environment (TME) is stressed in this particular study. TME comprises cellular components and non-cellular components like blood vessels and extra cellular matrix (ECM) surrounding a tumour. There is little evidence regarding the relation between LVI and TME. Epithelial–mesenchymal transition (EMT) plays a key role in the progression and metastasis of Breast cancer (BC). This research aimed to explore the clinicopathological importance of Lipocalin 2 (LCN2), Solute carrier Family 22 member 17 (SLC22A17), Cluster of Differentiation-276 (CD276 or B7-H3) and Leukocyte associated immunoglobulin like receptor-1 (LAIR-1) in BC cohort. LCN2 plays a major role in the BC transition from EMT, angiogenesis, cell migration, and invasion. Notably, LCN2 functions by involving multiple signalling pathways as an initiator of carcinogenesis and metastasis. The exact mechanism between LCN2 and SLC22A17 is not completely understood. CD276 is an important member of the B7 family of immune checkpoints expressed on antigen presenting cells and plays an important role in inhibiting the activity of T cells. Importantly, on a broad range of human solid tumours, CD276 is over-expressed and often associated with both adverse prognosis and bad clinical results in patients. LAIR-1 is an inhibitory receptor that is expressed on many leukocytes and on most types of hematopoietic cells and negatively regulate immune response, but the role of LAIR-1 in tumor micro-environment and its possible mechanism of action in LVI is clearly not understood. Thus, in the current study we evaluated each marker using a well characterized breast cancer cohort to evaluate the impact on TME.

Method: Biomarkers of interest were assessed at transcriptomic and proteomic level using multiple BC cohorts; the Molecular Taxonomy of BC International Consortium cohort (METABRIC; n = 1980) (mRNA), The Cancer Genome Atlas BC cohort (TCGA; n = 949) (mRNA) and the publicly available BC transcriptomic data hosted by BC Gene-Expression Miner (bc-GenExMiner v4.0) (mRNA), Kaplan–Meier plotter (mRNA and protein) and the Nottingham BC cohort (protein) (n=2000) prepared as tissue microarrays. The association between clinicopathological variables and patient outcome were investigated.

Results: *LCN2, CD276 and LAIR1* mRNAs showed significant positive associations with poor prognostic characteristics; high histological grade ($p<0.001$), HER2 status ($p<0.001$), and integrative Clusters 5 and 10 ($p<0.001$) which was associated with poorer clinical outcome. High expression of SLC22A17, CD276 and LAIR-1 protein (cytoplasmic) expressions was associated with high tumour grade ($p<0.001$), poor Nottingham Prognostic Index (NPI; $p=0.012$), hormone receptor negativity ($p<0.01$), among IHC associated with triple negative and human epidermal growth factor 2 (HER2) + tumours ($p=0.019$). However, SLC22A17 mRNA level was not aligned with SLC22A17 protein levels and LCN2 protein expression showed favourable outcome with few prognostic features. Separate multivariate (all four markers were individually analysed) analysis demonstrated that LCN2 nuclear protein expression is an independent predictor of BCSS [$p<0.001$; HR 1.7 (95% CI 1.4-2.1)], CD276 [$p=0.017$; HR 1.0 (95% CI 1.0-1.5)], LAIR-1 protein expression [$p=0.037$; HR 0.6 (95% CI 0.3-0.9)] however, SLC22A17 protein expression was not an independent predictor for BCSS [$p=0.973$; HR 0.9 (95% CI 0.7-1.3)].

Conclusion:

In conclusion, we demonstrated that all four markers were associated with high grade, more advanced tumours and poor patinet outcome. Furthur functional studies needed to elucidate the molecular mechanisms,their association with LVI and TME.

Table of Contents

Figure Legends 8
Table legends 10
Abbreviations 11
CHAPTER 1 12
Introduction 12
1.1 Epidemiology of breast cancer 12
1.2 Breast cancer morphology 12
1.2.1 Breast Cancer Molecular Subtypes 12
1.2.2 Luminal A Breast Cancer 13
1.2.3 Luminal B Breast Cancer 13
1.2.4 HER2 Positive Breast Cancer 13
1.2.5 Triple Negative/Basal-like Breast Cancer 14
1.2.6 Normal-like Breast Cancer 14
1.2.7 Outcome of Breast Cancer 14
1.3 Prognostic Variables In Breast Cancer 15
1.3.1 Tumour Size 15
1.3.2 Tumour Grade 15
1.3.3 Oestrogen and Progesterone Receptor 15
1.3.4 Human epidermal growth factor receptor [HER2] 16
1.4 Lymphovascular Invasion [LVI] 16
1.4.1 Tumour microenvironment and Lymphovascular Invasion [LVI] 17
CHAPTER 2 18
Materials and Methods 18
2.1. Study Cohorts 18
2.2 Tissue Arrays and Immunohistochemistry 20
2.3 Western blotting 21
2.4 Scoring 22
2.5 Statistical Analysis 22
2.6 Cell lines and Culture Media 23
2.7 Preparation of Cell Lysate: Adherent Cells 23
2.8 Cell Passage 24
2.9 Cryopreservation 25
2.10 Gene knockdown by SiRNA transfection in Mammalian cells 25
2.11 Migration and invasion assays 26
2.12 Proliferation Assay 27

2.13 Ethics *27*

CHAPTER 3 *28*

Role of Lipocalin 2 (LCN2) and SLC22A17 in breast Cancer *28*

3.1 Introduction *28*

3.2 Lipocalin 2 (LCN2/NGAL) *29*

3.3 SLC22A17 [LCN2-R] *32*

3.4 Association Between LCN2 and SLC22A17 *33*

3.5 Hypothesis *34*

3.6 Results: *35*

3.7 Western Blot (WB) *35*

3.8 LCN2 Immunohistochemistry *37*

3.9 SLC22A17 and LCN2 mRNA expression and clinicopathological parameters in the METABRIC cohort *38*

3.10 Expression of LCN2 in immunohistochemistry *40*

3.11 LCN2 protein expression *41*

3.12 Association between LCN2 protein expression and key clinicopathological variables *41*

3.13 Association with Key biomarkers *41*

3.14 Association with patient outcome *41*

3.15 Differential protein expression of LCN2 *44*

3.16 Migration *46*

3.17 Invasion Assay *49*

3.18 Proliferation Assay *50*

CHAPTER 4 *51*

Analysis of SLC22A17 *51*

4.0 SLC22A17 genomic profiling *51*

4.1 SLC22A17 protein expression *55*

4.2 Association of SLC22A17 with patient outcome *58*

4.3 DISCUSSION *61*

CHAPTER 5 *65*

CD276 as a Prognostic Biomarker in invasive Breast cancer *65*

5.1 Introduction *66*

5.2 Materials and Methods *67*

5.2.1 Transcriptomic evaluation *67*

5.2.2 Immunohistochemistry [IHC] *67*

5.2.4 Statistical Analysis *67*

5.2.5 Scoring *67*

5.3 RESULTS *68*

5.3.1 Western Blot (WB) 68

5.3.2 CD276 genomic profiling 69

5.3.3 CD276 protein expression 71

5.3.4 Association of CD276 with patient outcome 73

5.4 Discussion 77

CHAPTER 6 80

Leukocyte associated immunoglobulin like receptor-1 confers poor prognosis in Invasive Breast Carcinoma 80

6.1 Background 80

6.2 Methods 81

6.3 Results 82

Antibody validation 82

6.3.1 Western Blot 82

6.4 LAIR-1 genomic profiling 82

6.5 LAIR-1 protein expression 85

6.6 Discussion 89

7.0 Strengths and Limitations 91

7.1 Acknowledgements 92

8.0 Bibliography 93

Figure Legends

Fig. 1 *siRNA induced gene silencing. After transfection, the guide strand of the double-stranded siRNA is loaded into the RISC complex, while the passenger strand is degraded. The loaded RISC targets a specific mRNA which will be cleaved by Argonaute 2 (Adel et al., 2015). 26*

Fig. 2 *Role of LCN2 in different types of cancer (Ajaikumar B et al., 2014) 31*

Fig. 3 *String pathway Analysis showing the association between LCN2 and SLC22A17 (p<0.001). 34*

Fig. 4 *Western blot of A) LCN2 and B) SLC22A17 in breast cancer cell lines using rabbit monoclonal antibody against human LCN2 (LSBio – LS-C405956) and SLC22A17 (237539, abcam, UK). Green and red bands represent protein (LCN2/SLC22A17) and Beta-Actin (house-keeping), respectively. 36*

Fig. 5 *Morphological characteristics of LCN2 immunohistochemistry in breast cancer tissue. A) Invasive B) LVI. LCN2 protein expression in breast cancer TMA cores. C). Nuclear D). Cytoplasmic and E). Negative (all at 40X magnification). 40*

Fig. 6 *Kaplan Meier curves showing the relationship between LCN2 expression and BCSS. A) Nuclear expression at 15-year BCSS B). Nuclear expression at 20-year BCSS. 44*

Fig. 7 *Transfection of SKBr3 cell line - First two wells were Transfected (knockdown) cell lysates, next two Un-transfected (control) and last two were negative control. 46*

Fig. 8 *Transfection of MDA-MB-157 cell line - First two wells were Transfected (knockdown) cell lysates, next two Un-transfected (control) and last two were negative control. 46*

Fig. 9 *Representative images of the migration assay in the SKBr3 and MDA-MB-157 cells, the area of migrated cells were significantly increased in the un-transfected (control) cells after 48 hours compared to the transfected group. 47*

Fig. 10 *Bar graph A) SKBR3 migration from pre-migration till 48 hours. B) MDA-MB-157 migration. Black bar represents un-transfected (control), grey bar represents transfected (knockdown). 48*

Fig. 11 *Invasion ability of MDA-MB-157 and SKBR3. Black bar represents 49*

Fig. 12 *Cell proliferation was significantly reduced after LCN2 KD in both A) SKBr3 (p=0.007) and B) MDA-MB-157 (p=0.001) cell lines as detected by MTS assay (n=3). 50*

Fig. 13 *Kaplan–Meier plots of SLC22A17 expression and breast cancer patient outcome. At transcriptomic level (A) Violin plot- Nottingham Prognostic index (NPI) (B) Tumour Grade (C) PAM50 subtypes (D) BC gene miner overall survival. 52*

Fig. 14 *Immunohistochemical expression of SLC22A17 in BC. (a) Negative control (b) TDLU (c)*

DCIS and (d) Invasive BC cells. SLC22A17 protein expression in breast cancer TMA cores (e) Negative expression while (f) showing high cytoplasmic expressions at 40X magnification respectively.....55

***Fig. 15** Kaplan–Meier plots of SLC22A17 expression and breast cancer patient outcome. At transcriptomic level (a) KM plotter- Whole cohort overall survival (OS), (b) KM plotter- Whole cohort distant metastasis free survival (DMFS). 59*

***Fig. 16** Western blot and immunohistochemical expression of CD276 in BC. Western blotting results for CD276 expression in MCF7, SKBr3, MDA-MB-231 and HeLa using rabbit monoclonal antibody against human CD276 [227670, abcam (UK)]. Green and red bands represent CD276 and Beta-Actin (house-keeping), respectively.....68*

***Fig. 17** IHC image of CD276: In Full Face A) Tumour B) Invasive C) TDLU. CD276 expression in membrane in TMA cores D) Low expression E) High Expression. 72*

***Fig. 18** Kaplan–Meier plots of CD276 expression and breast cancer patient outcome. At transcriptomic level (A) METABRIC cohort CD276 (B) KM plotter- Whole cohort overall survival (C) KM plotter- Whole cohort Recurrence free survival (D) KM plotter- Whole cohort distant metastasis free survival. 74*

***Fig. 19** Kaplan–Meier plots of CD276 expression and breast cancer patient outcome. At transcriptomic level (a) METABRIC cohort CD276 – Overall survival b) Breast Cancer Gene-Expression Miner v4.0 Box plots - ER cases (c) BC gene miner PR cases (d) BC gene-miner TNBC (e) BC-gene miner-Histological grade (f) PAM50 subtypes METABRIC. 75*

***Fig. 20** Western blot image of LAIR-1. Green band LAIR-1 at 70kDa and Red band beta-actin at 42 kDa.....82*

***Fig. 21** IHC expression of LAIR-1 in TMA cores a) Low b) High 85*

***Fig. 22** Kaplan Meier BCSS in LAIR-1 A) METABRIC cohort B) HER2+ cohorts only.....88*

Table legends

Table 1 *Treatment Recommendation for Breast cancer subtypes (*St. Gallen International Expert Consensus 2011)* 13

Table 2- *Summary of the clinicopathologic data for Nottingham tenovus primary series.* 19

Table 3 *Elements of the Western Blot performed.* 35

Table 4*: A summary of conditions used in immunohistochemistry. Selected conditions are highlighted in bold* 37

Table 5: *Associations ..... between SLC22A17 and LCN2 mRNA expression and clinicopathological variables in the METABRIC cohort.* 39

Table 6: *Association of LCN2 nuclear and cytoplasmic expression in BC series.* 42

Table 7: *Associations between LCN2 expression and key biomarkers in BC* 43

Table 8: *Multivariate analysis of LCN2 expression compared with tumour stage, grade, size for breast cancer-specific survival* 44

Table 9 *Associations between SLC22A17 mRNA expression and clinicopathological variables in the METABRIC cohort.* 53

Table 10 *Clinicopathological associations of SLC22A17 protein expression in the Nottingham BC series.* 57

Table 11: *Associations of SLC22A17 IHC expression and other BC related biomarkers* 60

Table 12 *– Multivariate analysis of SLC22A17 expression compared with tumour stage, grade, size for breast cancer-specific survival* 61

Table 13 *Associations between CD276 mRNA expression and clinicopathological variables in the METABRIC cohort* 70

Table 14: *Associations between CD276 protein expression and clinicopathological parameters* 72

Table 15: *Associations of CD276 IHC expression and other BC related biomarkers within the Nottingham BC series.* 76

Table 16 *Multivariate analysis of CD276 expression compared with tumour stage, grade, size, CD8, CD68, CD3 status for breast cancer-specific survival.* 77

Table 17 *Associations between LAIR-1 mRNA expression and clinicopathological variables in the METABRIC cohort* 83

Table 18: *Association of LAIR-1 protein with other BC related biomarkers* 86

Table 19: *Associations of LAIR-1 IHC expression and other BC related biomarkers within the Nottingham BC series.* 87

Table 20 *Multivariate analysis of LAIR-1 expression compared with tumour stage, grade, size, ER, HER2, NPI status for breast cancer-specific survival.* 88

Abbreviations

BC- Breast Cancer

BCSS – Breast Cancer Specific Survival

CD276 – Cluster of Differentiation 276

CK5 – Cytokeratin 5

CK14 – Cytokeratin 14

DAB – 3,3'-Diaminobenzidine

DCIS – Ductal Carcinoma In Situ

DFI – Disease-Free Interval

DPX - Distyrene Plasticiser Xylene

EMT – Epithelial to mesenchymal transition

ER – Oestrogen Receptor

FFPE – Formalin-Fixed Paraffin-Embedded

GPG – Good Prognosis Group

H-score – Histochemical Score

HER2 – Human Epidermal Growth Factor Receptor 2

IHC - Immunohistochemical

IMS – Industrial Methylated Spirit

LAIR-1 - Leukocyte associated immunoglobulin like receptor-1

LCN2 – Lipocalin 2

LVI – Lymphovascular Invasion

METABRIC - Molecular Taxonomy of Breast Cancer International Consortium

MPG – Moderate Prognostic Group

NPI – Nottingham Prognostic Index

OD – Optical Density

PPG – Poor Prognostic Group

PR – Progesterone Receptor

SLC22A17 – Solute carrier 22A17

TAM – Tumour associated Macrophages

TMA – Tissue Micro-Array

TNBC – Triple Negative Breast Cancer

CHAPTER 1
Introduction

1.1 Epidemiology of breast cancer

Breast cancer (BC) is one of the most prevalent forms of cancer in general and the most frequent form of cancer in women (Office of National Statistics, 2017). BC is the world's second-largest cause of cancer-related deaths following lung cancer. In terms of mortality, BC was the world's fourth most common cause of death leading to 7% of cancer deaths in both sexes of 2017. (1). Despite advancements in early diagnosis and intervention, results modelling remains imprecise; thus, continued work is crucial to identifying future prognostic targets for improving BC care. It is a reality that many genes in cancer are apparently controlled up or down during the process of disease progression (2), the discovery and control of deregulated genes could therefore be valuable both to increase our knowledge of the condition and to strengthen the care protocol for cancer therapy.

1.2 Breast cancer morphology

Histological types

Breast cancer is categorised morphologically into several subtypes, based on distinctions and histological characteristics. Breast cancer includes more than 20 histological forms including ductal, no special type (NST), lobular, mucinous and tubular, and each subtype may have multiple morphological variations, according to the new WHO book classification (3) of breast tumours. Breast cancer is classified into 3 grades according to differentiation (Nottingham grading system) (4).

1.2.1 Breast Cancer Molecular Subtypes

Breast cancer tumours are heterogeneous, suggesting that different types exist and their classification system is continually being revised to adapt to new treatment strategies and to assess the prognostic characteristics of tumours. Present concepts of classification include: Luminal A, Luminal B, HER2 positive, basal / triple negative and natural classification (5, 6). Early classification was based on hormone receptor status such as; receptor of oestrogen (ER), receptor of progesterone (PR), and receptor of the human epidermal growth factor 2 (HER2). **Table 1** depicts possible treatment for specific BC subtypes.

Table 1 Treatment Recommendation for Breast cancer subtypes (**St. Gallen International Expert Consensus 2011)*

Systemic Treatment Recommendations for Breast cancer Subtypes			
Subtype		Clinico-pathologic definition	Treatment
LUMINAL A		• ER and/or PgR positive • HER2 negative • Ki-67 low (<14%)	• Endocrine therapy
LUMINAL B	HER2-	• ER and/or PgR positive • HER2 negative • Ki-67 high (>14%)	• Endocrine ± cytotoxic therapy
	HER2+	• ER and/or PgR positive • HER2 over-expressed or amplified • Any Ki-67	• Endocrine + cytotoxic therapy + anti-HER2
HER2+		• HER2 over-expressed or amplified • ER and PgR absent	• Cytotoxic + anti-HER2
TRIPLE-NEGATIVE		• ER and PgR absent • HER2 negative	• Cytotoxic

1.2.2 Luminal A Breast Cancer

Luminal A breast cancer is characterized by ER and/or PR expression, but does not display HER2 (6) and is trailed by weak Ki-67 expression (7), a proliferation marker (8). Luminal A tumour patients have a good long-term overall survival (9) and have more time to develop remote metastases (5), indicating a strong survival for this subtype.

1.2.3 Luminal B Breast Cancer

Luminal B breast cancer is also characterised by ER and/or PR expression but unlike luminal A, Luminal B has strong Ki-67 expression and is seen in few cases (7). As a high expression of Ki-67 correlated with a poor prognosis, this means that luminal B tumours have a worse survival than luminal A tumours (10).

1.2.4 HER2 Positive Breast Cancer

HER2-positive tumour are known as BC HER2-positive (5, 6). These tumours usually do not express either ER or PR (11). Patients with high HER2 amplification tumours tend to have decreased survival compared with those with low HER2 amplification and poor prognosis (12). Such HER2 receptors may be attacked by various treatments, including trastuzumab

(Herceptin), a humanised monoclonal antibody, but not all stable HER2 tumours do respond to them (13).

1.2.5 Triple Negative/Basal-like Breast Cancer

Triple Negative Breast Cancers (TNBC) receptors for ER, PR and HER2 (6, 7). As described above, such biomarkers offer therapeutic incentives to use a multitude of selective therapies against them to stop the progression of tumours. Nevertheless, because TNBC tumours don't activate these receptors, they're more difficult to target.

Basal-like breast cancers, a TNBC subgroup, exhibit a similar phenotype for TNBCs but also communicate a series of basal signals and present characteristics that distinguish them from TNBCs (14). TNBC patients tend to have lower mortality relative to those with hormone receptor positive while HER2-negative tumours. A retrospective study of breast cancer prognosis found that TNBC patients have the lowest overall survival prognosis for stable breast cancers relative to luminal A, luminal B and HER2 (9).

1.2.6 Normal-like Breast Cancer

Such tumours are distinguished by gene expression in adipose tissue and other forms of cells, including non-epithelial cells (5). This phenomenon is followed by decreased gene expression in luminal epithelial cells (6), this form of tumour is near the luminal A subtype due to the presence of ERs and PRs, accompanied by a lack of HER2 and Ki-67 expression(7) and large molecular weight cytokeratin 5 (CK5) (15).

1.2.7 Outcome of Breast Cancer

Breast cancer can be viewed as a class of diseases with a wide spectrum of individuals with substantially unpredictable actions and effect in terms of result and behavior. The result of breast cancer has generally improved after the implementation of screening system and the growing use of specific therapies. Recent figures show that women with invasive breast cancer have a 5-year survival rate of 90%. The overall survival rate is 83% over 10 years. If the disease is in the breast alone, women with breast cancer have a survival rate of 99% over 5 years. 62% (62%) of women with breast cancer are diagnosed with this stage.)(16).

1.3 Prognostic Variables In Breast Cancer

1.3.1 Tumour Size

Tumor size is one of the leading predictors of breast cancer tumour development. The incidence of nodal metastases in tumour cases below 1.0 cm is 10%-20%, and node-negative patients with tumours below 1.0 cm have a 10-year disease-free survival rate of around 90% (17).

1.3.2 Tumour Grade

The histological grade is based on a combination of mitotic results, nuclear grade and architectural morphological appearance. Several studies have shown that the tumour grade (especially high) is essential in predicting recurrence (17). Histological type is closely related to lymphovascular invasion, so tumours with lymphatic permeation have a worse prognosis even in the absence of nodal metastases. Invasive BC such as medullary types, for example, are of high grade with poor patient survival (18). Nonetheless, low-grade aggressive subtypes of breast cancer such as tubular, papillary, cribriform grade 1 (low grade) have a much-improved prognosis (Cancer research UK).

1.3.3 Oestrogen and Progesterone Receptor

Approximately 82% of tumours produce Oestrogen receptor binding protein (ER), which can be detected through radioligand assay and in practice by immunohistochemical examination, leading to the use of Oestrogen receptor as a method of selection in endocrine therapy. While survival in ER positive cancers is longer, this is primarily because women survive longer after first recurrence after a better response to hormone therapy. Oestrogen and the progesterone receptor (PR) also are effective in assessing reactions to endocrine therapy. Positive ER / PR tumours have a response rate of 60–70% compared with less than 10% for negative ER / PR tumours, whereas negative ER / PR tumours have an intermediate response rate (40%) (19).

1.3.4 Human epidermal growth factor receptor [HER2]

HER2-positive breast cancer cells produce too many versions of the HER2 gene, and are more aggressive and more likely to spread than HER2-negative breast cancer. They too are more likely to recur after treatment. This indicates that HER2-positive breast cancer has a less good prognosis than HER2-negative breast cancer (20).

1.4 Lymphovascular Invasion [LVI]

LVI is considered as an indicator of metastatic potential when morphologically identified in the peritumoural area, and is strongly associated with poor prognosis in many solid tumours, including breast cancer (BC). It is also identified by tumour emboli present in the breast surrounding invasive carcinoma within a given endothelial-lined area. The presence of LVI can help to identify who is at increased risk for axillary lymph node and distant metastasis, while LVI in patients with lymph node-negative invasive breast cancer has been acknowledged as a significant prognostic factor (21). LVI presence is associated with an increased risk of axillary lymph node and distant metastases (22). Although the LVI process has not been entirely elucidated, LVI is deemed a prognostic factor in patients with or without adjuvant therapy receiving metastatic axillary lymph nodes. *Liu et al* reported that LVI positive patients had the worse conditions for Recurrence Free Survival (RFS) and Overall Survival (OS) when classified along with HER2 overexpression. In comparison, the reviewers stated that in patients with LVI and triple negative subtype had the lowest RFS and OS. The population-based study showed that LVI is correlated with shorter RFS and OS in high-risk patients (positive lymph nodes, tumour size > 2 cm, strong histological score, negative hormone receptor status, or age less than 35 years) with operable breast cancer. (23).

1.4.1 Tumour microenvironment and Lymphovascular Invasion [LVI]

Breast cancer cells detach themselves from the tumour cell mass before they have access to vascular lumina, accompanied by infiltration and migration to the vascular walls through the extracellular matrix (ECM) (24). Consequently, certain steps are considered prerequisites for the LVI process. In the surrounding frontline, malignant cells infiltrate ECM as single cells or as clusters of malignant cells. BC cells at the tumour borders upregulate genes such as the Transforming Growth Factor (TGF-beta), the Epithelial Growth Factor Receptor (EGFR), and other transcriptional factors that promote the possible transition of malignant epithelial cells into a mesenchymal process by blocking E-cadherin and other cell adhesive molecules that result in increased motility (25). Tumor micro-environment regulates biological interactions between malignant cells and components of stroma (26). The association between malignant cells and tumour microenvironmental stromal components through genetic and epigenetic regulations has been documented to modify adherence and facilitate invasion and migration of malignant cells through the adjacent ECM with corresponding enhanced penetration into the vascular channels. (27).From the aforementioned studies we hypothesized that tumour microenvironment plays a role in the development of vascular invasion in breast cancer.

CHAPTER 2

Materials and Methods

2.1. Study Cohorts

The Molecular Taxonomy of BC International Consortium (METABRIC) (28) was used to evaluate mRNA expression. Data on gene expression is pre-processed and normalised as previously described (28). The association between *LCN2, SLC22A17, CD276 and LAIR-1* mRNA, clinicopathological parameters, and patient outcome were investigated. The Nottingham BC primary cohort were arrayed as previously described (29) using a TMA Grand-Master (3D Histech).

On the prospective basis, clinico-pathological evidence and clinical outcomes, including BC Specific Survival (BCSS) and the Disease-Free Interval (DFI) were preserved. The median cut-off was used to categorise the rates of mRNA and protein expression into subgroups high and low. Breast cancer-specific survival (BCSS) is characterised as the percentage of individuals in a research or patient community who have not died in a defined period of time from breast cancer. Disease-Free Interval (DFI) has been described as the time in months from diagnosis before local or regional recurrence occurs. Distant metastasis free survival (DMFS) was defined as the time in months from diagnosis until distant metastasis was developed in BC.

The mRNA expression was analyzed using the BC-GenExMiner v4.1 method to verify the findings of the METABRIC study (30). It consists of a prognosis part, and an inference system. The prognostic module measures the prognostic influence of the calculated chromosome, and the correlation module generates equations for data correlation. Digital software The Kaplan – Meier Plotter-(Breast Cancer; KM-Plotter; n=1967) (31), and Breast Cancer Gene Expression Miner v4.0 (30) were used as a supportive validation cohorts to evaluate them.

The Nottingham Tenovus Primary Series consists of 2000 primary invasive BC cases. **Table 2** shows a summary of patient cohorts, clinicopathological characteristics and biomarker status (32).

Table 2- Summary of the clinicopathologic data for Nottingham tenovus primary series.

Parameter	***Frequency (%)***	***Parameter***	***Frequency (%)***
Age at diagnosis		**TPN**	
<50 years	469 (23.7)	Positive	1661 (85.8)
≥50 years	1511 (76.3)	Negative	276 (14.2)
Menopausal status		**ER status**	
Pre	436 (22.1)	Positive	1498 (77.3)
Post	1533 (77.9)	Negative	439 (22.7)
Tumour size		**PR status**	
<2.0	19 (1.0)	Positive	1040 (47.5)
≥2.0	1941 (99.0)	Negative	940 (52.5)
Grade		**HER 2 status**	
1	170 (9)	Positive	247 (12.5)
2	770 (40.7)	Negative	1733 (87.5)
3	952 (50.3)	**P53**	
NPI		Wild Type	721 (36.4)
GPG	680 (34.3)	Mutant	99 (5)
MPG	1101 (55.6)	NA	1160 (58.6)
PPG	199 (10.1)	**LVI**	
Tumour type		Positive	635 (40.6)
Invasive ductal	1544 (84.1)	Negative	930 (59.4)
Invasive lobular	147 (8.0)		
Medullary	32 (1.7)		
Special type	113 (6.2)		

2.2 Tissue Arrays and Immunohistochemistry

Tumour samples of formalin-fixed paraffin embedded (FFPE) (Nottingham series) have been arrayed as previously described on tissue microarrays (TMAs) (29). TMAs were cut, 4 µm wide, on heavily loaded Leica Surgipath X-tra slides. Immunohistochemical staining was conducted using the detection system Novolink Max Polymer.

Sections of the full face and TMA were put on a hotplate at 60º C for 10 minutes to remove wax from the tissues. Upon cooling the slides were put for dewaxing (xylene) and rehydration in the Leica Auto Stainer [Industrial Methylated Spirit (IMS)]. For antigen recovery, heat-induced citrate antigen recovery (10mM citrate buffer with pH 6.0; microwave at 100W for 20 minutes) was used for all the markers. Flatbed approach was utilized after antigen retrieval. A hydrophobic membrane was built around the tissue nuclei, and a cap of Novolink peroxidase was applied to inhibit endogenous peroxidase action for 5 minutes. The slides were then washed (3X5), and the protein block Novolink was added for 5 minutes to block small fragments of non-specific proteins that might otherwise cause background staining. The slides were incubated with optimally diluted antibody following spray, and the antibodies were dissolved in a main antibody diluent Leica antibody diluent.

The Novolink post primary reagent was added for 5 minutes after primary antibody incubation to increase the penetration of the secondary agents. Novolink polymer, which is a secondary antibody tagged with Horse Radish Peroxidase, was added for 5 minutes. A chromogen, 3,3'-Diaminobenzidine (1:20 DAB Chromogen combined in DAB Substrate Buffer), has been applied for 5 minutes, and has been tackled by hematoxylin, a simple stain that stains acidic structures in violet. It allows the viewer to differentiate tumour cells from other types of cells in the central tissue. The slides in the Leica Autostainer were then dehydrated, and the slides were then covered with Distyrene Plasticiser Xylene (DPX) and left for 48 hours to dry. A supportive regulation was used: a tissue microarray comparing the portion of optimization stained with the same antibody concentration, thereby maintaining the method's accuracy between optimization and cohort staining. A negative test, where mere diluent was applied in place of the primary antibody, was also used to show that the staining of the cores was directly linked to the introduction of the antibody.

2.3 Western blotting

Western blotting is used to differentiate between a protein and a dynamic combination of different proteins. It was first incorporated into nitrocellulose sheets by Towbin, et al. in 1979 as a simple method of electrophoretic blotting of proteins. Western blotting procedures have since become a popular laboratory procedure for the immobilisation of proteins on a membrane. Although several changes were made to the initial protocol as well, the general premise persists. The macromolecules are separated and transferred to a membrane utilizing gel electrophoresis, which was nitrocellulose. Cell lysate (13µl) + Bolt NuPAGE LDS sample Buffer (4x) (5µl) + Bolt NuPAGE Reducing Agent (10x) (2µl) and de-ionized water were therefore prepared as follows. Samples to denature the proteins were put in a heat block at 100 ° C for 5 minutes. A MOPS running buffer was designed by de-ionized water diluting 50ml 20X MOPS SDS running buffer through 950ml. The wells of the electrophoresis gel were loaded with 20µl of the sample and 6µl PageRuler pre-stained protein marker (ladder) (Thermofisher Scientific 22616), as a reference. The running buffer was poured into the tank, at 160V for 60 minutes.

Mixing a 50ml 20X transfer buffer with 100ml methanol, 849ml de-ionized water and 1ml antioxidant formed a transfer buffer. A blot sandwich with the layers put in the following order was prepared on the cathode core: sponge, filter paper, gel, blotting membrane, filter paper, and then a sponge. The anode core was placed on top, after using a blotting roller to eliminate bubbles, and the package was extended for 1 hour in the 10V electrophoresis tank. This ensured that the proteins and respective markers are transferred from the gel to a nitrocellulose membrane. The blotting sandwich was removed after the transition was finished, and the membrane was stained with Ponceau stain to represent the transfer from gel to nitrocellulose membrane. A blocking solution was formulated at room temperature for an hour with 5% Marvel Milk and 0.1 per cent PBS-Tween 20 in required amount of washing buffer.

The mouse beta-actin (1:5000) (A5441, Sigma-Aldrich; Clone AC-15; Sigma, UK), a loading control, were diluted in blocking solution. A wash buffer was prepared by mixing Phosphate buffer saline (PBS) with 0.1% Tween-20. Anti-rabbit and anti-mouse secondary antibodies, bound with a fluorescent marker, were prepared at a dilution of 1:15000 in blocking solution 1 hour at room temperature. After 3 washes, the images were developed on a Li-cor Odyssey Fc with image studio 4.0 (LI-COR Biosciences), with wavelengths of 600 (ladder), 700 (antibody- rabbit host) and 800 (antibody – mouse host) nm used.

2.4 Scoring

The immune stained slides were scanned (NanoZoomer Hamamatsu Photonics, Welwyn Garden City, UK), and viewed at 20X magnification using slide-viewing software (NanoZoomer Digital Pathology viewing software, U12388-01, Hamamatsu). The cytoplasmic and nuclear positivity of the tumour cells were assessed using a modified histochemical score (H-score). The H-score includes both the intensity of the staining of the tumour cells, and the percentage of cells stained (33). The intensity is defined as negative (0), weak positive staining (1), moderate positive staining (2) and strong positive staining (3). The proportion of the core stained with the different intensities is substituted into the following formula in order to calculate the H score: 0(percentage of cells stained negative) +1(percentage of cells stained weakly positive) +2(percentage of cells stained moderately positive) +3(percentage of cells stained strongly positive).

TMA cores with less than 15% tumour cells, or showed Ductal Carcinoma in Situ (DCIS) were excluded. All slides were scored by the same observer, Narasimha PL and compared against a second, more experienced observer, Joseph C or Alsaleem M, where a consensus was reached.

2.5 Statistical Analysis

Statistical analysis was performed using SPSS 24.0 software. To assess the normality of the data, a histogram was produced. Cut-off scores were produced using the H-score (The H-score is a method of assessing the extent of nuclear immunoreactivity, applicable to steroid receptors like Oestrogen, Progesterone), and were used to classify the data by using either the median or the mean, with the spread of the data as portrayed in the normality test (for details, see results section). Associations between the expression of biomarker and the clinical data for the Nottingham Tenovus Primary Series (32) were assessed, by performing Pearson chi square analysis. Univariate survival analysis was performed using Kaplan-Meier curves, using a log rank test to determine statistical significance, and multivariate analysis was performed using the Cox regression method. Data was determined to be statistically significant if $p \leq 0.05$.

2.6 Cell lines and Culture Media

Based on our mRNA and proteomic evaluation differential expression of proteins in BC cell lysates were evaluated; ER-positive Luminal A (MCF-7), HER2+ (SKBr3) and Triple Negative (MDA-MB-157) cell lines were used for the quantitative assessment. All BC cell lines were bought from the American Type Culture Collection (ATCC, Manassas, VA USA) and cultured as recommended by ATCC. MCF-7 was grown in RPMI-1640 (Sigma), SKBr3 (Mcocy; M9309; Sigma) and MDA-MB-157 in RPMI-1640 (Sigma), all with a 10% fetal calf serum (FBS) supplement. Within a few passages (all; between passage 9-14) of the original stocks, cell lines obtained from ATCC were used, while other cell lines were authenticated by STR profiling and tested for mycoplasma contamination (CUL001B; R&D Systems) prior to experiments.

Transient knockdown was done using siRNA, Thermo-Fisher Scientific (Silencer ® Select siRNA, Ambion ®). Using Lipofectamine™ RNAiMAX Transfection Reagent (catalogue number: 13778155, Thermo-Fisher Scientific, UK) as per the manufacturer's protocol, transfection was achieved. Cell lysates were collected in the RIPA buffer (catalogue number:89900 Thermo-Fisher Scientific, UK), and transfection efficiency was confirmed through western blotting.

2.7 Preparation of Cell Lysate: Adherent Cells

Materials

Mammalian cells grown in adherent or suspension culture, ice cold RIPA Lysis Buffer. Ice cold PBS and ice.

Procedure

Cultured adherent cells to approximately 80% confluence on 100mm polystyrene tissue culture plates. Cells were in log phase and was healthy. We aspirated the media and kept plates on ice for all steps. We washed cells monolayer gently one time with 10 ml ice cold PBS. 500 µl of RIPA Lysis Buffer [50mL of PBS, Dissolve 1% Triton X-100, 0.5% SDS, 1mM EDTA, 1mM phenylmethylsulfonyl fluoride (PMSF), 1mM Sodium fluoride (NaF), 1 Tablet of Protease Inhibitor Cocktail (Complete, EDTA-free, Roche) was added. The final solution was prepared in 1mL aliquots and stored at -20°C, the cells were scraped and lysate was incubated on ice for 15 minutes. The lysate was centrifuged at 13,000 x g for 5 minutes at 4°C. Supernatant was collected (avoiding the pellet) and stored at -20ºC avoiding multiple freeze/thaw cycles.

2.8 Cell Passage

Materials

Culture vessels containing adherent cells, tissue-culture treated flasks, plates or dishes Complete growth medium, pre-warmed to 37°C. Disposable, sterile 15-mL tubes 37°C incubator with humidified atmosphere of 5% CO_2. Balanced salt solution such as Dulbecco's Phosphate Buffered Saline (DPBS), containing no calcium, magnesium, or phenol red and dissociation reagent such as trypsin.

Procedure

Old cell culture media was discarded from the culture vessel. Cells were washed using Dulbecco's Phosphate Buffered Saline (DPBS) (approximately 2 mL per 10 cm_2 culture surface area). Wash solution was added to the sides of the vessel opposite to the attached cell layer to avoid disturbing the cell layer, and the vessel was rocked back and forth several times. Wash solution was removed from the culture vessel. Pre-warmed dissociation reagent such as trypsin (Thermo-fisher scientific 15050065 - 0.25% phenol red 100 ml) were added to the side of the flask; trypsin was used to cover the cell layer (approximately 0.5 mL per 10 cm_2). Culture vessel was incubated at room temperature for approximately 2 minutes. Note that the actual incubation time varies with the cell line used. Cells were observed under the microscope for detachment. Culture vessel was gently tapped to expedite cell detachment. When ≥ 90% of the cells have detached, vessel was tilted for a few seconds to allow cells to drain. Equivalent to 2 volumes (twice the volume used for the dissociation reagent) of pre-warmed complete growth medium was added. Cells were transferred to a 15-mL conical tube and centrifuged at 200 × g for 5 minutes. Note that the centrifuge speed and time vary based on the cell type. Pellet was resuspended in a minimal volume of pre-warmed complete growth medium and a sample was taken for counting. The total number of cells and percentage viability was determined using a hemocytometer, cell counter and Trypan Blue exclusion method. Cell suspension was diluted according to the seeding density required for the cell line, and appropriate volume was pipetted into new cell culture vessels along with required growth media, and cells were kept back in incubator.

2.9 Cryopreservation

Procedure

Cryovials were labelled with the date, name of researcher, cell number, passage number and cell type. For adherent cells, removed the cell culture media, washed in PBS, added enough trypsin to cover the cells and incubated for 5 min in a 37°C CO2 incubator. Resuspended in cell culture media and transferred into a 50 mL Falcon tube. Cells were counted using a hemocytometer and their viability was determined. Cell viability was well above 75% for cryopreservation. Centrifuged for 5 min at 1,000 rpm at room temperature. freezing media was prepared (Cells cultured in FBS-containing media, 90% media + 10% DMSO). Supernatant was discarded and loosened the pellet gently. Freezing media was added to the required cell density. For mammalian cells this is usually 1,000,000/mL of freezing media. Cells should not be at room temperature in freezing media for more than 10 min. 1 mL was aliquoted into cryovials and transferred the cryovials into a -80°C freezer. The isopropanol ensured that the temperature decreases steadily by 1°C/minute. After approximately 24 h, cryovials were removed from the isopropanol container and transferred into liquid nitrogen for long term storage.

2.10 Gene knockdown by SiRNA transfection in Mammalian cells

The discovery of RNA interference mechanisms opened the way for gene expression in mammalian cells to be easily and effectively knocked down (34). Small interfering RNAs or siRNA are small double-stranded RNAs of approximately 21–23 nucleotides long capable of targeting and splitting complementary mRNAs (**Fig. 1**). SiRNAs can be synthesised and then transfected directly into the cell, or generated from a precursor of short hairpin RNA (shRNA). The mature siRNA (guide strand) is loaded into the RNA Induced Silencing Complex (RISC) once it is in cytoplasm.

The RISC structure is a molecule of multi-proteins. One of its components, the Argonaute 2 protein (Ago 2), has an RNase H-like domain involved in mRNA cleavage that occurs from the 5' end of the complementary siRNA at a position of 10 or 11 nucleotides (35). SiRNA knockdown is transitory and not necessarily 100% efficient, but is usually adequately enough to detect the results of targeted gene knockdown when transfected cells endure the procedure, even if an integral gene is blocked. In current study we transfected SKBR3 (HER2+) and MDA-MB-157 (Triple Negative) cell lines.

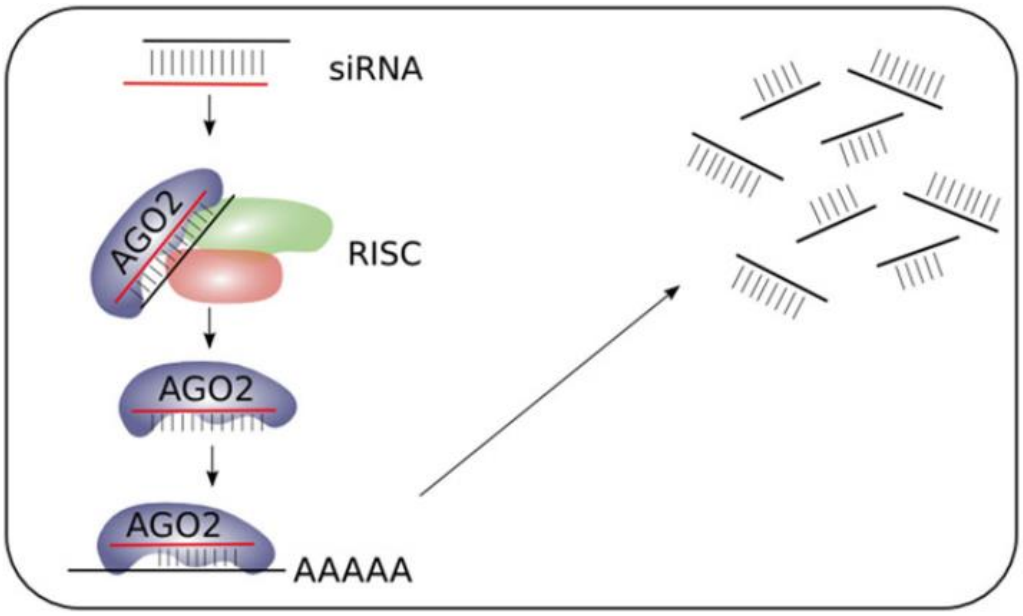


Fig. 1 siRNA induced gene silencing. After transfection, the guide strand of the double-stranded siRNA is loaded into the RISC complex, while the passenger strand is degraded. The loaded RISC targets a specific mRNA which will be cleaved by Argonaute 2 (Adel et al., 2015).

Positive, negative controls and un-transfected (control) cells, were included in all experiments. The positive control is beta-Actin and the negative control is a non-specific scrambled siRNA. It is recommended to carry out transfections in triplicate.

2.11 Migration and invasion assays

Cell migration was calculated using the Cell Biolabs (CBA-125; San Diego, CA) 24-well Radius™. Cells were seeded on Radius cell migration plates in this experiment, and were allowed to form monolayers before removing the gels. Following the manufacturer's instructions, the central gel layer was extracted after 24 h and the migration was examined using a Zeiss LSM-510 inverted microscope (Zeiss, Germany), photographing the plates at 24 and 48 h.

To test cell invasion, we used the CytoSelect 24-Well Cell Invasion Assay (Basement Membrane, Colorimetric) from Cell Biolabs (cat. no. CBA-110 San Diego, CA). Until detaching and seeding into matrix-coated trans tubes, cells were incubated overnight in serum-free water. The bottom chamber held media-added cells and 10% FBS.

After 24-hour incubation, the residual cells in the top chamber were extracted with moistened cotton swabs and handled from the package for 10 minutes with cell stain solution accompanied by the application of the extraction solution per manufacturer's instructions and calculated OD at 560 nm.

2.12 Proliferation Assay

The effect of knockdown on proliferation was assessed by the (Promega, (G3580); CellTitre 96 Aqueous One Solution Cell Proliferation Assay) 3–(4,5–dimethylthiazol-2–yl) -2,5–diphenyltetrazolium (MTS) assay. In brief, the control and knockdown cells were seeded at 3000 cells/well in 96-well plate at 37 °C in a 5% CO2 incubator. Proliferation was measured at 24, 48 and 72 hrs by adding MTS reagent to the wells as per the manufacturer's protocol. The plates were incubated in for 1 h and the absorbance of each well was measured using a Synergy™ 4 (BioTek Instruments, Winooski, VT, USA) at 490 nm.

2.13 Ethics

This study was approved by the Nottingham Research Ethics Committee 2 under the title 'Development of a molecular genetic classification of BC. All samples from Nottingham used in this study were pseudo-anonymized and collected prior to 2006 and therefore under the Human Tissue Act informed patient consent was not needed. Release of data was also pseudo-anonymized as per Human Tissue Act regulations.

CHAPTER 3

Role of Lipocalin 2 (LCN2) and SLC22A17 in breast Cancer

3.1 Introduction

Glycoproteins have a unique position in the pathogenesis of human diseases. Most of the commonly employed protein biomarkers are glycoproteins. Examples include CA19-9 (carbohydrate antigen 19-9) to follow-up patients with pancreatic cancer, CEA (carcinoembryonic antigen) for multiple solid tumours and CA125 (carbohydrate antigen 125) used in the diagnosis, follow-up and therapy of patients with ovarian cancer (36). Most of these glycoproteins are large molecules. However, there is a family of smaller, secreted glycoproteins (called lipocalins) that are important in the maintenance of health and in combating diseases effectively (37). A prototype of this family is a small, secreted glycoprotein called Neutrophil gelatinase associated lipocalin or LCN2. In recent years, LCN2 has emerged as a novel biomarker in several benign and malignant diseases. Further, *in-vitro* and *in-vivo* models have revealed a pivotal role for this molecule in several physiological processes and pathological conditions (38). Lipocalins are a family of small (160-180 long amino acids) secreted proteins that mediate a specific functional role, i.e. small hydrophobic ligands are transported. Most family of proteins are categorised in amino acid sequences, domain architecture, and three-dimensional protein structure based on similarity. Nevertheless, lipocalins are a peculiar exception in that the percentage of sequence identity among various members of the lipocalin family is sometimes even lower than the minimum identity (20%), reporting as stable alignment (39-43). The lipocalins are typically well-known as transport proteins that reside in the extracellular space and are involved in the transport of RBP (Retinol binding protein) that binds and delivers retinol (Vitamin A) from the liver to different organs (*Ma H* et al., 2019). Certain lipocalin-assigned roles include cell ageing control, survival and differentiation (probasin and purpurine), immune response modulation [Lipocalin 2 (LCN2), Alpha acid glycoprotein (AGP), Placental protein 14 (PP14) and apoptosis inhibitor of macrophages (AIM)] and prostaglandin synthesis (glutathione-independent PGD2 synthase) (44).

3.2 Lipocalin 2 (LCN2/NGAL)

Human LCN2 structurally contains a 20-amino acid signal peptide at the protein's N-terminal end followed by the "lipocalin" domain. Under physiological conditions, an important function of LCN2 is to serve as a bacteriostatic agent to protect the body from both Gram-negative bacteria and mycobacterial infections by binding strongly to bacterial iron binding proteins called siderophores, to mediates this role (43). Iron, a particularly ferrous material, is necessary for growth of bacteria. The extremely low free iron levels in the body, however, render it an important element that bacterial cells needed. Bacteria have evolved a mechanism for the expression of proteins (termed siderophores) that attach to free iron (present in the intestinal fluid and inside macrophages), particularly in its ferric shape, to bypass this necessity for iron. LCN2 has a strong affinity to bind to the iron-loaded siderophores. After binding to these proteins, cells expressing the cognate receptor for LCN2 take up the LCN2 siderophore complex and are therefore sequestered away from these iron laden proteins. In this manner, LCN2 prevents its replication by depriving bacteria of an essential nutrient (45, 46).

Other functions attributed to LCN2 include acting as a chemoattractant for neutrophils and as an inhibitor of cellular oxidative stress. LCN2 knock-out mice showed a significant decrease in the number of neutrophils infiltrating transplanted heart tissue compared to wild type mice (47-51). Though LCN2 first identified as a part of neutrophil late granules (52), is also strongly expressed in a variety of normal adult human tissues including non-neoplastic breast ducts, kidney, liver, lungs, trachea, small intestine, bone marrow, thymus, prostate, adipose tissue, and macrophages (53-55) . LCN2 is present in brain, heart, skeletal muscle, spleen, testes (56-60). The expression of LCN2 is altered under several adverse conditions, including inflammatory and metabolic disorders. Pancreatitis, meningitis, and myocarditis, are inflammatory diseases associated with increased expression of LCN2 (44). Metabolic disorders associated with LCN2 expression dysregulation include obesity, preeclampsia, and disease of the kidneys (61).

LCN2 expression in several solid and hematological tumours has been significantly increased and is correlated with both tumour characteristics and the tumour progression. Elevated levels of LCN2 expression have been reported in various cancers including ovarian cancer, pancreatic cancer, lung cancer, colon cancer and BC(62)., indicating there is a strong association between LCN2 expression and metastasis (63) (**Fig. 2**).

LCN2 tends to facilitate BC development, being higher in rapidly proliferating cells, in lymph node metastasis and human epidermal growth factor receptor 2(HER2+/ERBB2) positive tumours. In vitro studies rats suggest that HER-2 may be controlled by expression of LCN2 in breast cancer (64). Studies conducted on the LCN2 murine homolog (24p3/LCN2) showed that the malignant cells in leukemias, express BCR-ABL, (65, 66) a fusion protein. The leukemia cells release large quantities of 24p3/LCN2 into the bloodstream which acts via its receptor to induce cell death in the normal hematopoietic cells (44, 62, 66). Two potential pathways to clarify the anti-invasive impact of LCN2 have been proposed. One pathway includes inhibiting the FAK (focal adhesion kinase) of non-receptor tyrosine kinase. FAK interacts with Src (another non-receptor tyrosine kinase) and provides a scaffold for the activation of Ras-MAPK, a crucial metastasis mediator in cancer cells. Through inhibiting FAK, LCN2 would inhibit the Ras-MAPK pathway, thus preventing cancer cell invasion and metastasis. A second mechanism, based on previous research, indicates that ectopically expressed E-cadherin can increase LCN2 expression (67). E-cadherin is a protein that is found in calcium-dependent cell adhesion and facilitates the binding of epithelial cells to each other (thus avoiding metastasis). In fact, research in human pancreatic cancer cells also showed that LCN2 prevents angiogenesis (blood vessel formation) (67). **Fig. 2** depicts all possible cancers involving LCN2 in humans.

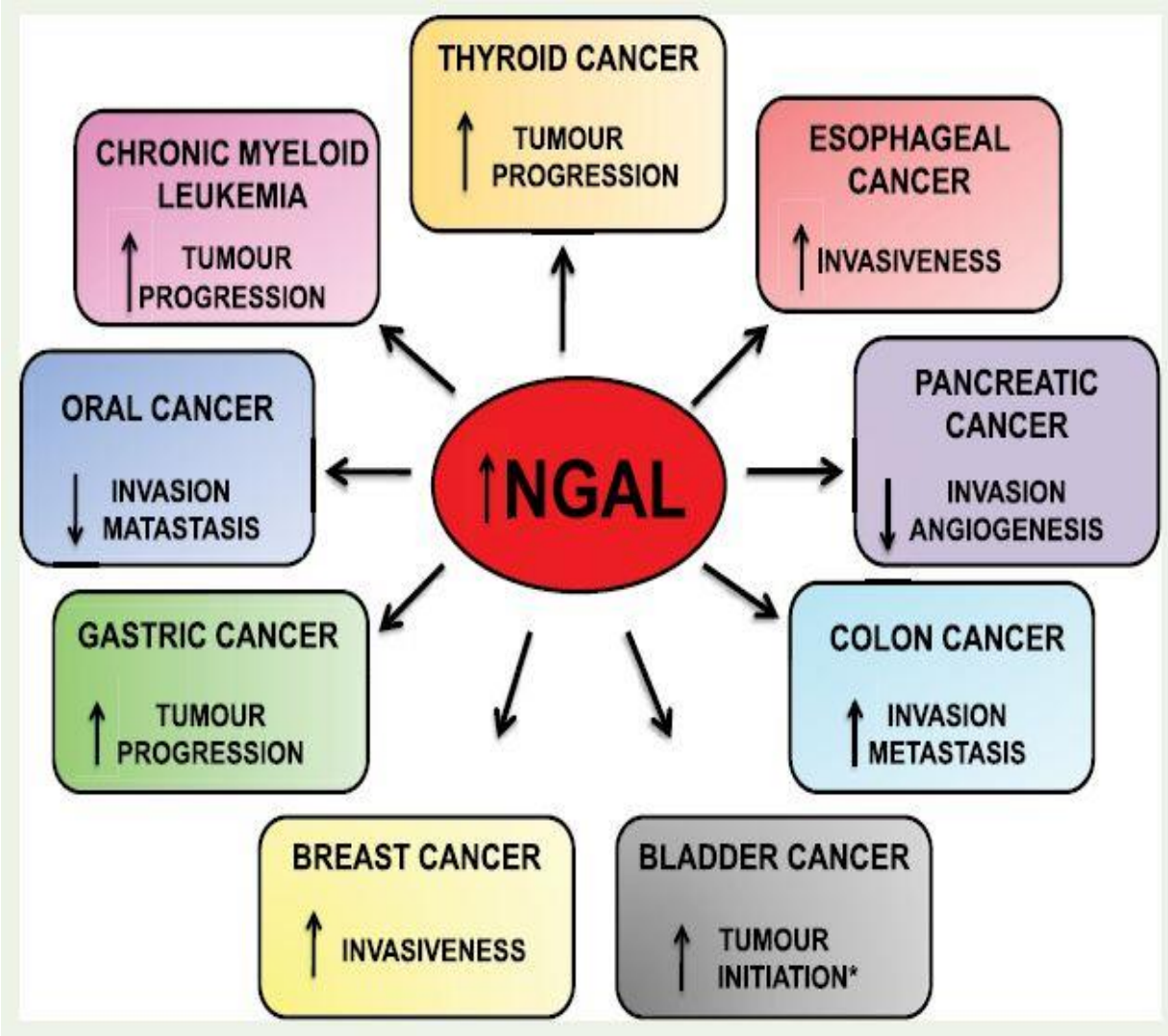


Fig. 2 *Role of LCN2 in different types of cancer.*

3.3 SLC22A17 [LCN2-R]

Epithelial-mesenchymal transition (EMT) is a highly dynamic process, where a lineage transition occurs allowing epithelial cells to undergo many biochemical changes to assume a mesenchymal cell type which involves increased migration, invasiveness, tumour progression and the generation of tumour cells with stem cell properties that play a major role in resistance to cancer treatment (68, 69). LCN2 may serve as a potential invasive biomarker for advanced BC, since elevated levels of LCN2 are detected in the urine of metastatic BC cancer patients compare to healthy controls (60, 70).

Recent study by *Sasagu Kurozumi et. al,* showed that LCN2 plays a role in breast cancer progression with loss of its nuclear expression which is associated with aggressive features and poor outcome (71). Solute Carrier Family 22 member 17 (SLC22A17) is a specific cell surface receptor for LCN2. SLC22A17 has a transmembrane domain and facilitates the transport of LCN2 across cytoplasmic or internal membranes (72). The physiological regulation of SLC22A17 and LCN2 expression maybe interlinked, in murine leukemia cell models inverse co-regulation of SLC22A17 and LCN2 expression has been observed (44). But, it had also been reported been reported about the co-existence of SLC22A17 and LCN2 in endometrial cancer types (73). For example, Du et al. reported that up-regulation of LCN2 and SLC22A17 in oesophageal squamous cell carcinoma, was associated with tumour progression (74).

3.4 Association Between LCN2 and SLC22A17

The siderocalin has attracted a lot of attention because LCN2 showed increased ability to bind to siderophores. Specifically, extensive studies are ongoing into exploring its possible pleiotropic roles. Nonetheless, how LCN2 will execute such pleiotropic roles remains unclear, although its capacity to modulate iron transfer across the cell seems to be the underlying mechanism that contribute its role in proliferation, apoptosis, and cancer progression. The exact mechanism that serves these pleiotropic roles remain unclear. The capacity of LCN2 to shield the matrix metalloprotease-9 (MMP9) from degradation by creating an MMP9-LCN2 complex (75, 76) may be the biochemical foundation underlying the role of LCN2 in cancer progression, but it cannot fully account for the contribution of LCN2 to cell division, apoptosis and inflammation. It was therefore suggested that LCN2's siderophore-mediated iron transport properties can play a role in these processes. This suggested mode of action has been verified by the identification of a cellular LCN2 receptor (LCN2-R / hLCN2-R in humans or 24p3-R, also known as SLC22A17), which promotes free and iron-bound LCN2 endocytosis together with the discovery of small molecules capable of acting as mammalian siderophores and retaining the iron-bound properties of LCN2. It has been shown that LCN2 can use these mammalian siderophores to transport iron into and out of the cell via its endo-and exocytosis using mLCN2-R (77) and thus control iron-responsive gene expression.

Given the relevant literature in which LCN2 and LCN2-R are implicated in inflammation and cancer, little is understood about the relationship between LCN2 and its cellular receptor. It has been shown that 24p3-R binds LCN2 with very high affinity (78) and that 24p3-R often exhibits strong avidity for specific ligands (such as transferrin or albumin) (79). Hence there could be an underlying mechanism involved in LCN2-LCN2R pathway and more research is needed to validate these findings. String pathway analysis revealed the association between the LCN2 receptor and LCN2 along with many other factors like MMP-9 which are known to involve in cancer development and progression (**Fig 3**).

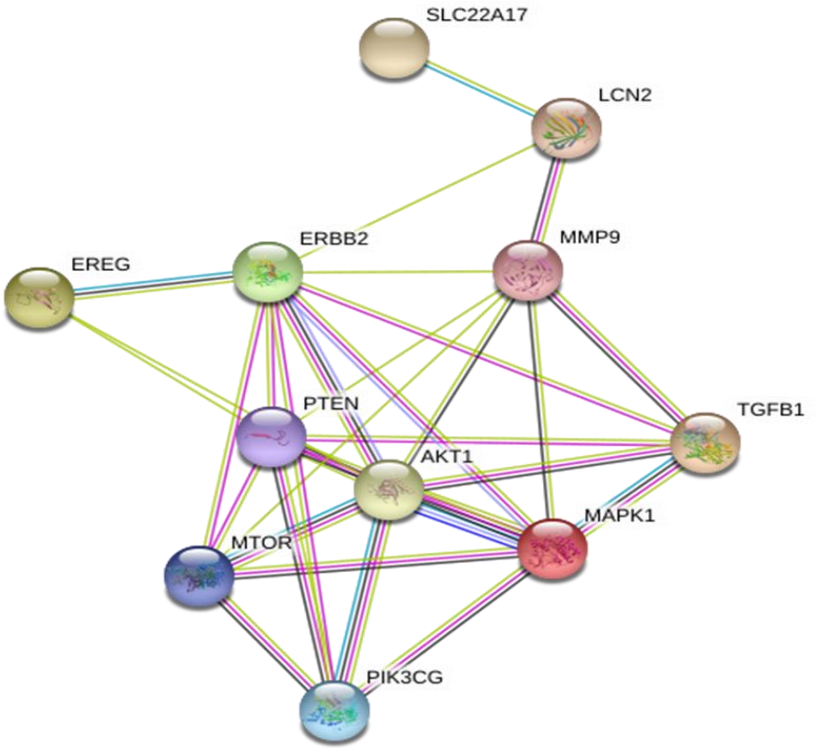


Fig. 3 *String pathway Analysis showing the association between LCN2 and SLC22A17 ($p<0.001$).*

3.5 Hypothesis

Thus, we hypothesise that SLC22A17 may play a major role in BC progression in conjunction with LCN2, involvement via LCN2/MMP9 pathway. However, little is known about the clinico-pathological features of SLC22A17 expression in human BC. Therefore, the goal of this study is to determine whether SLC22A17 play a role in the development, or progression, of breast carcinomas. For this purpose, *mRNA* and protein expression of SLC22A17 were evaluated using multiple BC cohorts.

3.6 Results: Antibody Validation

3.7 Western Blot (WB)

The LCN2 and SLC22A17 antibody specificity (LS-C405956; Lifespan Biosciences, Seattle, WA) (dilution: 1:500) was confirmed using different BC cell lines (SKBr3, MDA-MB-157, MDA-MB-231 and MCF-7) (obtained from the American Type Culture Collection; Rockville, MD, USA). The LCN2 antibody detected as single protein of 70 KDa in the SKBR3, MDA-MB-231, MDA-MB-157 and MCF-8 cell lysate and a single band visualised for the SLC22A17 antibody at approximately 50 KDa in the MCF-7, SKBR3 cell lysate (**Fig 4**). The anti-actin antibody (red band) showed a single band at a molecular weight of 41kDa and **Table 3** represents the optimum conditions of western blot was performed.

Table 3 *Elements of the Western Blot performed.*

Antibody	**Lysates**	**Dilution of Protein**	**Secondary Antibody**	**Dilution of Secondary Antibody**	**Predicted Band Size (kDa)**
Anti-LCN2/LCN2 polyclonal rabbit antibody, LSBio (LS-C405956)	157, SKBR3, 231, MCF-7	1:250	Li-cor Biosciences, IRDye 800CW Donkey anti-rabbit antibody	1:15000	70
Anti-SLC22A17, Rabbit monoclonal antibody, 237539, abcam UK	157, 231, MCF-7, SKBR3	1:500	Li-cor Biosciences, IRDye 800CW Donkey anti-rabbit antibody	1:15000	50

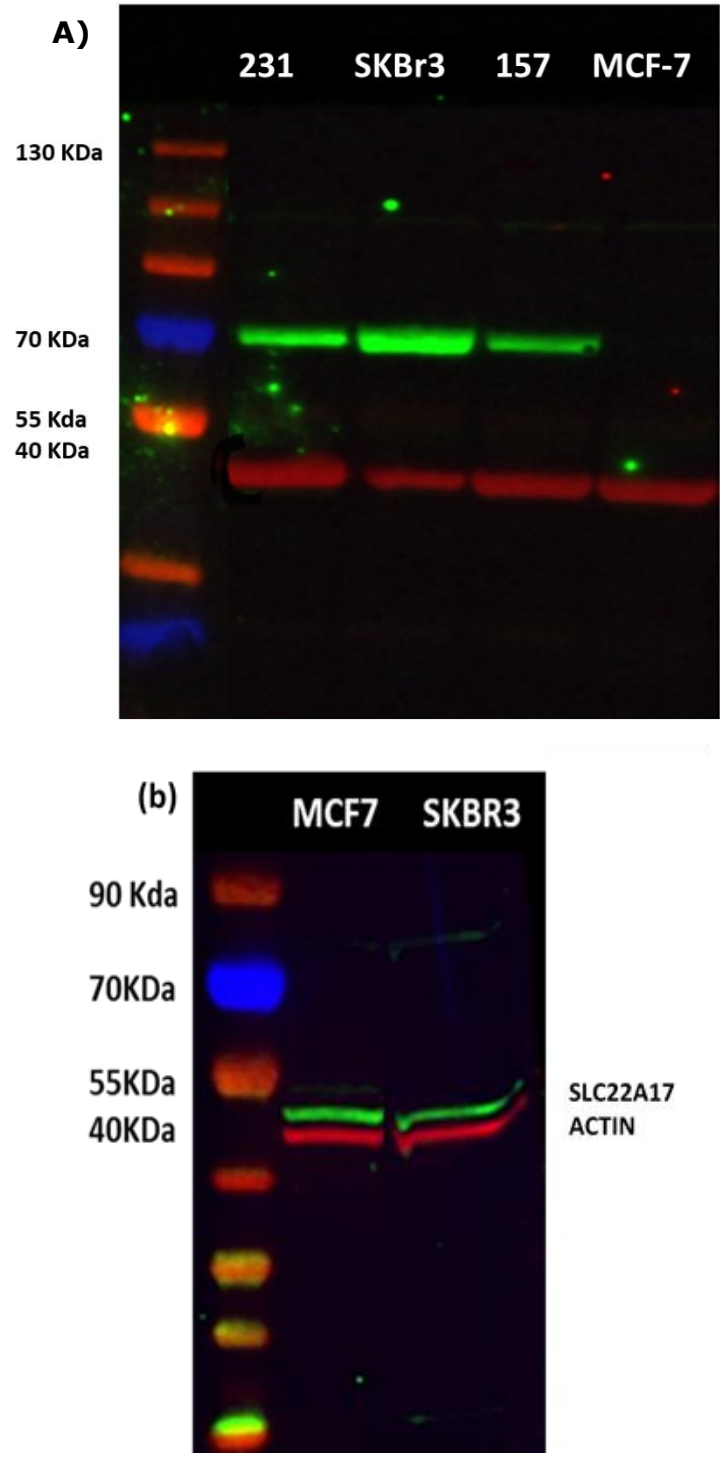


Fig. 4 Western blot of A) LCN2 and B) SLC22A17 in breast cancer cell lines using rabbit monoclonal antibody against human LCN2 (LSBio – LS-C405956) and SLC22A17 (237539, abcam, UK). Green and red bands represent protein (LCN2/SLC22A17) and Beta-Actin (house-keeping), respectively.

3.8 LCN2 Immunohistochemistry

To examine LCN2 expression, immunohistochemical staining was performed on full-face breast cancer tissue and TMA (Nottingham Series) sections (4-µm) using Novolink polymer detection system as described earlier (Section 2.2). **Table 4** represents IHC of LCN2 and SLC22A17.

Table 4: A summary of conditions used in immunohistochemistry. Selected conditions are highlighted in bold

Dilution with BC optimization sections		***Incubation***	**Antigen retrieval**
LCN2	**SLC22A17**	30 minutes at room temperature.	Heat induced Citrate retrieval at pH6 for 20 minutes.
1/1000	1/1000		
1/750	1/750		
1/500	1/800	Overnight incubation at 4◦C constant room temperature.	
1/300	1/700		
1/100	1/100		
1/150	1/250		
1/200	**1/500**		

3.9 *SLC22A17* and *LCN2* mRNA expression and clinicopathological parameters in the METABRIC cohort

High *SLC22A17* mRNA expression was positively associated with low histological grade (p<0.001), ER+ and PR+ (p<0.001) status. When BC was classified using the intrinsic (PAM50) subtypes, high expression was associated with Luminal A (p<0.001) similarly, within the METABRIC Integrative Clusters (4), elevated *SLC22A17* mRNA expression was associated with IC cluster 3 (Luminal A) associated with good prognosis, and showed low expression for IC clusters 9 (ER+ Lum B) respectively (p<0.001;**Table 5**).

However, *LCN2* mRNA expression showed significant positive associations with high histological grade (p<0.001), HER2 status (p<0.001) and triple negative status (p<0.001; **Table 5**). High *LCN2* mRNA expression was significantly associated with integrative Clusters 5 and 10 (p<0.001) which was associated with poorer clinical outcome in the METABRIC cohort.

Table 5: Associations between SLC22A17 and LCN2 mRNA expression and clinicopathological variables in the METABRIC cohort.

Clinicopathological Criteria	***SLC22A17***		***x2 & (p Value)***	***LCN2***		***x2 & (p Value)***
	Low (%)	High (%)		Low (%)	High (%)	
Histological grade						
1	53 (31.2)	117 (68.8)	77.676 (**<0.001**)	104 (61.2)	66 (38.8)	47.791 **(<0.001)**
2	347 (45.1)	423 (54.9)		441 (57.3)	329 (42.7)	
3	584 (61.3)	368 (38.7)		402 (42.2)	550 (57.8)	
Tumour type						
Ductal	908 (53.4)	793 (46.6)	40.967 (**<0.001**)	809 (49.5)	825 (50.5)	1.419 **(0.701)**
Lobular	55 (37.4)	92 (62.6)		73 (49.7)	74 (50.3)	
Special type	11 (23.9)	35 (76.1)		44 (56.4)	34 (43.6)	
Other invasive	4 (33.3)	8 (66.7)		6 (50)	6 (50)	
NPI						
GPG	272 (40.0)	408 (60.0)	57.193 (**<0.001**)	400 (58.8)	280 (41.2)	34.779 **(<0.001)**
MPG	622 (56.5)	479 (43.5)		510 (46.3)	591 (53.7)	
PPG	125 (62.8)	74 (37.2)		80 (40.2)	119 (59.8)	
PAM50 subtype						
Luminal A	300 (41.8)	418 (58.2)	153.73 (**<0.001**)	433 (60.3)	285 (39.7)	265.742 **(<0.001)**
Luminal B	269 (55.1)	219 (44.9)		335 (68.6)	153 (31.4)	
Basal	136 (56.7)	104 (43.3)		66 (20.1)	263 (79.9)	
HER2	253 (76.9)	76 (23.1)		96 (40)	144 (72.4)	
Normal-like	60 (30.2)	139 (69.8)		55 (27.6)	144 (72.4)	
IntClustMemb						
IntClustMemb 1	90 (64.7)	49 (35.3)	160.147 (**<0.001**)	90 (64.7)	49 (35.3)	178.968 **(<0.001)**
IntClustMemb 2	30 (41.7)	42 (58.3)		43 (59.7)	29 (40.3)	
IntClustMemb 3	109 (37.6)	181 (62.4)		160 (55.2)	130 (44.8)	
IntClustMemb 4	140 (40.8)	203 (59.2)		173 (50.4)	170 (49.6)	
IntClustMemb 5	100 (52.6)	90 (47.4)		59 (31.1)	131 (68.9)	
IntClustMemb 6	41 (48.2)	44 (51.8)		66 (77.6)	19 (22.4)	
IntClustMemb 7	82 (43.2)	108 (56.8)		120 (63.2)	70 (36.8)	
IntClustMemb 8	146 (48.8)	153 (51.2)		164 (54.8)	135 (45.2)	
IntClustMemb 9	91 (62.3)	55 (37.7)		74 (50.7)	72 (49.3)	
IntClustMemb 10	190 (84.1)	36 (15.9)		41 (18.1)	185 (81.9)	
ER						
Negative	334 (70.5)	140 (29.5)	90.060 (**<0.001**)	94 (21.4)	345 (78.6)	187.248 **(p<0.001)**
Positive	685 (45.5)	821 (54.5)		877 (58.5)	621 (41.5)	
PR						
Negative	563 (59.9)	377 (40.1)	50.902 (**<0.001**)	395 (42)	545 (58)	45.571 **(<0.001)**
Positive	456 (43.8)	584 (56.2)		595 (57.2)	445 (42.8)	
HER2						
Negative	890 (51.4)	843 (48.6)	0.065 (0.797)	911 (52.6)	822 (47.4)	36.640 **(<0.001)**
Positive	129 (52.2)	118 (47.8)		79 (32.0)	168 (68.0)	

*Significant p values are highlighted in bold.

3.10 Expression of LCN2 in immunohistochemistry

Full-face tissue sections were from Nottingham BC cohort which showed LCN2 expression in tumour and LVI (**Fig**. **5 A & B**). In contrast, LCN2 immunopositivity was observed in the cytoplasm/membrane of invasive cancer cells, which was stronger compared to the normal epithelial cells. On TMAs, variable degree of LCN2 protein expression in BC is shown in (**Fig 5 C, D & E**) LCN2 showed cytoplasmic and nuclear staining. The variation in intensity amongst the cores was observed and figures 5 and 6 show patterns of the staining identified in breast cancer TMAs.

On TMAs (Nottingham series), there were 714 positive cores out of which 72.1% and 27.9% showed negative/low and high cytoplasmic expression respectively. For the nuclear staining, 30% showed negative/low expression while 70% showed high expression. Staining of both nuclear and cytoplasmic LCN2 varied from low to high intensity (**Fig 5 C & E**).

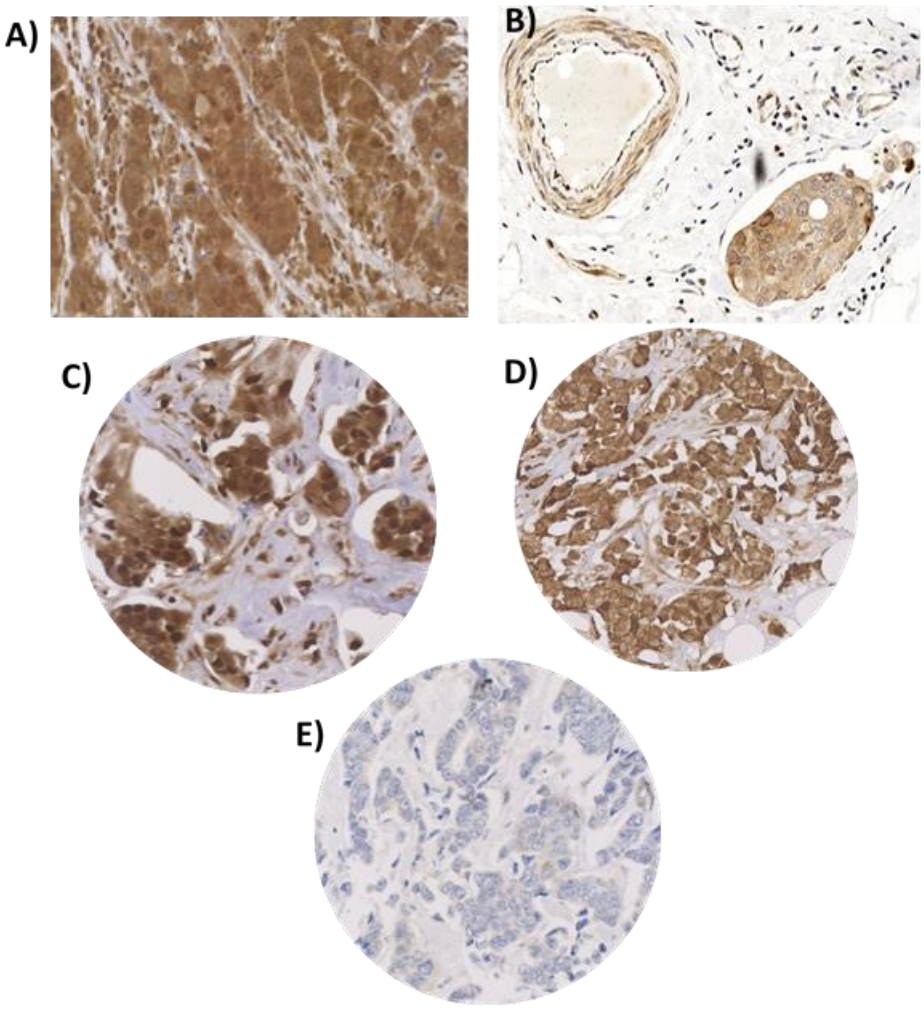


Fig. 5 Morphological characteristics of LCN2 immunohistochemistry in breast cancer tissue**.** A) Invasive B) LVI. LCN2 protein expression in breast cancer TMA cores. C). Nuclear D). Cytoplasmic and E). Negative (all at 40X magnification).

3.11 LCN2 protein expression

Immunoreactivity of LCN2 expression observed in the cytoplasm/nucleus of invasive cancer cells (**Fig 5 C & D**) and low immunoreactivity was observed in TDLU and DCIS. In both the cytoplasm and nucleus of malignant epithelial cells, LCN2 displayed poor staining in the stroma. The expression of LCN2 was moderate to strong in the nuclei of adjacent apparently normal duct-lobular terminal units. By contrast, invasive cancer cells ' LCN2 nuclear immunoreactivity was lower than that of adjacent normal epithelial cells. In the cytoplasm of cancer cells, the immunoreactivity of LCN2 was moderate compared to that in the nucleus. Also, both cytoplasmic/nuclear LCN2 expression did not follow a normal distribution therefore the expression of LCN2 protein was dichotomized using cut points derived from prediction of patient survival using X-tile (80), BCSS as endpoint.

3.12 Association between LCN2 protein expression and key clinicopathological variables

At the protein level, favourable prognostic lobular tumours displayed higher LCN2 nuclear expression in comparison to other subtypes ($p<0.001$). High nuclear expression was associated with low- grade tumours ($p=0.001$), moderate nuclear pleomorphism ($p=0.003$), low mitotic activity ($p<0.001$) and Luminal A tumours (comprising 78.9% of cases; $p=0.004$). Cytoplasmic LCN2 expression was also high in low-grade tumours ($p=0.021$) and special-type tumours ($p=0.003$) as well as tumours with well differentiated tubules ($p=0.033$) (Summarised in **Table 6**).

3.13 Association with Key biomarkers

High nuclear LCN2 expression showed negative association with cytokeratin 5 ($p=0.002$), Ki67 ($p<0.001$) and LVI ($p=0.040$) while positively associated with hormone receptor positivity ($p=0.014$ and 0.044 respectively; summarized in **Table 7**).Low nuclear expression was significantly associated with high Ki67 labelling index ($p < 0.001$), N-cadherin ($p = 0.00052$), TWIST2 ($p = 0.039$), CK5/6 ($p = 0.0088$) and EGFR positivity ($p = 0.019$) (**Table 7**).

3.14 Association with patient outcome

Univariate analysis (Nottingham series) displayed significant associations with high nuclear LCN2 expression and improved BCSS at 15 and 20-year endpoints ($p=0.004$ and 0.007 respectively; **Fig 6**). Using multivariate Cox regression, LCN2 nuclear protein expression is an independent predictor of BCSS [$p<0.001$; HR 1.7 (95% CI 1.4-2.1); **Table 8**].

Table 6: Association of LCN2 nuclear and cytoplasmic expression in BC series.

Clinico-pathological Criteria	***LCN2 nuclear expression***		***x2 (p Value)***	***LCN2 cytoplasmic expression***		***x2 (p Value)***
	Low (%)	***High (%)***		***Low (%)***	***High (%)***	
Age at Diagnosis						
≤50 years	*77 (29.3)*	*186 (70.7)*	*0.096 (0.757)*	*180 (68.4)*	*83 (31.6)*	2.817 ***(0.093)***
>50 years	*137 (30.4)*	*314 (69.6)*		*335 (74.3)*	*116 (25.7)*	
Tumour size						
≤2.0cm	*91 (27.6)*	*239 (72.4)*	*2.058 (0.151)*	*232 (70.3)*	*98 (29.7)*	1.438 ***(0.23)***
>2.0cm	*123 (32.5)*	*255 (67.5)*		*281 (74.3)*	*97 (25.7)*	
Histological grade						
1	*24 (21.8)*	*86 (78.2)*	*18.220 (**0.001**)*	*74 (67.3)*	*36 (32.7)*	7.754 ***(0.021)***
2	*61 (23.8)*	*195 (76.2)*		*201 (78.5)*	*55 (21.5)*	
3	*129 (37.9)*	*211 (62.1)*		*236 (69.4)*	*104 (30.6)*	
Tumour type						
Ductal	*194 (33.0)*	*394 (67.0)*	*22.567 (**0.0004**)*	*422 (71.8)*	*166 (28.2)*	17.774 ***(0.003)***
Lobular	*6 (8.6)*	*64 (91.4)*		*60 (85.7)*	*10 (14.3)*	
Medullary like	*5 (31.3)*	*11 (68.8)*		*10 (62.5)*	*6 (37.5)*	
Special type	*9 (31.0)*	*20 (69.0)*		*16 (55.2)*	*13 (44.8)*	
NPI						
Good prognostic group	*44 (21.3)*	*163 (78.7)*	*11.543 (**0.003**)*	*160 (77.3)*	*47 (22.7)*	5.237 *(0.07)*
Moderate prognostic group	*129 (33.2)*	*259 (66.8)*		*279 (71.9)*	*109 (28.1)*	
Poor prognostic group	*41 (36.3)*	*72 (63.7)*		*74 (65.5)*	*39 (34.5)*	
IHC subtypes						
Luminal A	*34 (21.1)*	*127 (78.9)*	*13.589 (**0.004**)*	*121 (75.2)*	*40 (24.8)*	1.473 ***(0.68)***
Luminal B	*67 (31.6)*	*145 (68.4)*		*154 (72.6)*	*58 (27.4)*	
HER2+	*31 (30.1)*	*72 (69.9)*		*71 (68.9)*	*32 (31.1)*	
TNBC	*49 (41.5)*	*69 (58.5)*		*83 (70.3)*	*35 (29.7)*	
Pleomorphism						
1	*6 (42.9)*	*8 (57.1)*	*11.918 (**0.003**)*	*11 (78.6)*	*3 (21.4)*	2.913 ***(0.233)***
2	*62 (22.8)*	*210 (77.2)*		*205 (75.4)*	*67 (24.6)*	
3	*136 (34.7)*	*256 (65.3)*		*273 (69.6)*	*119 (30.4)*	
Mitotic figures						
1	*48 (21.3)*	*177 (78.7)*	*19.935 (**<0.001**)*	*176 (78.2)*	*49 (21.8)*	6.184 ***(0.045)***
2	*40 (26.3)*	*112 (73.7)*		*106 (69.7)*	*46 (30.3)*	
3	117 (38.7)	185 (61.3)		208 (68.9)	94 (31.1)	

*significant values are highlighted in bold

Table 7: Associations between LCN2 expression and key biomarkers in BC

Biomarker	***LCN2 nuclear expression***		***x2 (p Value)***	***LCN2 cytoplasmic Expression***		***x2 (p Value)***
	Low (%)	***High (%)***		***Low (%)***	***High (%)***	
Cytokeratin 5						
			9.821 (**0.002**)			0.674 (0.412)
Negative	39 (43.8)	50 (56.2)		61 (68.5)	28 (31.5)	
Positive	24 (32.9)	49 (67.1)		51 (69.9)	22 (30.1)	
P16						
Negative	93 (26.1)	263 (73.9)	2.458 (0.117)	194 (33.0)	394 (67.0)	5.615 **(0.018)**
Positive	62 (32.5)	129 (67.5)		6 (8.6)	64 (91.4)	
ER						
Negative	65 (37.4)	109 (62.6)	6.043 (**0.014**)	118 (67.8)	56 (32.2)	2.307 (0.153)
Positive	147 (27.5)	387 (72.5)		392 (73.4)	142 (26.6)	
PR						
Negative	96 (34.4)	183 (65.6)	4.040 (**0.044**)	199 (71.3)	80 (28.7)	0.398 (0.528)
Positive	110 (27.2)	294 (72.8)		297 (73.5)	107 (26.5)	
HER2						
Negative	171 (29.3)	413 (70.7)	0.012 (0.913)	426 (72.9)	158 (27.1)	0.609 (0.435)
Positive	31 (29.8)	73 (70.2)		72 (69.2)	32 (30.8)	
TPN						
Negative	160 (27.6)	419 (72.4)	8.330 (**0.004**)	322 (74.7)	109 (25.3)	3.047 (0.081)
Positive	48 (41.0)	69 (59.0)		191 (68.7)	87 (31.3)	
LVI						
Negative	92 (27.1)	247 (72.9)	4.209 **(0.040)**	253 (74.6)	86 (25.4)	1.367 (0.242)
Positive	78 (35.3)	143 (64.7)		155 (70.1)	66 (29.9)	
Ki67						
Negative	51 (22.5)	176 (77.5)	12.759 **(<0.001)**	161 (70.9)	66 (29.1)	**0.382 (0.536)**
Positive	116 (36.8)	199 (63.2)		231 (73.3)	84 (26.7)	
N-CADHERIN						
Negative	83 (60.6)	54 (39.4)	**0.0005**	75 (54.7)	62 (45.3)	0.48
Positive	140 (42.7)	188 (57.3)		167 (50.9)	161 (49.1)	
TWIST2						
Negative	106 (58.6)	75 (41.4)	**0.039**	97 (53.6)	84 (46.4)	0.92
Positive	118 (48.2)	127 (51.8)		129 (52.7)	116 (47.3)	
EGFR						
Negative	245 (51.0)	235 (49)	**0.019**	248 (51.7)	232 (48.3)	0.61
Positive	47 (38.8)	74 (61.2)		59 (48.8)	62 (51.2)	

*significant values are highlighted in bold

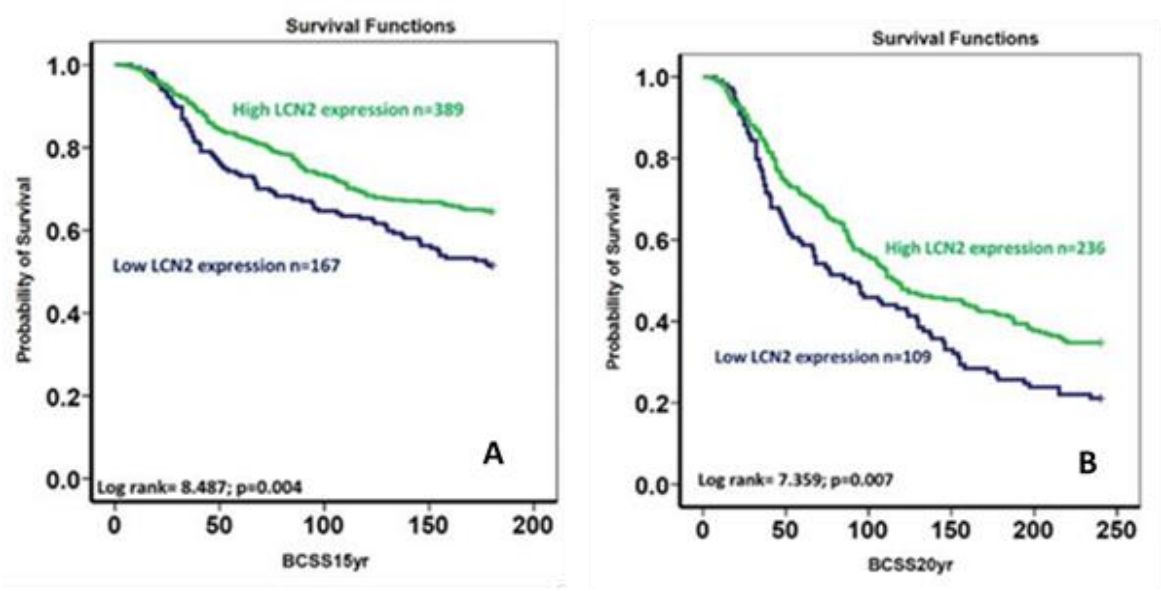


Fig. 6 Kaplan Meier curves showing the relationship between LCN2 expression and BCSS. A) Nuclear expression at 15-year BCSS B). Nuclear expression at 20-year BCSS.

Table 8: Multivariate analysis of LCN2 expression compared with tumour stage, grade, size for breast cancer-specific survival

Variable	Breast cancer-specific survival		
	Multivariate		
	HR	95%CI	p value
Whole cohort			
Stage	1.3	1.2-1.8	**<0.001**
Grade	1.5	1.6- 2.4	**<0.001**
Tumour size	1.0	1.0-1.6	**0.003**
LCN2	1.7	1.4-2.1	**<0.001**

Significant p values are highlighted in bold

3.15 Differential protein expression of LCN2

As described in the methodology, cell lines were selected based on the differential protein expression on Western blot hence, SKBR3 and MDA-MB-157 were optimised for knockdown. For the optimisation of the knockdown protocol two LCN2 siRNAs were used (s8113-4392420, s8114-4392420) and a scrambled negative control (4390843).

Optimization of siRNA transient transfection of LCN2

Pre designed LCN2 siRNAs (5nM) were diluted at 25nM concentration and tested it against a negative non-specific scrambled control and un-transfected cells in all experiments.

Prepared a 10µM working stock by carrying out a 1:10 dilution from the 100µM stock using nuclease-free water. 10µM stock of siRNA is equivalent to 10pmol/µl, transfections were carried out in triplicates.

LCN2 siRNA and the scrambled negative control siRNA was prepared at 10µmol concentration. Lipofectamine RNAiMAX was used as a transporter of LCN2 SiRNA. Solution was mixed gently and incubated at RT for 15 minutes. Cells were trypsinised and viability was calculated using haemocytometer. Seeding was done between 2×10^5 cells in McCoy (SKBR3) and RPMI (MDA-MB-157) medium in 24 wells plates. Cells were incubated at 37 °C with 5 % CO2 overnight.

To each well containing siRNA-Lipofectamine complexes, required number of cells were added. Plate was gently moved using rocker. Incubated between 24-72hours at 37°C in CO2 incubator. On fifth day cells were collected on ice in lysis buffer. Samples were stored at -20 for western blot analysis to measure the knock-down efficacy. For each cell line and each target, depending on well plate specific protocol was followed and was previously optimised. Prior to transfections, cells were tested for mycoplasma and was mycoplasma free since mycoplasma can interfere with transfection efficiency and the results.

SKBr3 and MDA-MB-157 were selected for Transfection (Knockdown) and prominent bands were seen in WB images. Initially transient gene knockdown was optimised. Optimised knockdown protocol was followed as previously described and two SiRNA was used. Cells were harvested on Day 3 and Day 5 respectively and Western blot image showing the expression of LCN2 in both the cell lines (**Fig. 7 & Fig. 8**).

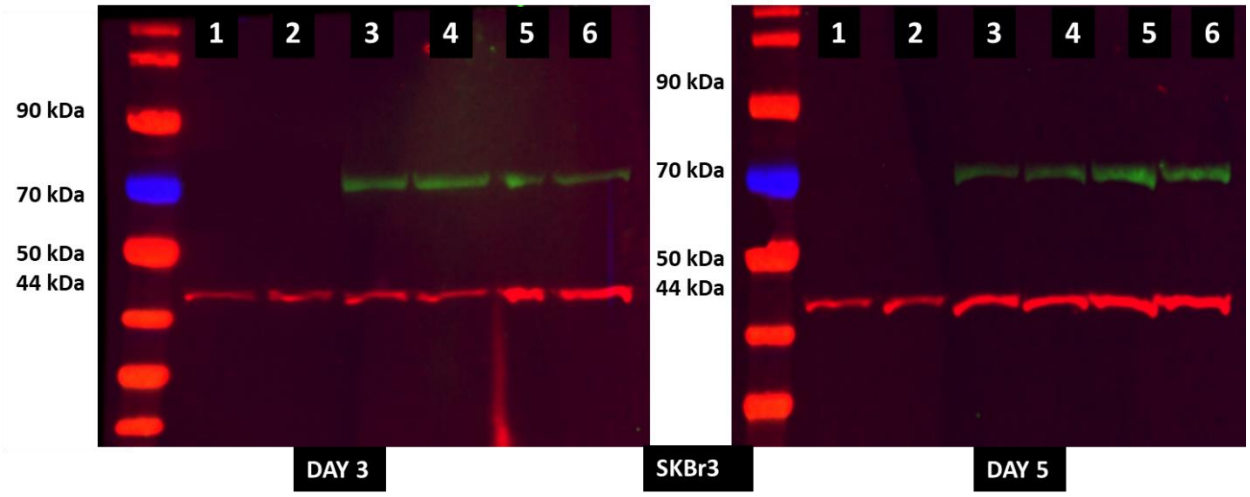


Fig. 7 Transfection of SKBr3 cell line - First two wells were Transfected (knockdown) cell lysates, next two Un-transfected (control) and last two were negative control.

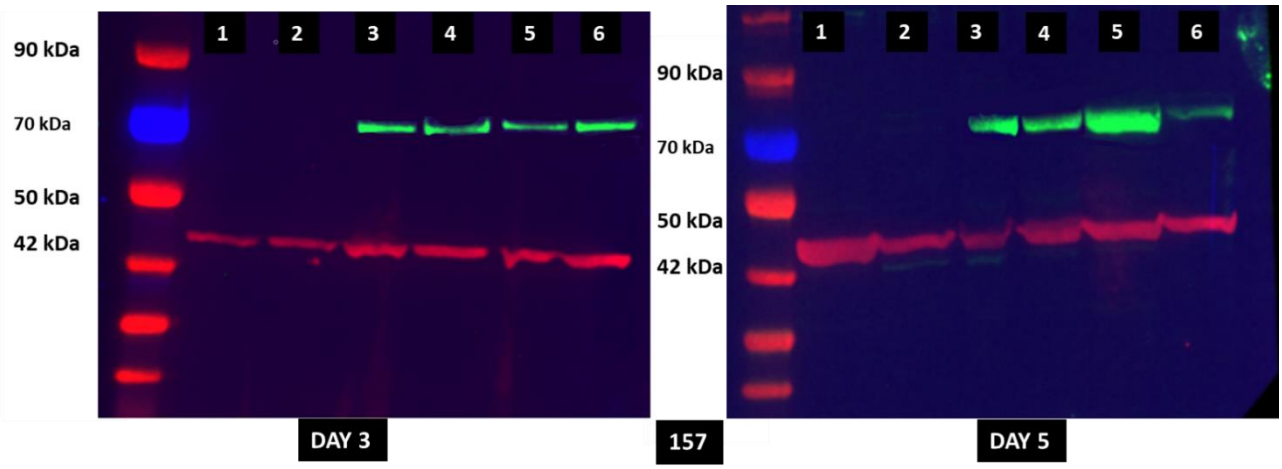


Fig. 8 Transfection of MDA-MB-157 cell line - First two wells were Transfected (knockdown) cell lysates, next two Un-transfected (control) and last two were negative control.

3.16 Migration

As previously described migration was followed after knockdown, using Un-transfected and Transfected cells. Pre-migration treatment were obtained after the seeding day (i.e., Day 2) and after 48 hours images were taken to deduce the area of migration in both un-transfected and transfected (**Fig 9**).

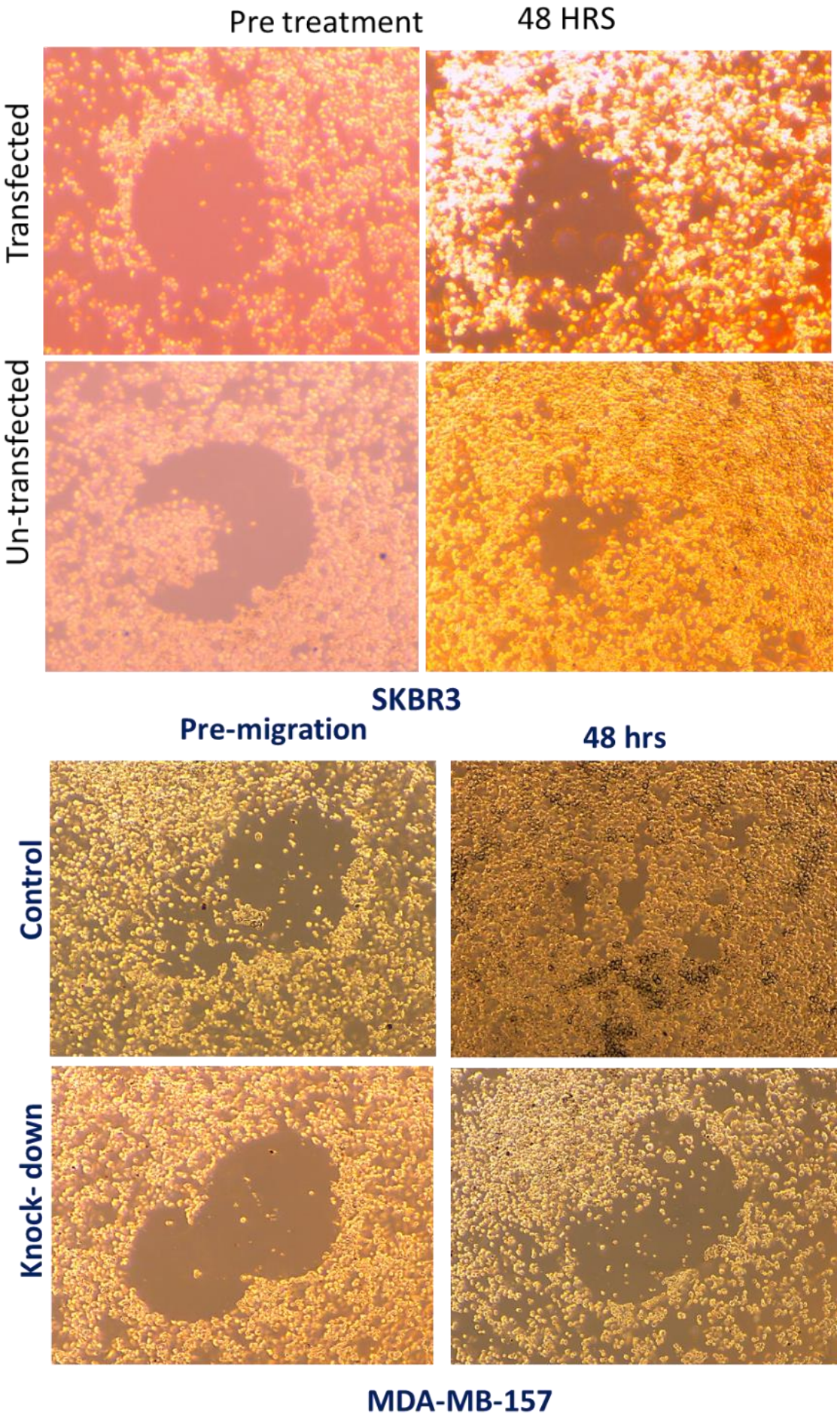


Fig. 9 Representative images of the migration assay in the SKBr3 and MDA-MB-157 cells, the area of migrated cells were significantly increased in the un-transfected (control) cells after 48 hours compared to the transfected group.

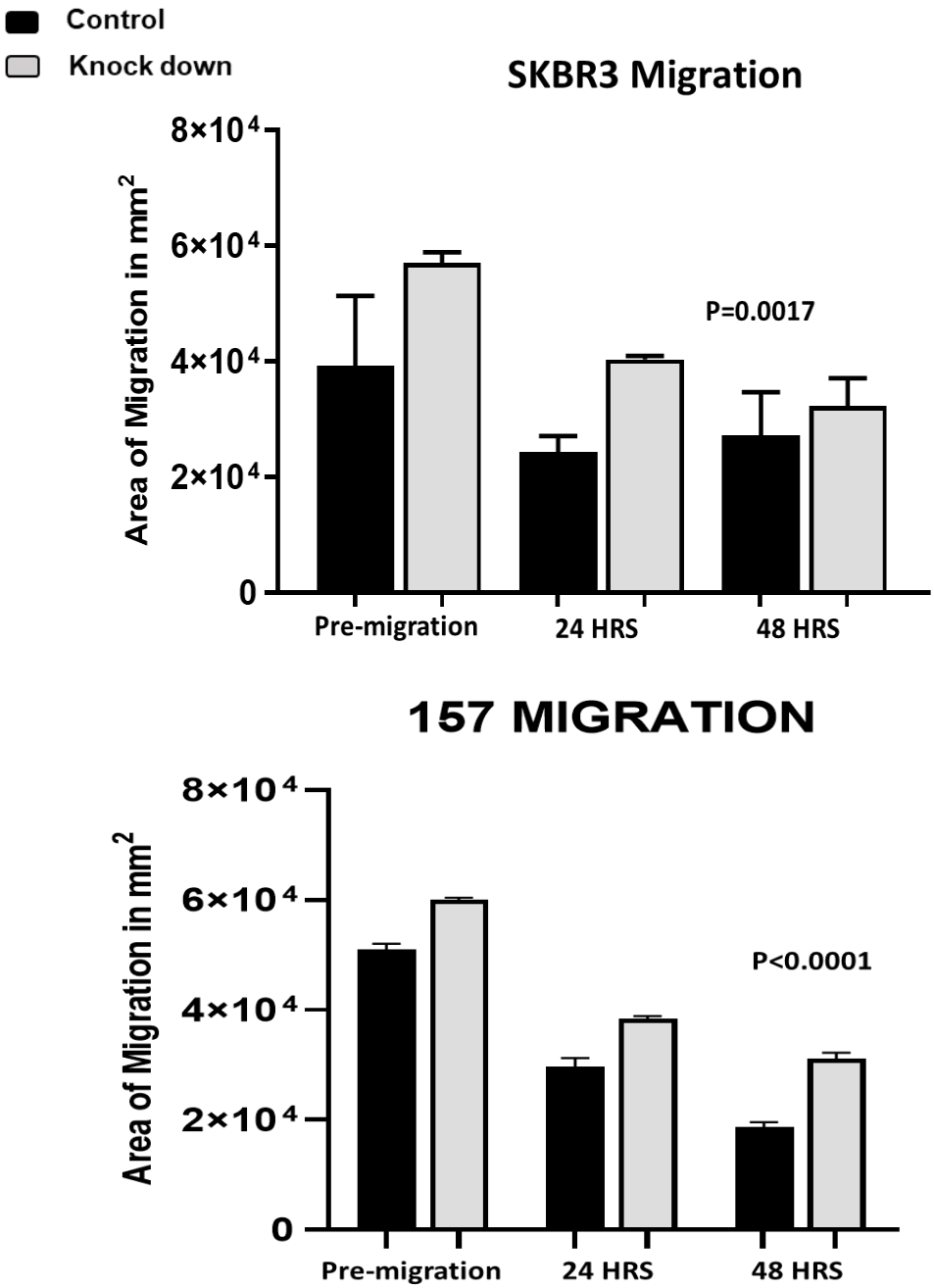


Fig. 10 Bar graph A) SKBR3 migration from pre-migration till 48 hours. B) MDA-MB-157 migration. Black bar represents un-transfected (control), grey bar represents transfected (knockdown).

Transfection of LCN2 using SiRNA's reduces the migration of BC cells. Both SKBr3 and MDA-MB-157 cells showed that the migration rate was significantly lowered in the *LCN2* transfected cells compared to the un-transfected groups (n=3; p=0.0017 and p<0.001 respectively) (**Fig 10**).

3.17 Invasion Assay

Trans-well Invasion assay displayed that the number of invaded cells was significantly decreased in the SKBr3 KD cells compared with the control group (p=0.008), followed by MDA-MB157 (p=0.002) (**Fig. 11**).

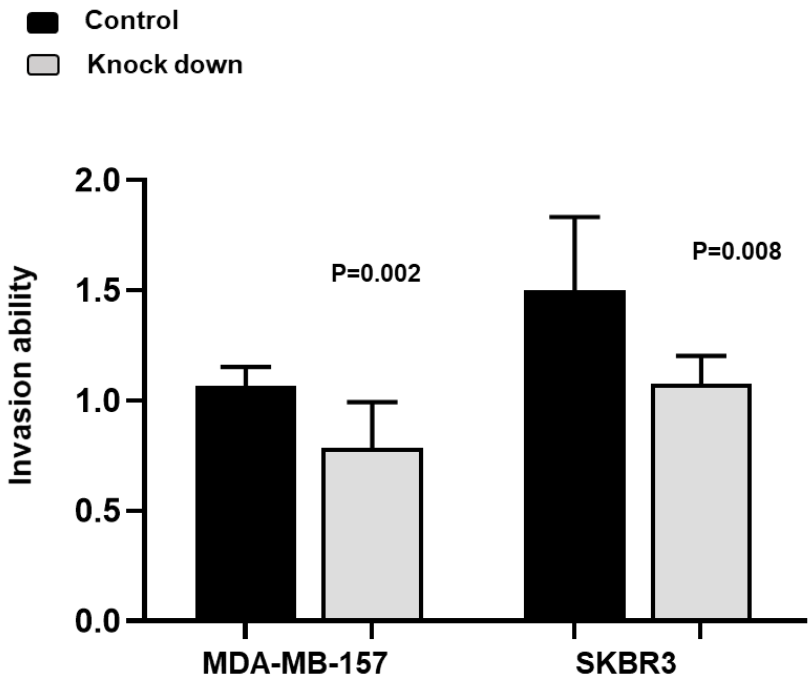


Fig. 11 Invasion ability of MDA-MB-157 and SKBR3. Black bar represents Un-transfected (control) which had invaded more compared to grey bar which was Transfected (knockdown) respectively.

3.18 Proliferation Assay

Proliferation assay displayed that transfected *LCN2* showed significant reduction in the proliferation of cells compared to un-transfected, cells. (**Fig. 12**).

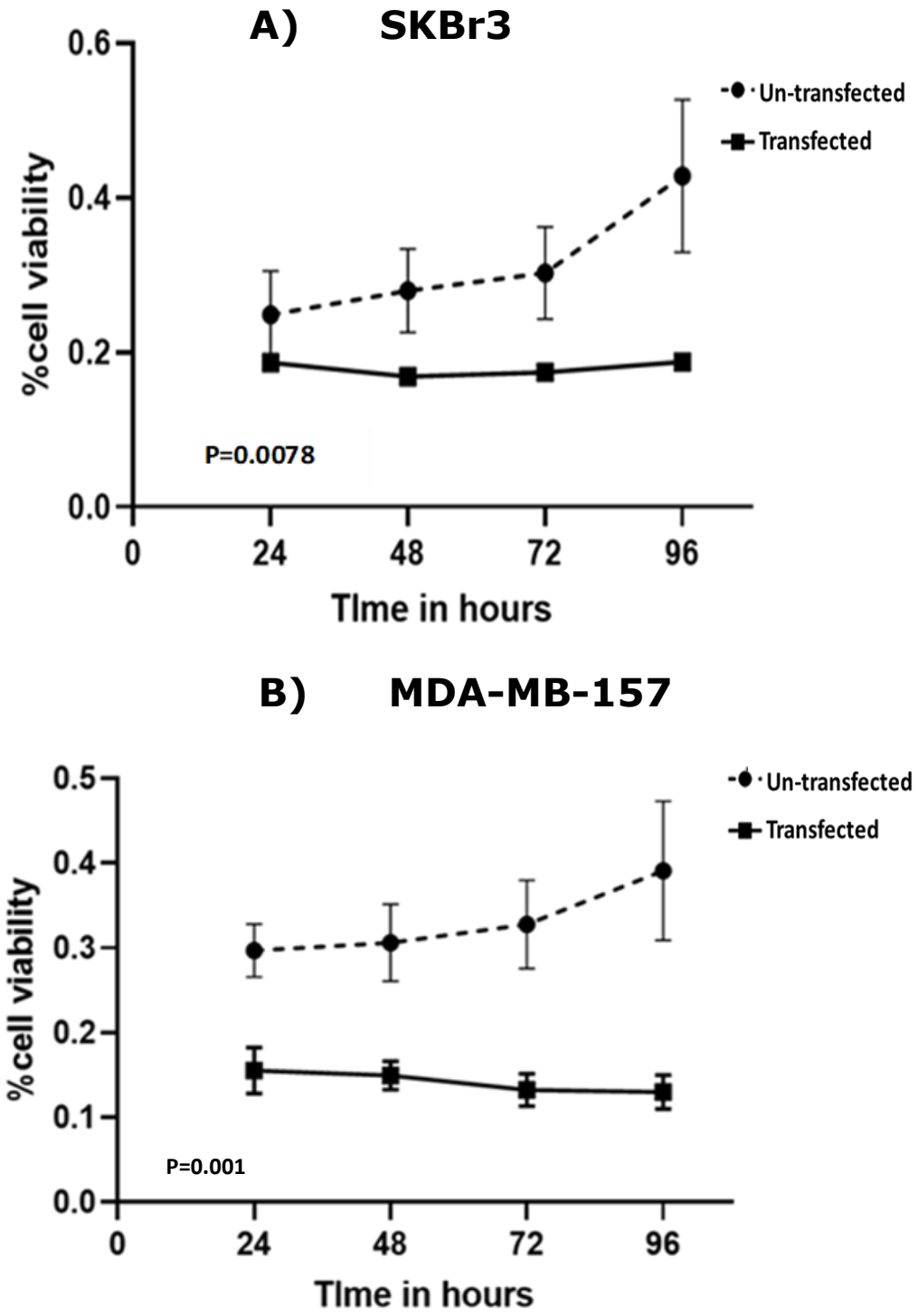


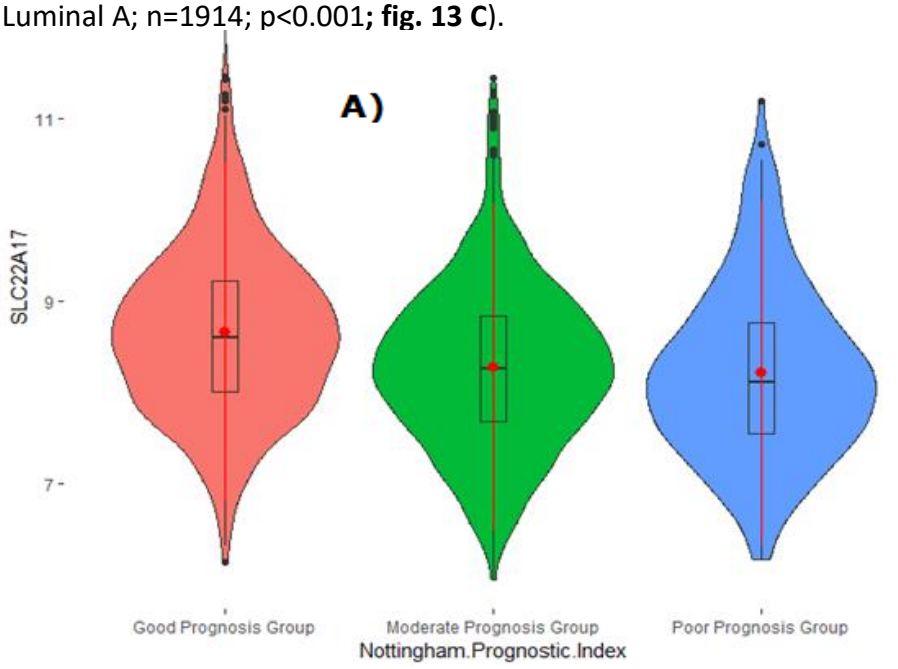
Fig. 12 Cell proliferation was significantly reduced after LCN2 KD in both A) SKBr3 (p=0.007) and B) MDA-MB-157 (p=0.001) cell lines as detected by MTS assay (n=3).

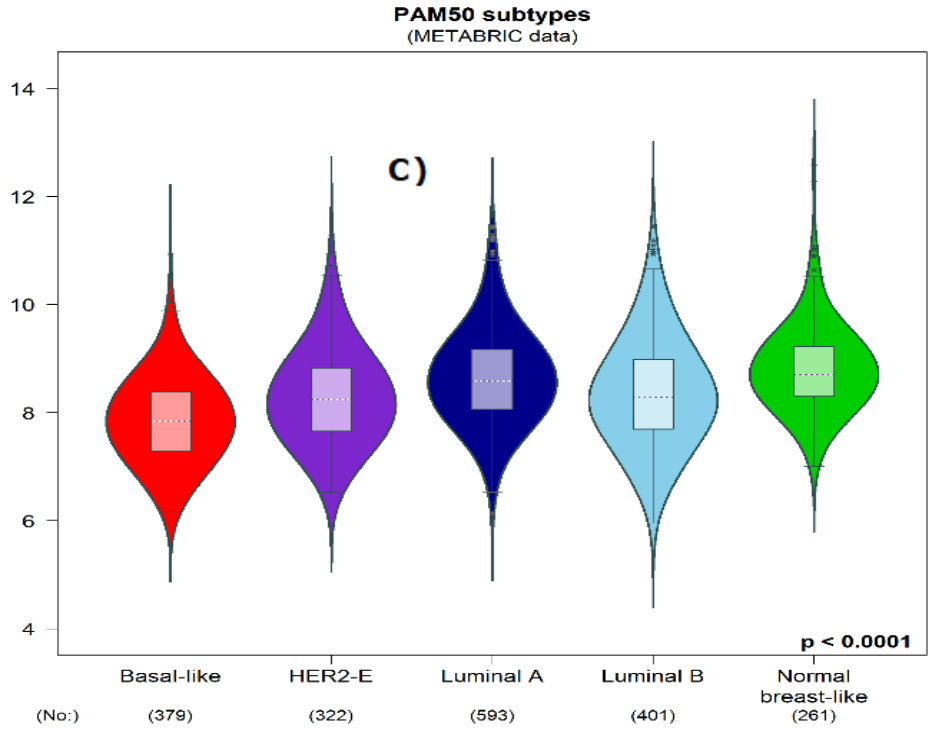
CHAPTER 4

Analysis of SLC22A17

4.0 SLC22A17 genomic profiling

High *SLC22A17* mRNA expression was positively associated with low histological grade (p<0.001), ER+ and PR+ (p<0.001) status. When BC was classified using the intrinsic (PAM50) subtypes, high expression was associated with Luminal A (p<0.001) similarly, within the METABRIC Integrative Clusters (4), elevated *SLC22A17* mRNA expression was associated with IC cluster 3 (Luminal A) associated with good prognosis, and showed low expression for IC clusters 9 (ER+ Lum B) respectively (p<0.001;**Table 9**). Using BC Gene-Expression Miner v4.0, *SLC22A17* mRNA was associated with overall survival (n=965; p=0.02), low tumour grade (n=973; p<0.001; **fig. 13 D & B**) and good Nottingham Prognostic Index (n=573; p<0.001; **fig. 13 A**). BC Gene-Miner showed positive association between *SLC22A17* mRNA with PAM50 subtypes (Luminal A; n=1914; p<0.001**; fig. 13 C**).





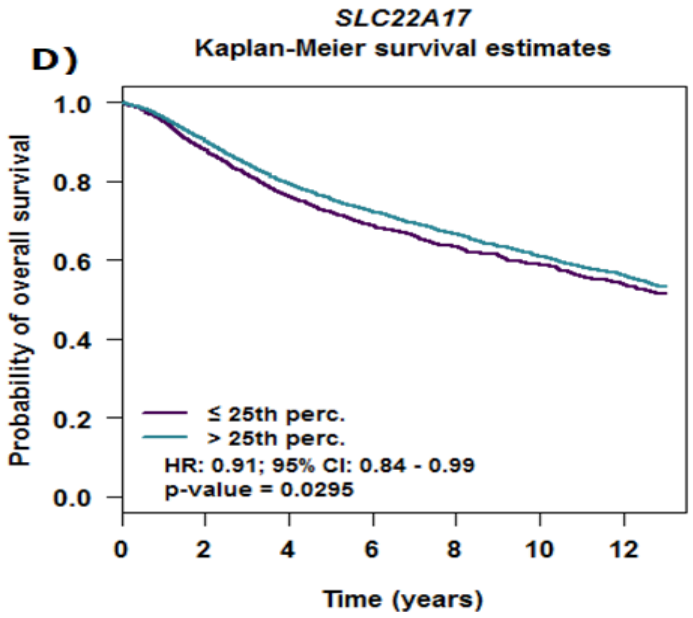


Fig. 13 Kaplan–Meier plots of SLC22A17 expression and breast cancer patient outcome. At transcriptomic level (A) Violin plot- Nottingham Prognostic index (NPI) (B) Tumour Grade (C) PAM50 subtypes (D) BC gene miner overall survival.

Table 9 Associations between *SLC22A17* mRNA expression and clinicopathological variables in the METABRIC cohort.

Clinico-pathological Criteria	***SLC22A17 mRNA expression***		***χ2 & p Value***
	Low Expression N (%)	***High Expression N (%)***	
Age at Diagnosis			
≤50	234 (55.2)	190 (44.8)	2.995 (0.083492)
>50	785 (50.4)	771 (49.6)	
Tumour Size			
≤2.0	430 (50.1)	428 (49.9)	0.971 (0.324)
>2.0	577 (52.4)	525 (47.6)	
Histological Grade			
1	53 (31.2)	117 (68.8)	77.676 **(<0.001)**
2	347 (45.1)	423 (54.9)	
3	584 (61.3)	368 (38.7)	
Tumour Type			
Ductal	908 (53.4)	793 (46.6)	40.967 **(<0.001)**
Lobular	55 (37.4)	92 (62.6)	
Medullary-like	26 (81.3)	6 (18.8)	
Special type	11 (23.9)	35 (76.1)	
Miscellaneous	4 (33.3)	8 (66.7)	
Nottingham Prognostic Index (NPI)			
Good Prognostic Group	272 (40.0)	408 (60.0)	57.193 **(<0.001)**
Moderate Prognostic Group	622 (56.5)	479 (43.5)	
Poor Prognostic Group	125 (62.8)	74 (37.2)	
PAM50 subtype			
Luminal A	300 (41.8)	418 (58.2)	153.573 **(<0.001)**
Luminal B	269 (55.1)	219 (44.9)	

Basal	136 (56.7)	104 (43.3)	
Her2	253 (76.9)	76 (23.1)	
Normal like	60 (30.2)	139 (69.8)	
IntClustMemb			
IntClustMemb 1	90 (64.7)	49 (35.3)	
IntClustMemb 2	30 (41.7)	42 (58.3)	160.147
IntClustMemb 3	109 (37.6)	181 (62.4)	**(<0.001)**
IntClustMemb 4	140 (40.8)	203 (59.2)	
IntClustMemb 5	100 (52.6)	90 (47.4)	
IntClustMemb 6	41 (48.2)	44 (51.8)	
IntClustMemb 7	82 (43.2)	108 (56.8)	
IntClustMemb 8	146 (48.8)	153 (51.2)	
IntClustMemb 9	91 (62.3)	55 (37.7)	
IntClustMemb 10	190 (84.1)	36 (15.9)	
Oestrogen Receptor (ER)			
Negative	334 (70.5)	140 (29.5)	90.060
Positive	685 (45.5)	821 (54.5)	**(<0.001)**
Progesterone Receptor (PR)			
Negative	563 (59.9)	377 (40.1)	50.902
Positive	456 (43.8)	584 (56.2)	**(<0.001)**
Human epidermal growth factor receptor 2 (HER2)			
Negative	890 (51.4)	843 (48.6)	0.065
Positive	129 (52.2)	118 (47.8)	(0.797)

*significant p-values are highlighted in bold

4.1 SLC22A17 protein expression

Full-face tissue sections were from Nottingham BC cohort and selected based on tumour grade, LVI status, and histological type, were used to evaluate the pattern of SLC22A17 protein expression prior to staining of TMAs. Full-face tissue sections showed weak SLC22A17 expression in normal glandular epithelium and DCIS (**Fig 14 A** & **C**). In contrast, SLC22A17 immunopositivity was observed in the cytoplasm of invasive cancer cells (**Fig 14 D**).

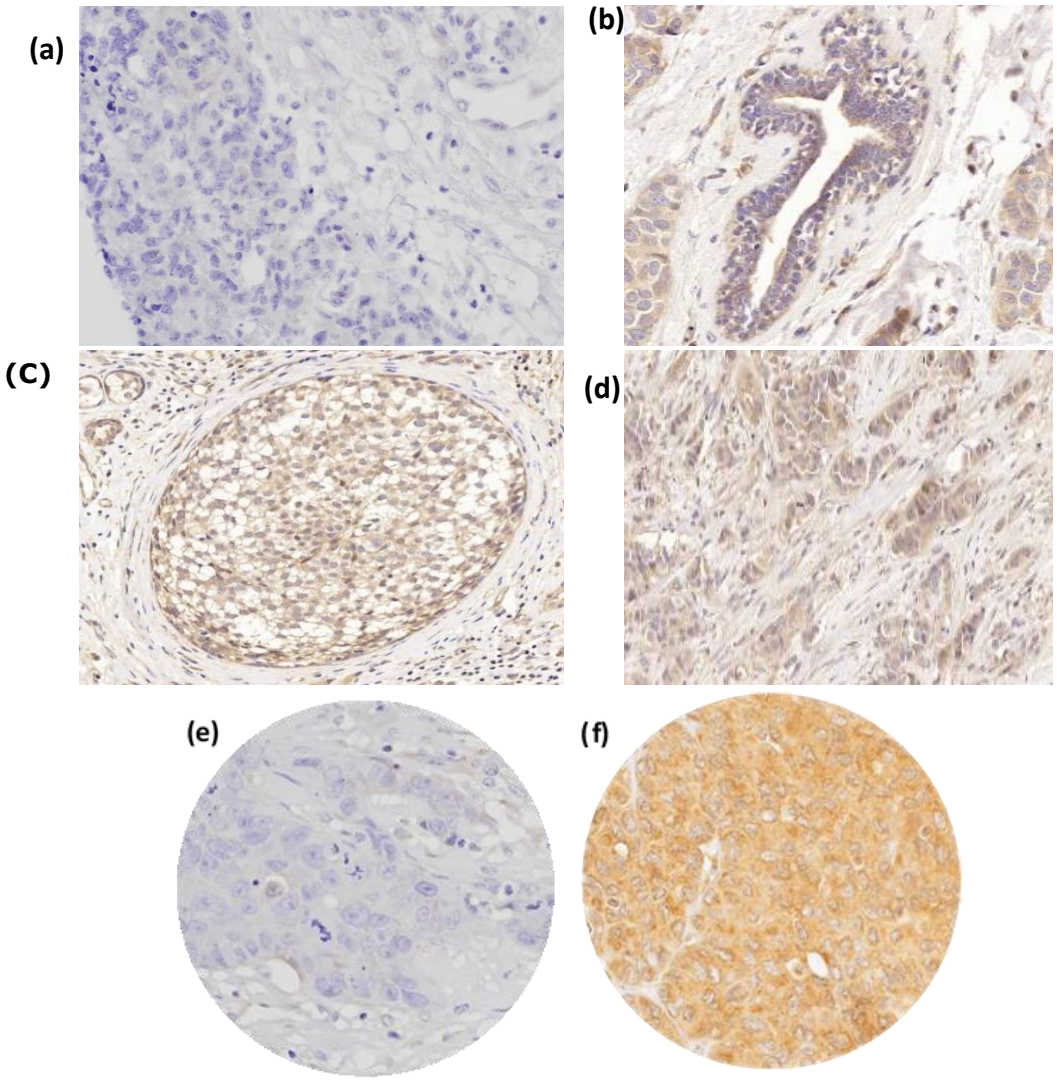


Fig. 14 Immunohistochemical expression of SLC22A17 in BC. (a) Negative control (b) TDLU (c) DCIS and (d) Invasive BC cells. SLC22A17 protein expression in breast cancer TMA cores (e) Negative expression while (f) showing high cytoplasmic expressions at 40X magnification respectively.

On TMAs (Nottingham series), a variable degree of SLC22A17 protein expression was observed as shown in **Fig. 14 (E-F).** Of the 645 informative cores, the median cut-off point for SLC22A17 was set at 50 where low expression was defined as H-score <50 (48%) and above 50 (52%) was considered high. High SLC22A17 protein expression was associated with LVI positivity (p= 0.025), high histological grade (p<0.001), high pleomorphism (p<0.001), mitotic figure (p<0.001) and poor Nottingham Prognostic Index (NPI; p<0.001) (**Table 10**).

Elevated SLC22A17 expression positively associated with Ki67 (p=0.008), p53 status (p<0.001) Proline-, glutamic acid- and leucine-rich protein 1 (PELP1) (p=0.005). Moreover, high SLC22A17 showed positive association with EMT markers such as N-cadherin (p=0.012) and TGF-β (p=0.036) (**Table 11**). However, when protein expression of SLC22A17 was correlated with LCN2 (cytoplasmic) expression we found out that there was a significant association between the two, although nuclear expression had a trend but showed no significance (p=0.269) respectively.

Table 10 Clinicopathological associations of SLC22A17 protein expression in the Nottingham BC series.

Clinico-pathological Criteria	***SLC22A17 Cytoplasmic Staining N (%)***		***χ2 & p Value***
	Low Expression (%)	***High Expression (%)***	
Age at Diagnosis			
<50	118 (52.9)	105 (47.1)	3.366
≥50	252 (60.4)	65 (39.6)	0.067
Histological Grade			
1	71 (76.3)	22 (23.7)	31.163
2	134 (65.4)	71 (34.6)	**<0.001**
3	166 (48.1)	179 (51.9)	
Pleomorphism			
1	10 (71.4)	4 (28.6)	19.152
2	145 (69.0)	65 (31.0)	**<0.001**
3	209 (51.2)	199 (48.8)	
Mitosis			
1	163 (74.8)	55 (25.2)	44.500
2	58 (56.9)	44 (43.1)	**<0.001**
3	143 (45.7)	170 (54.3)	
IHC subtypes			
Luminal B	118 (54.4)	99 (45.6)	
Luminal A	110 (69.6)	48 (30.4)	15.087
Triple Negative	59 (48.0)	64 (52.0)	**<0.002**
HER2+	43 (55.1)	35 (44.9)	
Histological Type			
Ductal	395 (68.9)	178 (31.1)	40.590
Lobular	39 (81.3)	9 (18.7)	**<0.001**
Medullary-like*	8 (47.1)	9 (52.9)	
Special type	18 (78.3)	5 (21.7)	
Stage			

I	240 (60.6)	156 (39.4)	7.600 **0.006**
II	103 (53.6)	89 (46.4)	
III	28 (50.9)	27 (49.1)	
Tumour Size			
≥ 2.0cm	202 (63.1)	118 (36.9)	3.672 0.348
< 2.0cm	167 (52.4)	152 (47.6)	
Nottingham Prognostic Index			
Good Prognostic Group	138 (74.6)	47 (25.4)	33.025 <**0.001**
Moderate Prognostic Group	182 (53.1)	161 (46.9)	
Poor Prognostic Group	49 (44.1)	62 (55.9)	

*significant p-values are highlighted in bold

4.2 Association of SLC22A17 with patient outcome

In the whole METABRIC cohort, *SLC22A17* mRNA showed a trend of poor patient outcome but it did not reach statistical significance. The KM plotter showed significant association with overall survival (n=1402; p<0.04) and DMFS (n=1747; p<0.002) suggesting that poor patient outcome and less time to distant metastasis. However, the BC gene-miner showed poor overall survival (n=4359; p<0.015). **Fig.15 A & B**]. Regarding BC metastasis high SLC22A17 protein levels were associated with development of distant metastasis to the bone (p=0.028), while there was no significant association with developing distant metastasis to lung or liver. Furthermore, results from the bc-GenExMiner v4.0 datasets showed that cases with high expression of *SLC22A17* mRNA had shorter overall survival rate (p=0.04; **Fig.15A**). Multivariate analysis of SLC22A17 protein expression was not an independent predictor for BCSS [p=0.973; HR 0.9 (95% CI 0.7-1.3); **Table 12**].

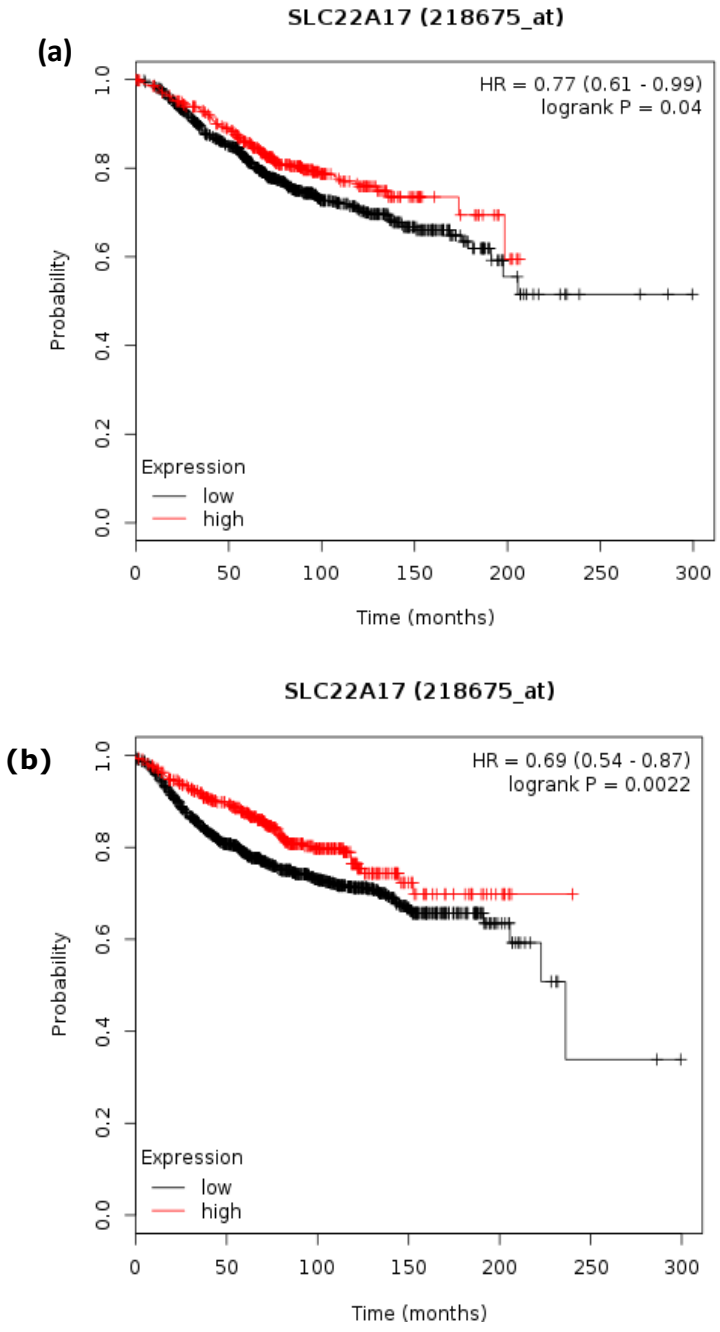


Fig. 15 Kaplan–Meier plots of SLC22A17 expression and breast cancer patient outcome. At transcriptomic level (a) KM plotter- Whole cohort overall survival (OS), (b) KM plotter- Whole cohort distant metastasis free survival (DMFS).

Table 11: Associations of SLC22A17 IHC expression and other BC related biomarkers

Clinico-pathological Criteria	***SLC22A17 Cytoplasmic Staining***		***X2 & p Value***
	Low expression N (%)	***High expression N (%)***	
Oestrogen Receptor (ER)			
Negative	90 (52.3)	82 (47.7)	3.013 0.083
Positive	283 (60.0)	189 (40.0)	
Progesterone (PR)			
Negative	146 (55.5)	117 (44.5)	0.982 0.322
Positive	220 (59.5)	150 (40.5)	
Human epidermal Growth Factor receptor 2 (HER2)			
Negative	322 (58.5)	228 (41.5)	0.328 0.567
Positive	43 (55.1)	35 (44.9)	
P53			
Negative	280 (63.3)	162 (36.7)	17.861 **<0.001**
Positive	87 (45.3)	105 (54.7)	
Epidermal Growth Factor Receptor (EGFR)			
Negative	308 (59.7)	208 (40.3)	5.141 0.233
Positive	58 (48.3)	62 (51.7)	
Ki67			
Negative	131 (64.9)	71 (35.1)	7.052 **0.008**
Positive	172 (53.1)	152 (46.9)	
Lymphovascular Invasion (LVI)			
Negative	220 (60.1)	146 (39.9)	5.025 **0.025**
Positive	90 (50.0)	90 (50.0)	
Phosphatidylinositol-4,5-bisphosphate 3-kinase, catalytic subunit alpha (PIK3CA)			
Negative	163 (55.3)	132 (44.7)	2.411 0.120
Positive	419 (50.0)	419 (50.0)	
Mucin 3			
Negative	17 (70.8)	7 (29.2)	5.296 **0.021**
Positive	181 (46.6)	207 (53.4)	
Transforming Growth Factor 1 (TGFβ1)			
Negative	121 (53.5)	105 (46.5)	4.399 **0.036**
Positive	132 (44.3)	166 (55.7)	

*Significant values are highlighted in bold

Table 12 – Multivariate analysis of SLC22A17 expression compared with tumour stage, grade, size for breast cancer-specific survival

Variable	Breast cancer-specific survival		
	Multivariate		
	HR	95%CI	p value
Whole cohort			
Stage	1.5	1.3-1.9	**<0.001**
Grade	1.6	1.2- 2.2	**<0.001**
Tumour size	1.1	0.8-1.6	0.343
SLC22A17	0.9	0.7-1.3	0.973

*Significant p values are highlighted in bold

4.3 DISCUSSION

Numerous studies investigated SLC22A17 and LCN2 functions in BC development, growth, and prognosis. Nonetheless, minimal research was done to show the mRNA and protein production of these markers and compare the results in an expanded population of patients with clinicopathological variables. Therefore, the purpose of this study was to evaluate if LCN2 and SLC22A17 were associated with tumour grade BC morphology, LVI, and patient outcome.

EMT plays a major role in breast cancer metastasis (81). In accordance with previous studies, we found that high *LCN2* mRNA expression was significantly associated with poor prognostic tumour characteristics such as high histological grade, younger age, HER2 + , and triple negative status (62, 82). Association between high histological grade and LCN2 indicates its role as a marker of poor prognosis in BC. High expression of LCN2 has also been linked with triple negative breast cancer (TNBC), which is another indication of its low prognostic status in BC. TNBC is an acute BC subtype linked to high mortality within five years of diagnosis (83). LCN2 is expressed through the modulation of NF-kB pathway by cells that are immune to chemotherapy (84). Through growth-factor and cytokine regulated signaling pathways such as PI3K / PTEN / Akt / mTORC1/GSK-3, Ras / Raf / Mek / ERK, and Jak / STAT, this pathway can be activated. Radiation and chemotherapy activate NF-kB by causing reactive oxygen species resulting in a corresponding transcription of LCN2 downstream (84).

A weak nuclear expression of LCN2 has been substantially associated with high N-cadherin and TWIST2 activity in the present study. N-cadherin, a transmembrane glycoprotein component, facilitates tumour-stroma interactions and induces cell motility, invasion, and metastasis (85, 86). TWIST2's over-expression facilitates breast cancer metastasis by

stimulating EMT and improving the cancer-like stem cell self-renewal system (87). Previous studies showed that LCN2 controls the Ras pathway behavior and regulates cell proliferation and EMT (88, 89). The low nuclear expression of LCN2 has been significantly associated in the present study with the positive expression of basal markers like CK5/6 and EGFR. Several studies suggested a strong correlation between basal cytokeratin expression and cell proliferation (6, 88). EGFR is not a basal-like unique marker such as CK5, but is expressed in the basal-like form and greatly assists in this sort of immunohistochemical identification (90, 91).

The Nottingham Prognostic Index + is based on the biological class evaluation in combination with established clinicopathological prognostic variables, including CK5/6 and EGFR. This index enhances patient outcome stratification for invasive breast cancer (92). Previously, it has been suggested to use molecular-targeted treatment for EGFR-positive breast cancer (e.g., neratinib (93), pertuzumab (94), and lapatinib (95)). LCN2 association with basal-like breast cancers can define a subset of patients that are more likely to benefit from treatment with these agents

LCN2's reduced nuclear expression was strongly associated with high tumour grade, HER2 positivity, and weak patient outcome. Notably, other research has shown that LCN2's elevated cytoplasmic expression is associated with reduced disease-free survival in patients with invasive breast cancer (63, 96).

The cytoplasmic expression of LCN2 was correlated with lymph node metastasis in the present study. The tumour microenvironment regulates the cancer cell LCN2-autocrine pathway by stress-dependent endoplasmic reticulum and reticulum-independent mechanisms (97). After release into the extracellular compartment, LCN2 drives iron sequestration and internalization through receptors established to promote cell survival and EMT (97, 98). Such factors may be responsible for the clinicopathologically important difference between the nuclear expression of LCN2 and the cytoplasmic expression.

Some previous studies showed the potential value of EMT-related biomarkers as prognostic factors and proposed their effectiveness in predicting the reaction to chemotherapy from invasive breast cancer. Over the last decade there have been paucity of information exploring the role of SLC22A17 as a potential prognostic marker but SLC22A17 was reported to be a predictor of patient survival for various cancers including ovarian cancer, glioma and colorectal cancer (99-101)**.** Transcriptomic results revealed that high expression was associated with good prognostic characteristics whereas proteomic results showed significant poor prognostic characteristics.

To our knowledge, this is one of the few studies to define the prognostic role of SLC22A17 in BC using large clinical data sets with long-term follow up (102). Our study showed that high mRNA expression of *SLC22A17* showed good prognosis and clinically relevant subgroups like ER/PR positive and HER2 negative tumours. It was also strongly associated with clinicopathological variables with good prognosis including low grade and Good Nottingham prognostic index, highlighting a potential tumour suppressive role in BC. Although these were not consistent with SLC22A17 protein expression, except for HER2 which could be attributed to the discrepancy of post-transcriptional/translational modifications and proteins may differ substantially in their *in-vivo* stages (103, 104). Further confirmation in larger cohorts of both HER2-positive and HER2-negative cases is warranted to determine the exact role of SLC22A17 in HER2-positive BC. Within the METABRIC integrative clusters, high *SLC22A17* mRNA expression was associated with clusters 3 (Luminal A) IC which is good prognosis and provides further support for potential hormonal therapy. Luminal A is associated with good clinical outcome and non-resistant to chemotherapy (105).

However, high SLC22A17 protein expression was significantly associated poor performing histological subtypes such as medullary-like tumours and also showed a positive correlation with EMT genes (TGFβ1, PELP) which could also have its role in tumour progression. TGFβ1 acts as an oncogene in tumour progression by inducing cell invasion, dissemination to distant sites and angiogenesis (106). High expression Mucin 3 (MUC3) correlates with poor prognosis, MUC3 expression was detected in 91% of cases and its expression was associated with increased local recurrence, and lymph node stage (107). Previous study by Emad Rakha et. al., suggested that the elevated expression of MUC3 shown to be associated with high grade, poorer NPI and ER negative status (107). Moreover, metastasis to bone in our study suggests the involvement of tumour spread and LVI plays a major role in the metastatic process, placing patients at the highest risk for early metastasis and death (108).

Our results suggest that increased SLC22A17 protein expression promotes BC progression. This is in concordance with previous reports indicating that high SLC22A17 protein expression facilitates metastasis in different types of cancer which further reinforces its role as a oncogene (109). High SLC22A17 expression in BC is associated with favorable prognostic parameters. SLC22A17 appears to play a role in inhibiting tumour cells proliferation, invasion and metastasis.

Few studies have suggested that there is an inverse relation between LCN2 and SLC22A17, wherein apo-LCN2 plays an important role in antibacterial innate immunity (110), and have demonstrated that apo-LCN2 induces apoptosis in LCN2-R expressing cells (78, 111), whereas holo-LCN2 is anti-apoptotic and may even promote cell proliferation, e.g. in cancer cells (112). *Devireddy et al., 2005* suggested that apoptosis is initiated by reduction in intracellular iron via endosome recycling pathway as like several other endocytosed receptor-ligand complexes, also proved that forced expression of SLC22A17 induces apoptosis in BCR-ABL-transformed mouse cell lines, indicating that downregulation of SLC22A17 is critical for survival of tumour (78). Further functional studies to decipher the role of SLC22A17/LCN2 and its mechanism of action as a tumour suppressor is required.

The difference in mRNA and protein analysis is may be due to posttranslational modification (103). Over last two decades few studies have suggested that the mRNA to protein ratio is not directly proportional since there are many factors involved in post-translation. The central dogma is very well understood but the post-transcriptional and post-translational modification is still ongoing. The mRNA would undergo lot of changes like intron splicing or can correlate to the variation of mRNA to protein concentration which arises from same genes across different individuals or conditions.

CHAPTER 5

CD276 as a Prognostic Biomarker in invasive Breast cancer

Purpose: CD276/B7-H3 is part of the B7 superfamily of immune regulatory ligands and plays an important role in regulating T cells in the adaptive immune response of co-inhibitory / stimulatory factors. However, the extent to whichCD276 directly affects mechanisms of tumour immune evasion remains unclear, especially in breast cancer patients.

Methods: *CD276* mRNA and protein expression were assessed in the METABRIC cohort and utilizing a large well-characterised BC cohort using immunohistochemistry. Association with well-established clinicopathological characteristics, BC-related biomarkers and patient outcome were investigated.

Results: High expression of *CD276* mRNA levels were associated with characteristics of poor prognosis such as high tumour grade, poor Nottingham Prognostic Index (NPI), and hormone receptor negativity (all; $p<0.001$). High CD276 protein expression was positively associated with high histological grade, medullary tumour type ($p<0.001$) and poor NPI ($p<0.001$). Multivariate analysis revealed that CD276 protein expression was an independent predictor for BC specific survival.

Conclusion: CD276 expression was associated with poor breast cancer prognosis. The expressions were correlated suggesting that expression of CD276, regardless of any biomarker, plays an independent role in tumour immune evasion.

5.1 Introduction

CD276 [CD276] is part of the B7 family's most significant co-inhibitory molecule and can adjust the immune response of T-cells by inhibiting activation and proliferation of T-cells (113). There was no clear identification of the receptor for CD276, so the mechanisms underlying the effects of CD276 on the immune system remain unclear, especially in terms of targeting T cells for suppression. CD276 protein expression was detected in several tumour cell lines along with human lymphoma (114), ovary (115), lung (116), stomach (117), prostate (118) and pancreas malignancies (119), and colorectal carcinoma (120). It has been reported that CD276 is a type-1 transmembrane protein (121). Two possible receptors on T cells for CD276 have been postulated, one giving rise to the activation of signals, while the other exerts inhibitory signals (122). In mice, CD276 is constitutively expressed on competent antigen-presenting cells (APCs) and upregulated with lipopolysaccharide (LPS) activation on dendritic cells [DCs] (123). CD276 co-inhibitory function was described using the fusion protein CD276-Ig, where it decreased proliferation, and the production of T-cells activated with anti-CD3 interleukin-2 (IL-2) and interferon-π (IFN-π) (124). In humans, during T-cell activation, CD276 was first identified as a positive co-stimulator in DCs that enhanced the development of Interferon (IFN-π) (125).

However, more recently, during T-cell activation, a study showed a potent inhibition of the production of IFN-α, IL-2, IL-10, and IL-13 (122). Until now, the CD276 receptor has not been characterised. CD276 expression has been identified as a poor prognostic factor in cancer patients. For example, CD276 expression is associated with advanced tumour stage, tumour size, and lymph node metastasis in patients with non-small cell lung cancer (126). The protein expression of CD276 is elevated in sarcoma and assists in tumour progression (127) but still , the underlying mechanism of CD276 action in cancer is ill-defined.

CD276 was expressed in human tumour microenvironment and inhibition of CD276 controlled tumour growth and anti-tumour immunity depended on cells of CD8 + T and natural killer (124) cells. In comparison, CD276 specifically prevented NK cell activation (124).

In the current study we examined the function of CD276 using well characterised breast cancer cohorts. Therefore, CD276 acts as a crucial negative regulator of tumour immunity and could be aimed in cancer immunotherapy in general.

5.2 Materials and Methods

5.2.1 Transcriptomic evaluation

The Molecular Taxonomy of Breast Cancer International Consortium [METABRIC] [19], comprising 1980 early invasive breast cancer, was used to explore and analyses the prognostic value of *CD276* mRNA. The Kaplan–Meier Plotter-[Breast Cancer] [KM-Plotter; n=1967] online dataset (31), and Breast Cancer Gene Expression Miner v4.0 (30) were used to validate the prognostic significance of *CD276* mRNA. For CD276 protein expression, we investigated the Nottingham Breast Cancer Primary Series (32), as previously described in section 2.1.

5.2.2 Immunohistochemistry [IHC]

Specificity of CD276 [rabbit monoclonal antibody; 227670, abcam, UK] was verified by western blot analysis of whole cell lysates of MCF-7, SKBr3 and MDA-MB-157 cell lines [obtained from the American Type Culture Collection; Rockville, MD, USA] using 1:750 dilution of the primary antibody, and fluorescent secondary antibodies at [1:15000] [IR Dye 800CW donkey anti-rabbit and 680RD donkey anti-mouse, LI-COR Biosciences, UK] as previously described (sections 2.2). The specificity of the antibody was validated by the presence of a single specific band at the predicted size [55 kDa; Figure 15].

5.2.4 Statistical Analysis

This study was conducted according to recommendations for tumour marker prognostic studies [REMARK] criteria (128). Statistical analysis was performed using SPSS 24.0 [Chicago, IL, USA]. The interclass correlation coefficient [ICC] test was used to assess the concordance rate of the CD276 scoring between both observers. Associations between the CD276 expression and the clinical data for the Nottingham Breast Cancer Primary Series were assessed by performing Pearson chi square analyses. Univariate survival analysis was performed using Kaplan-Meier curves, using a log rank test to determine statistical significance, and multivariate analysis was performed using the Cox regression method. Data was determined to be statistically significant if $p<0.05$.

5.2.5 Scoring

The TMA (Nottingham series) slides produced from immunohistochemistry were analysed using the method previously described (Section 2.2).

CD276 showed both cytoplasmic and membrane immuno-reactivity. TMA cores with less than <15% tumour cells, or showed Ductal Carcinoma in Situ (DCIS) were excluded. All slides were scored by the same observer, Pavan and compared against a second, more experienced observer, Chitra Joseph or Mansour Alsaleem, where a consensus was reached.

5.3 RESULTS

Antibody Validation

5.3.1 Western Blot (WB)

Antibody was validated by Western Blotting as described earlier, CD276 expression in MCF7, SKBr3, MDA-MB-231 and HeLa (Figure 8) breast cancer cell lines using rabbit monoclonal antibody against human CD276 [227670, abcam (UK)]. Green and red bands represent CD276 and Beta-Actin (house-keeping), respectively. The anti-CD276 showed a band at 55 KDa and the anti-actin antibody (**Fig. 16**) showed a single band at a molecular weight of 44kDa, and the single band indicates specificity of the antibody.

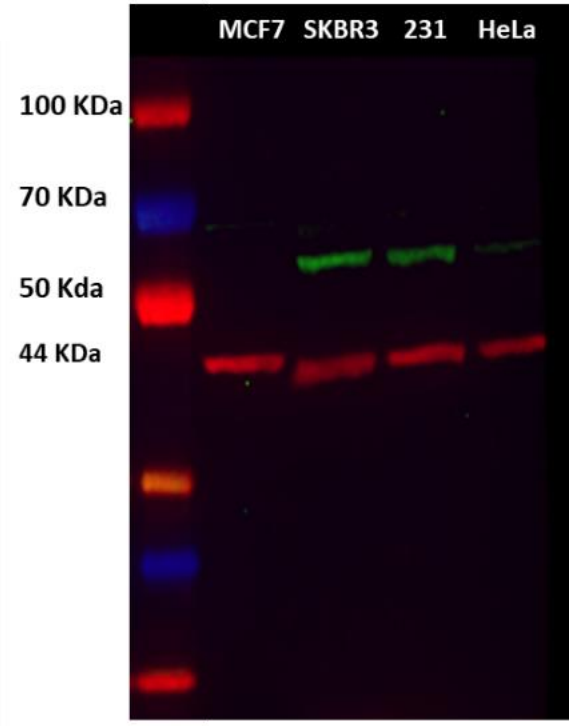


Fig. 16 Western blot and immunohistochemical expression of CD276 in BC. Western blotting results for CD276 expression in MCF7, SKBr3, MDA-MB-231 and HeLa using rabbit monoclonal antibody against human CD276 [227670, abcam (UK)]. Green and red bands represent CD276 and Beta-Actin (house-keeping), respectively.

5.3.2 CD276 genomic profiling

High expression of *CD276* mRNA was positively associated with high histological status (p<0.001), ER-/PR- (p<0.001), and HER2+ (p<0.001). When BC was classified using intrinsic [PAM50] subtypes, high expression was associated with Basal and HER2 positive status [p<0.001] similarly, elevated CD276 mRNA expression was associated with IC cluster 5 [HER2 enriched] associated with poor prognosis and also showed high association with IC clusters 6 (ER+) respectively (p<0.001;**Table 13**), also high expression was associated with Triple-negative status (p<0.001; **Table 13**).

Using BC Gene-Expression Miner v4.0, high expression of CD276 mRNA was correlated with ER- and PR- status (n=2024; p=0.004), high tumour grade (n=1639; p=0.0075) and BC Gene-Miner revealed a positive association between CD276 mRNA and PAM50 subtypes (basal and triple-negative; n=520; p=0.006) in agreement with METABRIC.

Table 13 Associations between CD276 mRNA expression and clinicopathological variables in the METABRIC cohort

Clinico-pathological Criteria	***CD276 mRNA expression***		***χ2 & p Value***
	Low Expression N (%)	***High Expression N (%)***	
Age at Diagnosis			
≤50	190 (45.3)	229 (54.7)	5.465 (**0.0193**)
>50	797 (51.8)	771 (48.2)	
Tumour Size (cm)			
≤2.0	421 (49.8)	425 (50.2)	0.923 (0.762)
>2.0	551 (50.5)	541 (49.5)	
Histological Grade			
1	99 (58.9)	69 (41.1)	13.672 **(<0.001)**
2	404 (52.9)	359 (47.1)	
3	434 (46.1)	507 (53.9)	
Tumour Type			
Ductal	817 (48.6)	863 (51.4)	23.805 **(<0.001)**
Lobular	98 (67.1)	48 (32.9)	
Medullary-like	17 (53.1)	15 (46.9)	
Special type	30 (65.2)	16 (34.8)	
Miscellaneous	8 (66.7)	8 (33.3)	
Nottingham Prognostic Index (NPI)			
Good Prognostic Group	367 (54.6)	305 (45.4)	7.290 **(0.026)**
Moderate Prognostic Group	524 (48.1)	566 (51.9)	
Poor Prognostic Group	96 (49.0)	100 (51.0)	
PAM50 subtype			
Luminal A	394 (55.6)	314 (44.4)	47.893 **(<0.001)**
Luminal B	241 (49.9)	242 (50.1)	
Basal	94 (39.7)	143 (60.3)	
Her2	129 (39.4)	198 (60.6)	
Normal like	125 (63.5)	72 (36.5)	
IntClustMemb			
IntClustMemb 1	64 (47.1)	72 (52.9)	60.264 **(<0.001)**
IntClustMemb 2	40 (55.6)	32 (44.4)	
IntClustMemb 3	167 (58.0)	121 (42.0)	
IntClustMemb 4	183 (53.8)	157 (46.2)	
IntClustMemb 5	61 (32.4)	127 (67.6)	
IntClustMemb 6	35 (41.7)	49 (58.3)	

IntClustMemb 7	98 (52.1)	90 (47.9)	
IntClustMemb 8	178 (61.0)	114 (39.0)	
IntClustMemb 9	72 (49.7)	73 (50.3)	
IntClustMemb 10	89 (39.6)	136 (60.4)	
Oestrogen Receptor (ER)			
Negative	186 (39.5)	285 (60.5)	29.574 **(<0.001)**
Positive	801 (53.9)	686 (46.1)	
Progesterone Receptor (PR)			
Negative	438 (46.9)	495 (53.1)	8.551 **(0.003)**
Positive	549 (53.6)	476 (46.4)	
Human epidermal growth factor receptor 2 (HER2)			
Negative	898 (52.4)	815 (47.6)	22.215 (**<0.001**)
Positive	89 (36.3)	156 (63.7)	
Triple Negative (TPN) status			
Negative	863 (52.4)	783 (47.6)	16.887 **(<0.001)**
Positive	124 (39.7)	188 (60.3)	

*significant values are highlighted in bold.

5.3.3 CD276 protein expression

Full-face BC tissue from Nottingham series sections selected based on tumour grade, LVI status, and histological type, were used to evaluate the pattern of CD276 protein expression prior to staining of TMAs. Full-face tissue sections showed weak CD276 expression in normal glandular epithelium and TDLU (**Fig. 17A & 17D**). In contrast, CD276 immunopositivity was observed in the membrane of invasive cancer cells (**Fig. 17B**). On TMAs, a variable degree of CD276 protein expression was observed as shown in (**Fig. 17 D & E)**.

The median cut-off point for CD276 was set at 50, out of the 385 cores where low expression was described as H-score <50 (49%) and >50 (51%).

High CD276 protein expression was associated with high histological grade ($p<0.001$), high pleomorphism ($p<0.001$), mitotic figure ($p<0.001$) and poor Nottingham Prognostic Index (NPI; $p<0.001$) (**Table 14**). CD276 protein was also associated with positive ER, PR and HER2 status ($p=0.013$; $p=0.010$ and $p=0.021$ respectively), P53 association was also seen ($p=0.002$) along with pAKT ($p<0.001$) (**Table 15**).

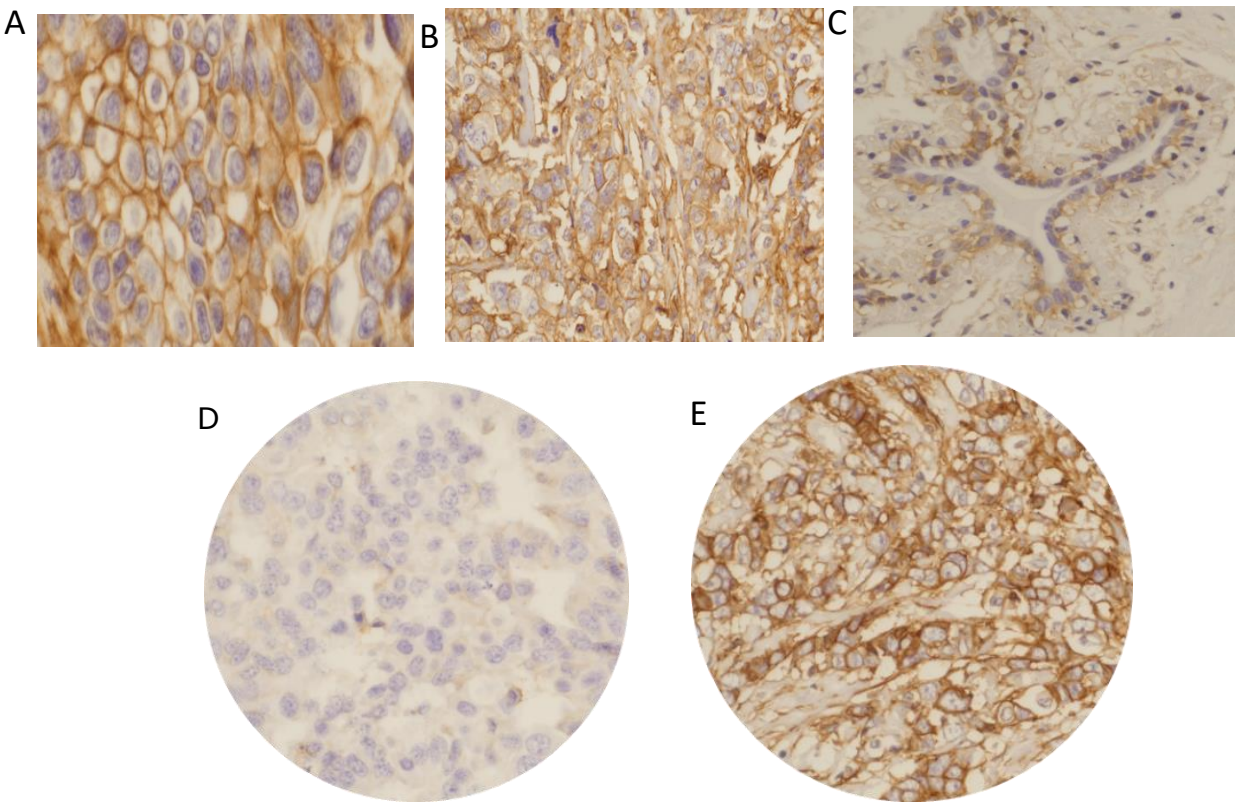


Fig. 17 IHC image of CD276: In Full Face A) Tumour B) Invasive C) TDLU. CD276 expression in membrane in TMA cores D) Low expression E) High Expression.

Table 14: Associations between CD276 protein expression and clinicopathological parameters

Clinico-pathological Criteria	***CD276 membrane staining N (%)***		***χ2 & p Value***
	Low Expression	***High Expression***	
Age at Diagnosis			
<50	112 (62.2)	68 (37.8)	1.605 (0.205)
≥50	203 (67.9)	96 (32.1)	
Histological Grade			
1	53 (85.5)	9 (14.5)	31.629 **<0.001**
2	115 (77.2)	34 (22.8)	
3	151 (55.7)	120 (44.3)	
Pleomorphism			
1	4 (100)	0 (0)	26.104 **<0.001**
2	132 (81.0)	31 (19.0)	
3	181 (58.6)	128 (41.4)	
Mitosis			
1	123 (83.7)	24 (16.3)	34.323 **<0.001**
2	59 (70.2)	25 (29.8)	
3	135 (55.1)	110 (44.9)	
IHC subtypes			
Luminal B	119 (67.2)	58 (32.8)	

Luminal A	84 (81.6)	19 (18.4)	19.004 **<0.001**
Triple Negative	52 (57.1)	39 (42.9)	
HER2+	33 (53.2)	29 (46.8)	
Stage			
I	184 (65.7)	96 (34.3)	2.057 0.561
II	103 (66.5)	52 (33.5)	
III	32 (68.1)	15 (31.9)	
Tumour Size			
≥ 2.0cm	161 (70.6)	67 (29.4)	4.312 **0.038**
< 2.0cm	154 (61.6)	96 (38.4)	
Nottingham Prognostic Index			
Good Prognostic Group	95 (82.6)	20 (17.4)	18.906 <**0.001**
Moderate Prognostic Group	160 (60.2)	106 (39.8)	
Poor Prognostic Group	60 (61.9)	37 (38.1)	

*Significant values are highlighted in bold

5.3.4 Association of CD276 with patient outcome

CD276 mRNA has shown a trend of poor patient outcome throughout the METABRIC cohort but did not reach a statistical significance, but CD276 protein expression showed poor patient outcome (n=453; p=0.009) (**Fig.18A**). The KM plotter showed a significant correlation with overall survival (n=626; p=0.048) (**Fig.18B**) and DMFS (n=664; p=0.0016) (**Fig.18D**) indicating low patient overall survival and was also associated with poor RFS (n=1764; P=0.035) (**Fig.18C**). In comparison, evidence from the bc-GenExMiner v4.0 datasets found that cases with elevated *CD276* mRNA expression had a shorter overall survival rate [n=614; p=0.0072; **Fig.19A**), ER- and PR- (n=2127; p<0.001 and n=1534; p=0.004 respectively) (**Fig. 19 B & C**). Also showed correlation with positive Basal/TNBC status and higher grade (n=186; p=0.006 and n=767; p=0.007). Multivariate analysis demonstrated that CD276 as an independent predictor of BC-specific survival (10 year) [p=0.017; HR 1.0 (95% CI 1.0-1.5); **Table 16**] and higher probability of distant metastasis.

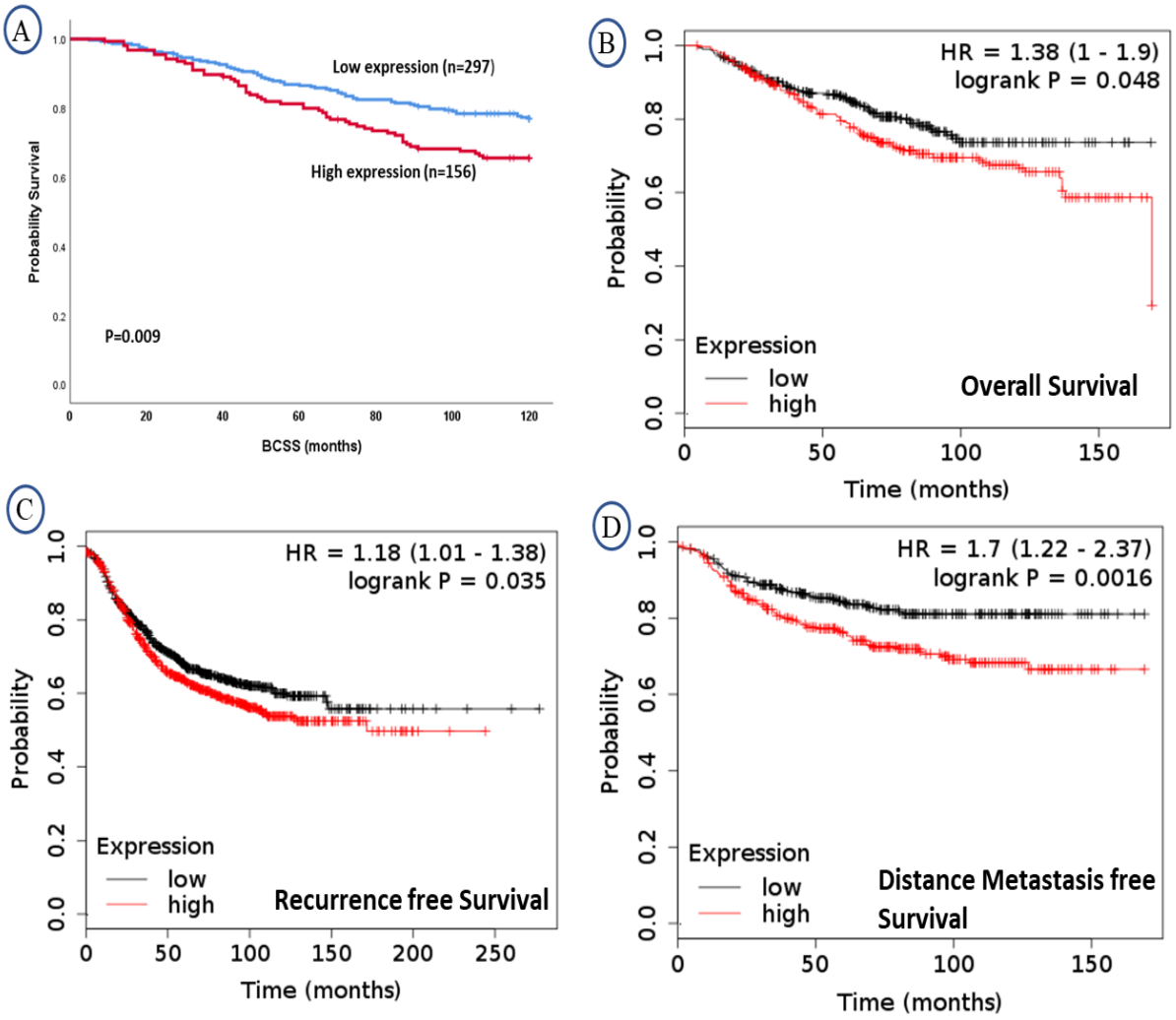


Fig. 18 Kaplan–Meier plots of CD276 expression and breast cancer patient outcome. At transcriptomic level (A) METABRIC cohort CD276 (B) KM plotter- Whole cohort overall survival (C) KM plotter- Whole cohort Recurrence free survival (D) KM plotter- Whole cohort distant metastasis free survival.

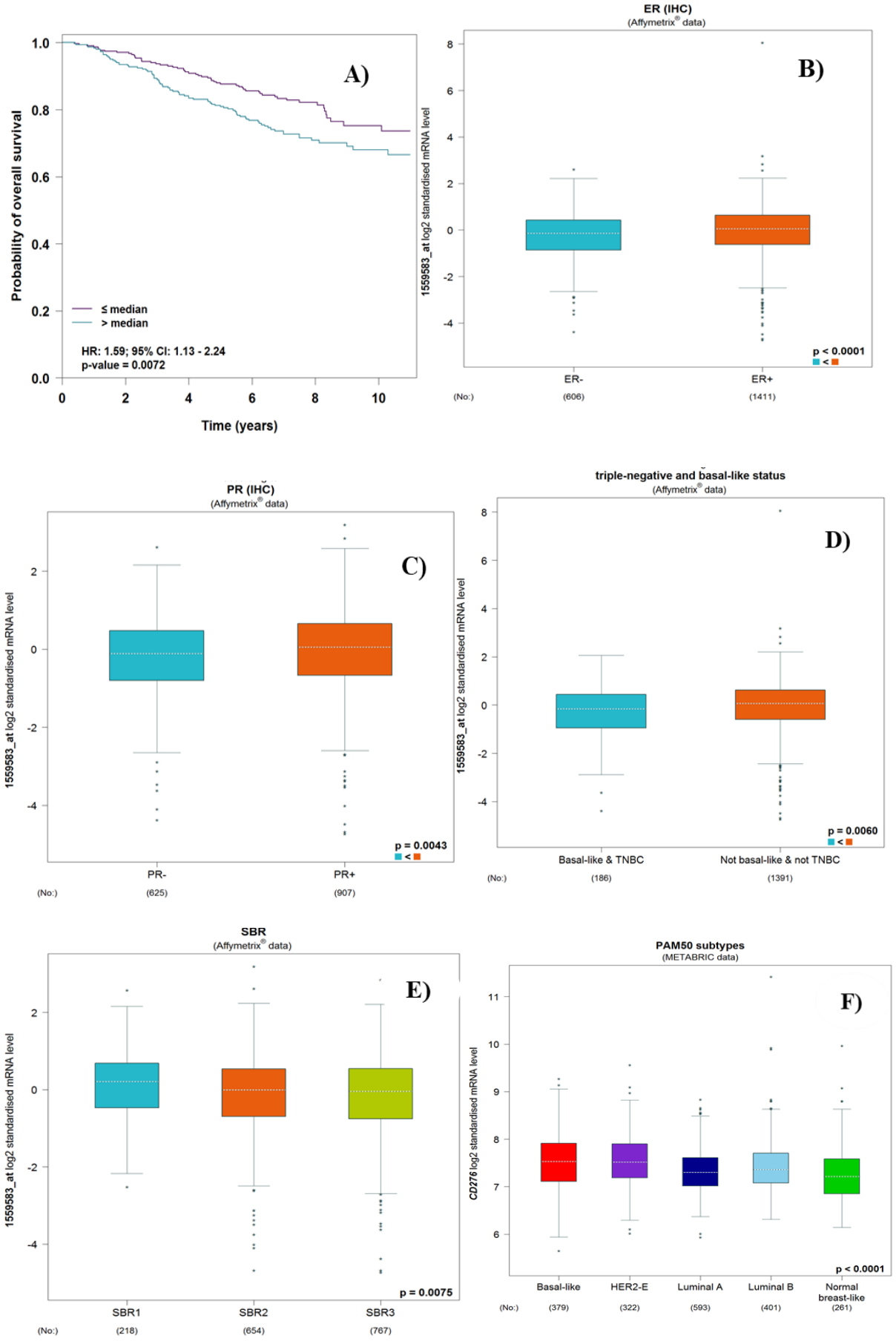


Fig. 19 Kaplan–Meier plots of CD276 expression and breast cancer patient outcome. At transcriptomic level (a) METABRIC cohort CD276 – Overall survival b) Breast Cancer Gene-Expression Miner v4.0 Box plots - ER cases (c) BC gene miner PR cases (d) BC gene-miner TNBC (e) BC-gene miner-Histological grade (f) PAM50 subtypes METABRIC.

Table 15: **Associations of CD276 IHC expression and other BC related biomarkers within the Nottingham BC series.**

Clinico-pathological Criteria	***CD276 membrane staining***		***χ2 & p Value***
	Low expression N (%)	***High expression N (%)***	
Estrogen Receptor (ER)			
Negative	74 (57.4)	55 (42.6)	6.120 **0.013**
Positive	245 (69.4)	108 (30.6)	
Progesterone (PR)			
Negative	111 (59.0)	77 (41.0)	6.635 **0.010**
Positive	203 (70.5)	85 (29.5)	
Human epidermal Growth Factor receptor 2 (HER2)			
Negative	276 (68.1)	129 (31.9)	5.348 **0.021**
Positive	33 (53.2)	29 (46.8)	
P53			
Negative	233 (70.8)	96 (29.2)	9.724 **0.002**
Positive	82 (56.2)	64 (43.8)	
Epidermal Growth Factor Receptor (EGFR)			
Negative	308 (59.7)	208 (40.3)	5.141 0.233
Positive	58 (48.3)	62 (51.7)	
Ki67			
Negative	97 (70.8)	40 (29.2)	2.168 0.141
Positive	163 (63.4)	94 (36.6)	
Lymphovascular Invasion (LVI)			
Negative	189 (69.7)	82 (30.3)	2.711 0.100
Positive	87 (61.7)	54 (38.3)	
CK5/6			
Negative	223 (66.4)	113 (33.6)	0.16 0.899
Positive	43 (67.2)	21 (32.8)	
Protein Kinase B (AKT)			
Negative	39 (48.8)	41 (51.2)	13.018 **<0.001**
Positive	198 (70.5)	83 (29.5)	
Cluster of Differentiation 3 (CD3)			
Negative	171 (72.5)	65 (27.5)	8.535 **0.003**
Positive	99 (58.6)	70 (41.4)	
Cluster of Differentiation-68 (CD68)			
Negative	202 (71.9)	79 (28.1)	18.651 **0.001**
Positive	48 (48)	52 (52)	
Cluster of Differentiation-8 (CD8)			
Negative	181 (70.2)	77 (29.8)	10.672 **0.001**
Positive	67 (53.2)	59 (46.8)	

*****Significant values are highlighted in bold.

Table 16 Multivariate analysis of CD276 expression compared with tumour stage, grade, size, CD8, CD68, CD3 status for breast cancer-specific survival.

Variable	Breast cancer-specific survival		
	Multivariate		
	HR	95%CI	p value
Whole cohort			
Stage	**2.7**	**1.6-2.0**	**<0.001**
Grade	**2.3**	**1.6-2.1**	**0.003**
Tumour size	1.6	1.3-1.8	0.212
CD276-Membrane	**1.0**	**1.0-1.5**	**0.017**
CD71	1.1	0.4-0.8	0.651
CD8	1.0	0.8-1.3	0.784
CD68	1.1	1.1-1.7	0.587
CD3	0.7	0.8-1.3	0.460

*significant values are highlighted in bold

5.4 Discussion

This study has demonstrated that high expression of CD276 in BC is associated with poor prognostic characters and poor BC patient's outcome, over the last decade (129) there have been very few studies looking into the role of CD276 as a potential prognostic marker and predictor of patient survival for various cancers including lung cancer (130), pancreatic cancer (130), renal cell carcinomas (131). CD276 has been reported as a negative regulator that preferentially downregulates T helper type 1-mediated immune responses (121). CD276 is found on many different types of tissues and cells. Non-lymphoid and lymphoid organs such as liver, heart, prostate, spleen, and thymus are ubiquitously found at the mRNA level (132). Given the broad expression of mRNA, protein expression is constrained at a steady state, indicating an important post-transcription control mechanism to be present. Additionally, CD276 is also detected on natural killer cells, B cells, and a minor population of T cells following PMA/ionomycin stimulation (133).

CD276 being reported to down-regulate and avoid host immunity, though, its clinical and functional importance is still uncertain (134). *In vivo* studies suggested that B7–H3 was involved in inhibitory immunoregulation in non-small-cell lung and prostate cancers (118), patients with strong expression of CD276 in prostate cancer had a worse prognosis compared to patients with low expression of CD276 (118).

In our current study high expression of *CD276* mRNA was significantly associated with poor prognostic characteristics, including high histological grade, younger age, poor NPI, ER−/PgR− tumours and histological subtypes of poor prognosis. This is in agreement with studies of other cancer sites. For example, CD276 is significantly associated with tumour aggressiveness and poor prognosis in lung cancer (135), gastric (136) and renal cell carcinomas (131).

CD276 mRNA overexpression was significantly associated with TNBC as previously documented (137). Within the METABRIC Integrative Clusters, high *CD276* mRNA expression was associated with clusters 10 (TNBC/basal-like) and cluster 5 (HER2 enriched) IC, which provides further support for a potential role in TNBC with HER2+. TNBC is synonymous with chemotherapy resistance and strongly linked with worse clinical results, which means that CD276 plays a role in tumourigenic processes and could be a predictor for weak TNBC prognosis.

High CD276 protein expression was associated with p53 and pAKT suggesting the involvement of cell growth, proliferation and survival. An overactive PI3K / AKT / mTOR pathway can either be triggered by loss of tumour suppressor gene activity (phosphatase and tensin homolog (PTEN), p53) or benefit of PI3 K function, resulting in increased glucose uptake, glycolytic flux, and a change from mitochondrial respiration to lactate development. Inhibitors of proteins in the AKT/mTOR pathway, including everolimus, are currently being tested in the clinic as new therapeutic agents in breast cancer patients (137).

The expression of CD276 did not alter the activation of the AKT/mTOR pathway, but the high levels of expression of CD276 in tumour cells increased the cell survival and glycolysis. The presence of API-2 or everolimus inhibitors did not alter the expression of CD276, but their inhibitory effect on both cell growth and glycolysis depended on the levels of endogenous expression of CD276.

Together, these results suggest that putative different mechanisms would act with each other by inhibiting API-2 and everolimus along with knockdown of CD276 (138). Further recognition and comprehension of the CD276 signaling pathway and possible receptor(s) in breast cancer is required which offers new therapeutic strategies.

CHAPTER 6

Leukocyte associated immunoglobulin like receptor-1 confers poor prognosis in Invasive Breast Carcinoma

6.1 Background

Leukocyte-associated immunoglobulin-like receptor-1 (LAIR-1/CD305) is a transmembrane glycoprotein and a member of the superfamily of immunoglobulin, expressed on most immune cells. LAIR-1 is an inhibitory receptor that is involved in immune response down-regulation and cell differentiation (139-141). The immune system plays an important role in actions and consequence of breast cancer (BC). Tumour-infiltrating lymphocytes (TILs) are correlated with outcome in BC and their presence before chemotherapy is a healthy phenomenon (142) however lymphocytes secreteIL-6 and IL8 which in effect stimulate PI3K / AKT, STAT3 signaling and create a positive feedback loop between the tumour cells and the immune microenvironment. Most TILs with prominent CD8 + T cells are linked to better prognosis (143) whereas Foxp3 + or PD-1+ T cells infiltration mediates worse prognosis (144). Additionally, multiple transmembrane and extracellular matrix collagens, which are ligands of high affinity for LAIR-1 (145), have been implicated as metastasis avenues in BC [8]. The expression of LAIR-1 in both tumour cells and immune cells indicates a regulatory role for LAIR-1 in tumour biology, but further studies are required; the biological role of LAIR-1 in BC has yet to be clarified.

6.2 Methods

Specificity of LAIR-1 antibody was validated by western blotting prior to immunohistochemistry (IHC). Full-face BC tissue sections and TMAs (Nottingham series) were immunoassayed using Novolink Max Polymer Detection system (Leica, Newcastle, UK) as previously described (146). Immunoreactivity of LAIR-1 cytoplasmic expression in invasive tumour cells were individually assessed using the histochemical score (H-score) and its association with clinico-pathological paraments and patient outcome were evaluated.

Immunohistochemistry

Specificity of LAIR-1 [rabbit monoclonal antibody; NOVUS, UK] was verified by western blot analysis using 1:500 dilution of the primary antibody, and fluorescent secondary antibodies at [1:15000] [IR Dye 800CW donkey anti-rabbit and 680RD donkey anti-mouse, LI-COR Biosciences, UK] as previously described (section 2.2).

6.3 Results

Antibody validation

6.3.1 Western Blot

Antibody was validated by Western Blotting as described earlier (section 2.3), LAIR-1 expression in MCF7 and HeLa (**Fig. 20**) breast cancer cell lines using rabbit monoclonal antibody against human LAIR-1 [NBP1-84590, polyclonal rabbit, NOVUS (UK)]. Green and red bands represent LAIR-1 and Beta-Actin (house-keeping), respectively. The anti-LAIR-1 showed a band at 70kDa and the anti-actin antibody showed a single band at a molecular weight of 42kDa, and the single band indicates specificity of the antibody.

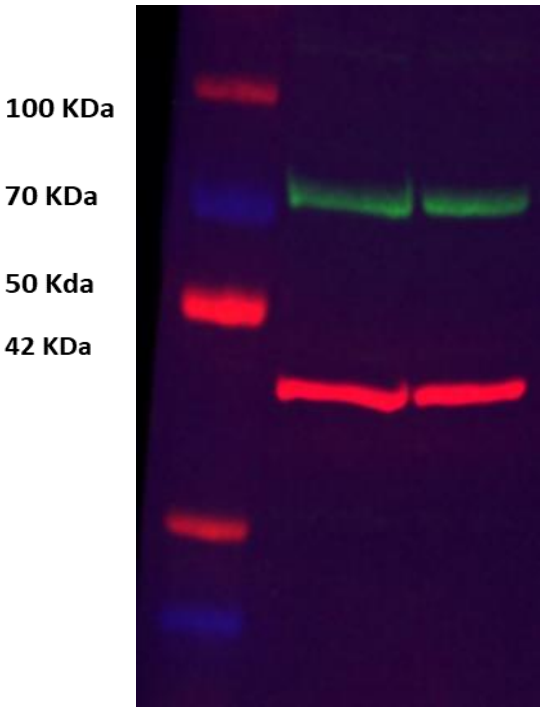


Fig. 20 Western blot image of LAIR-1. Green band LAIR-1 at 70kDa and Red band beta-actin at 42 kDa.

6.4 LAIR-1 genomic profiling

In the large METABRIC BC cohort (n=1980), we evaluated the *LAIR-1* mRNA. This showed a positive association of up-regulation of *LAIR-1* mRNA with higher histological grade ($p<0.001$), Nottingham Prognostic Index weak prognostic category ($p<0.001$) (**Table 17**), medullary-like tumours ($p=0.024$), and triple negative phenotype ($p<0.05$). High levels of LAIR-1 mRNA expression were significantly associated with METABRIC Integrative Clusters with upregulation within intClust.10 ($p=<0.001$) representing poor-outcome patients and basal-like intrinsic PAM50 subtype (**Table 17**).

Table 17 Associations between *LAIR-1* mRNA expression and clinicopathological variables in the METABRIC cohort

Clinicopathological Criteria	***LAIR-1 mRNA expression***		***χ2 & p Value***
	Low Expression N (%)	***High Expression N (%)***	
Age at Diagnosis			
≤50	234 (55.2)	190 (44.8)	0.764 (0.764)
>50	846 (54.6)	710 (45.6)	
Tumour Size (cm)			
≤2.0	488 (56.9)	370 (43.1)	3.280 (0.070)
>2.0	581 (52.8)	520 (47.2)	
Histological Grade			
1	112 (65.9)	58 (34.1)	56.994 **(<0.001)**
2	479 (62.2)	291 (37.8)	
3	435 (45.7)	517 (54.3)	
Tumour Type			
Ductal	926 (54.4)	775 (45.6)	11.279 (0.024)
Lobular	92 (62.6)	55 (37.4)	
Medullary-like	10 (31.3)	22 (68.8)	
Special type	29 (59.2)	20 (40.8)	
Miscellaneous	12 (57.1)	9 (42.9)	
Nottingham Prognostic Index (NPI)			
Good Prognostic Group	438 (64.4)	242 (35.6)	50.501 **(<0.001)**
Moderate Prognostic Group	564 (51.2)	537 (48.8)	
Poor Prognostic Group	78 (39.2)	121 (60.8)	
Stage			
I	290 (57.9)	211 (42.1)	17.033 **(0.001)**
II	417 (50.5)	408 (49.5)	
III	53 (44.9)	65 (55.1)	
PAM50 subtype			
Luminal A	478 (66.6)	240 (33.4)	81.734 **(<0.001)**
Luminal B	254 (52.0)	234 (48.0)	
Basal	127 (38.6)	202 (61.4)	
Her2	116 (48.3)	124 (51.7)	
Normal like	101 (50.8)	98 (51.7)	
IntClustMemb			
IntClustMemb 1	71 (51.1)	68 (48.9)	
IntClustMemb 2	33 (45.8)	39 (54.2)	
IntClustMemb 3	178 (61.4)	112 (38.6)	

IntClustMemb 4	145 (42.3)	198 (57.7)	126.426 **(<0.001)**
IntClustMemb 5	94 (49.5)	96 (50.5)	
IntClustMemb 6	52 (61.2)	33 (38.3)	
IntClustMemb 7	130 (68.4)	60 (31.6)	
IntClustMemb 8	221 (73.9)	78 (26.1)	
IntClustMemb 9	76 (52.1)	70 (47.9)	
IntClustMemb 10	80 (35.4)	146 (64.6)	
Oestrogen Receptor (ER)			
Negative	189 (43.1)	250 (56.9)	30.648 **(<0.001)**
Positive	869 (58.0)	629 (42.0)	
Progesterone Receptor (PR)			
Negative	423 (45.0)	517 (55.0)	65.768 **(<0.001)**
Positive	657 (63.2)	383 (36.8)	
Human epidermal growth factor receptor 2 (HER2)			
Negative	963 (55.6)	770 (44.4)	5.863 (**0.015**)
Positive	117 (47.4)	130 (52.6)	
Triple Negative (TPN) status			
Negative	863 (52.4)	783 (47.6)	16.887 **(<0.001)**
Positive	124 (39.7)	188 (60.3)	
Lymph node (LN)			
Negative	609 (58.8)	426 (41.2)	15.516 **(<0.001)**
Positive	469 (50.0)	469 (50.0)	

*significant values are highlighted in bold

6.5 LAIR-1 protein expression

Full-face BC tissue sections were used to evaluate the pattern of LAIR-1 protein expression prior to staining of TMAs (Nottingham series). This showed uniformly weak LAIR-1 expression in normal glandular epithelium and DCIS. On TMAs, a variable degree of LAIR-1 protein expression in invasive BC was observed. Out of 569 informative TMA cores, 49.4% showed negative/low expression (Fig. **21a**) in the cytoplasm while 50.6% showed high expression (Fig. **21b**).

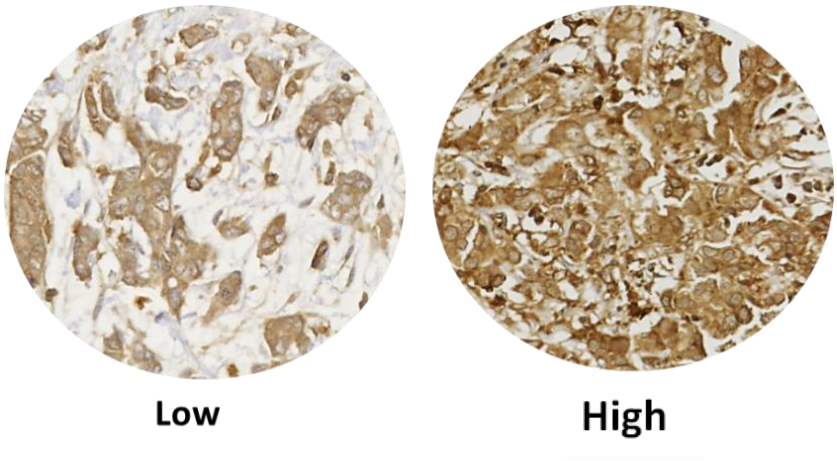


Fig. 21 IHC expression of LAIR-1 in TMA cores a) Low b) High

High LAIR-1 cytoplasmic expressions were associated with high tumour grade ($p<0.001$), poor Nottingham Prognostic Index (NPI; $p=0.012$), hormone receptor negativity ($p<0.01$), among IHC subtypes associated with triple negative and human epidermal growth factor 2 (HER2) + tumours ($p=0.019$) (**Table 18**). High LAIR-1 expression positively associated with Cyclin B1 ($p=0.010$) and signaling pathway associated markers; epidermal growth factor receptor (EGFR; $p=0.045$). Elevated expression of LAIR-1 was also associated with T-cell markers (CD3, CD8, and FOXP3; $p<0.01$) and histiocytic marker (CD68; $p<0.001$) (**Table 19**). Breast cancer-specific survival (BCSS) of patients with tumours expressing high cytoplasmic LAIR-1 was significantly shorter than that of the negative/low expression subgroup ($p=0.002$) and HER2 only cohort ($p=0.019$) (**Fig. 22**). Multivariate analysis revealed that increased LAIR-1 protein is an independent risk factor for shorter BCSS [$p=0.037$; HR 0.6 (95% CI 0.3-0.9); **Table 20**].

Table 18: Association of LAIR-1 protein with other BC related biomarkers

Clinico-pathological Criteria	***LAIR-1 cytoplasmic staining N (%)***		***χ2 & p Value***
	Low Expression	***High Expression***	
Histological Grade			
1	41 (54.7)	34 (45.3)	23.004 **(<0.001)**
2	115(62.2)	70 (37.8)	
3	122 (40.0)	181 (60.0)	
Pleomorphism			
1	4 (100)	0 (0)	26.104 **<0.001**
2	132 (81.0)	31 (19.0)	
3	181 (58.6)	128 (41.4)	
Mitosis			
1	103 (62.4)	62 (37.6)	23.849 **<0.001**
2	64 (55.2)	52 (44.8)	
3	102 (39.1)	159 (60.9)	
IHC subtypes			
Luminal A	69 (61.6)	43 (38.4)	9.979 **0.019**
Luminal B	86 (49.4)	88 (50.6)	
Triple Negative	46 (42.2)	63 (57.8)	
HER2+	41 (44.1)	52 (55.9)	
Stage			
I	175 (51.2)	167 (48.8)	1.158 (0.763)
II	84 (46.9)	95 (53.1)	
III	19 (45.2)	23 (54.8)	
Tumour Size			
≥ 2.0cm	161 (70.6)	67 (29.4)	4.312 **0.038**
< 2.0cm	154 (61.6)	96 (38.4)	
Nottingham Prognostic Index			
Good Prognostic Group	88 (59.9)	59 (40.1)	8.866 (**0.012)**
Moderate Prognostic Group	153 (46.5)	176 (53.5)	
Poor Prognostic Group	39 (43.3)	51 (56.7)	

*significant values are highlighted in bold

Table 19: Associations of *LAIR-1* IHC expression and other BC related biomarkers within the Nottingham BC series.

Clinico-pathological Criteria	***LAIR-1 membrane staining***		***χ2 & p Value***
	Low expression N (%)	***High expression N (%)***	
Estrogen Receptor (ER)			
Negative	64 (41.0)	92 (59.0)	6.143 **0.013**
Positive	216 (52.7)	194 (47.3)	
Progesterone (PR)			
Negative	112 (47.1)	126 (52.9)	0.891 (0.345)
Positive	161 (51.1)	154 (48.9)	
Human epidermal Growth Factor receptor 2 (HER2)			
Negative	233 (50.7)	227 (49.3)	1.113 (0.291)
Positive	42 (44.7)	52 (55.3)	
P53			
Negative	211 (54.7)	175 (45.3)	11.755 **(0.001)**
Positive	63 (38.7)	100 (61.3)	
Triple Negative (TPN)			
Negative	231 (51.2)	220 (48.8)	3.528 (0.060)
Positive	44 (41.1)	63 (58.9)	
Ki67			
Negative	91 (56.9)	69 (43.1)	3.057 (0.080)
Positive	135 (48.2)	145 (51.8)	
Lymphovascular Invasion (LVI)			
Negative	142 (52.6)	128 (47.4)	0.431 (0.512)
Positive	91 (49.5)	93 (50.5)	
Matrix Metalloproteinase-15 (MMP-15)			
Negative	136 (61.0)	87 (39.0)	35.041 **(<0.001)**
Positive	66 (32.4)	138 (67.6)	
Matrix Metalloproteinase-14 (MMP-14)			
Negative	140 (56.7)	107 (43.3)	19.691 **(<0.001)**
Positive	65 (35.1)	120 (64.9)	
Forkhead box P3 (FOXP3)			
Negative	97 (58.1)	70 (41.9)	8.960 **(0.003)**
Positive	136 (43.7)	175 (56.3)	
CD3			
Negative	124 (55.6)	99 (44.4)	8.320 **(0.004)**
Positive	109 (42.4)	148 (57.6)	
CD68			
Negative	158 (51.1)	151 (48.9)	5.225 **(0.002)**
Positive	54 (39.4)	83 (60.3)	
CD8			
Negative	156 (51.0)	150 (49.0)	7.149 **(0.007)**
Positive	54 (37.5)	90 (62.5)	

**Significant values are highlighted in bold*

Table 20 Multivariate analysis of LAIR-1 expression compared with tumour stage, grade, size, ER, HER2, NPI status for breast cancer-specific survival.

Variable	Breast cancer-specific survival		
	Multivariate		
	HR	95%CI	p value
Whole cohort			
Stage	2.4	1.4-3.8	**<0.001**
Grade	4.9	2.1-11.4	**<0.001**
Tumour size	1.8	1.3-3.2	**0.037**
LAIR-1-Cytoplasmic	0.6	0.3-0.9	**0.037**
Oestrogen (ER)	0.5	0.3-0.9	**0.019**
HER2	1.9	1.2-3.0	**0.003**
Nottingham Prognostic Index (NPI)	0.6	0.4-1.8	0.690

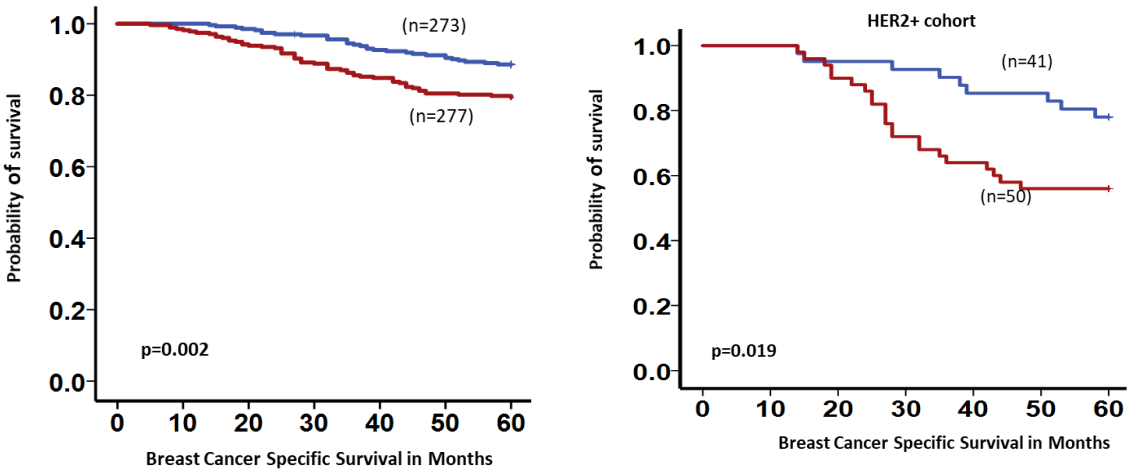


Fig. 22 Kaplan Meier BCSS in LAIR-1 A) METABRIC cohort B) HER2+ cohorts only.

We suggest that from the above-mentioned studies that expression LAIR-1 is associated with poor prognosis in BC. Therefore, we explored in this analysis the relationship between LAIR-1, clinicopathological factors and the amount of patient outcome protein in a well-characterized early stage BC cohort. In addition, we also investigated the relationship between total and subtype LAIR-1 protein expression (B and T cell and histiocytic markers (147, 148).

6.6 Discussion

The immunoglobulin-like receptor-1 (LAIR-1) associated with leukocytes is a superfamily member of the immunoglobulin (Ig) and is a type of transmembrane glycoprotein. LAIR-1 consists of an Ig-like domain of type C2 and two inhibition motifs (ITIMs) centered on the immunoreceptor tyrosine. It is commonly distributed on many immune cells, such as T-cells, B-cells, and NK cells. LAIR-1 was recently studied as an immuno-phenotypic precursor in acute leukaemia (149). LAIR-1 is primarily found in immune cells and is also found in hematopoietic progenitor cells, MKs and osteoclasts $CD34^{+}$ (150, 151). Previous study by *Poggi et al., (*152*)* showed that LAIR-1 was not expressed in chronic lymphocytic leukemia (CLL), however the intensity was associated with higher stage and progression of CLL. Although only a few studies are looking into the effects of LAIR-1 in breast cancer. Since LAIR-1 is an inhibitory receptor, it acts by binding to SH2 domain of phosphatases leading to dephosphorylation of kinases (152).

Our current study suggests that high cytoplasmic expression of LAIR-1 was associated with poor prognosis such as high tumour grade, poor Nottingham prognostic index and HER2+ status. LAIR-1 was positively associated with cyclin B1, which is essential for transition from G2 phase to mitosis and in many breast cancer cases (153) cyclin B1 is mutated leading to survival of cancer cells. A previous study by *Shen et al., (*154*)* suggested that highly expressed cyclin B1 attaches to Cdk1 in G1 step, which phosphorylates a variety of substrates irrespective of the cell cycle process and contributes to the violent proliferation of neoplastic tissues. Epidermal growth factor receptor (EGFR) which suggests a potential role in cell signaling, tumour progression and in correlation with HER2+ status. Many studies has suggested that EGFR plays a major role in breast cancer progression and survival due to inhibition of apoptosis by EGFR (155).

Association of high LAIR-1 was also perceived with T- cell markers suggesting an involvement in evading the immune system if mutated, FOXP3 this gene plays a crucial role in immune system and also helps in production of CD4+ regulatory T cells (Tregs), and the loss of FOXP3 activity contributes to a deficit of Tregs, contributing to lethal auto-aggressive lymphoproliferation (156). Previous study by *Ni C et al., (*157*)* suggested that CD68 which is known as a macrophage marker and is used to distinguish macrophages of different types of cancer, including breast cancer. CD68 is considered to be Tumour associated marker (TAM) when mutated can correlate with TNBC and also HER2+ status in few breast cancer cases (158, 159).

Conclusions: This study provides evidence for the prognostic value of LAIR-1 in invasive BC. Strong positive association with immune cell markers and LAIR-1 warrant further studies to assess them individually and in combination along with the immune check point proteins.

7.0 Strengths and Limitations

One of the important strength in this whole project is use of different well characterised datasets for reliable results. Some procedures have been put in place to ensure reliability of results produced in this report. Another individual ranked the whole group, to assess the accuracy of the ranking. A second partner, more qualified, then again scored a subset of the sample to check that the initial H scores were correct. In all studies, use of positive and negative measures has shown that the experimental procedures have been correctly observed. In Western Blotting, a mouse anti-beta-actin antibody was used to ensure that the protocol was properly performed, and that any other bands found is due to the addition of those particular antibodies. A negative and positive regulation was used for the immunohistochemistry. The negative control revealed that any staining seen was due to the addition of the antibodies, and the positive control suggested that the staining strength was associated with optimizations.

Because of these modifications, we can be sure of the quality of the western blots and the processed staining. Including TMAs (Nottingham series) in the project also made it possible to stain a large cohort with greater ease for the marker. That increased the study's power, and hence the results ' reliability.

However, one disadvantage of using TMAs is that they may not reflect the heterogeneity of marker expression within the tumour. Tumors can show heterogeneity, suggesting that tumour regions may be negative for all four markers whereas other regions may show high expression. Because TMAs require analysing a small core of the tumour, it may be lacking differences in expression. We tried to reduce this however by ranking multiple samples from many tumours.

Experiments involving the application of LCN2 and CD276-specific agonists to tumours of breast cancer may also be useful in the future to investigate their use in innovative cancer therapies.

This is one of the few trials to specifically investigate the expression of LCN2, SLC22A17, CD276 and LAIR-1 in breast cancer to the best of our knowledge, and as such these findings will need to be replicated to confirm such tests.

7.1 Acknowledgements

My heartfelt gratitude goes out to everyone involved in this project. I want to thank Professor Emad Rakha, my boss, for his constant support and guidance throughout the project. I would also like to thank my co-supervisor, Dr Chitra Joseph, who has also given extensive support throughout the project and offered advice on many aspects of the project, including Western Blotting, statistical analysis and dissertation selection. I would like to express my thanks to Christopher Nolan, who have contributed to the laboratory experiments. I would also like to credit Mansour Alsaleem for rating the TMA slides in double scoring and helping with cell culture experiments.

8.0 Bibliography

1. Ferlay J, Soerjomataram I, Dikshit R, Eser S, Mathers C, Rebelo M, et al. Cancer incidence and mortality worldwide: sources, methods and major patterns in GLOBOCAN 2012. Int J Cancer. 2015;136(5):E359-86.
2. Feng Y, Spezia M, Huang S, Yuan C, Zeng Z, Zhang L, et al. Breast cancer development and progression: Risk factors, cancer stem cells, signaling pathways, genomics, and molecular pathogenesis. Genes Dis. 2018;5(2):77-106.
3. Hoon Tan P, Ellis I, Allison K, Brogi E, Fox SB, Lakhani S, et al. The 2019 WHO classification of tumours of the breast. Histopathology. 2020.
4. Rakha EA, Reis-Filho JS, Baehner F, Dabbs DJ, Decker T, Eusebi V, et al. Breast cancer prognostic classification in the molecular era: the role of histological grade. Breast Cancer Res. 2010;12(4):207.
5. Sorlie T, Perou CM, Tibshirani R, Aas T, Geisler S, Johnsen H, et al. Gene expression patterns of breast carcinomas distinguish tumor subclasses with clinical implications. Proc Natl Acad Sci U S A. 2001;98(19):10869-74.
6. Perou CM, Sorlie T, Eisen MB, van de Rijn M, Jeffrey SS, Rees CA, et al. Molecular portraits of human breast tumours. Nature. 2000;406(6797):747-52.
7. Dai X, Li T, Bai Z, Yang Y, Liu X, Zhan J, et al. Breast cancer intrinsic subtype classification, clinical use and future trends. Am J Cancer Res. 2015;5(10):2929-43.
8. Warth A, Cortis J, Soltermann A, Meister M, Budczies J, Stenzinger A, et al. Tumour cell proliferation (Ki-67) in non-small cell lung cancer: a critical reappraisal of its prognostic role. Br J Cancer. 2014;111(6):1222-9.
9. Hennigs A, Riedel F, Gondos A, Sinn P, Schirmacher P, Marme F, et al. Prognosis of breast cancer molecular subtypes in routine clinical care: A large prospective cohort study. BMC Cancer. 2016;16(1):734.
10. de Azambuja E, Cardoso F, de Castro G, Jr., Colozza M, Mano MS, Durbecq V, et al. Ki-67 as prognostic marker in early breast cancer: a meta-analysis of published studies involving 12,155 patients. Br J Cancer. 2007;96(10):1504-13.
11. Hon JD, Singh B, Sahin A, Du G, Wang J, Wang VY, et al. Breast cancer molecular subtypes: from TNBC to QNBC. Am J Cancer Res. 2016;6(9):1864-72.
12. Xuan Q, Ji H, Tao X, Xu Y, Zhang Q. Quantitative assessment of HER2 amplification in HER2-positive breast cancer: its association with clinical outcomes. Breast Cancer Res Treat. 2015;150(3):581-8.
13. Boekhout AH, Beijnen JH, Schellens JH. Trastuzumab. Oncologist. 2011;16(6):800-10.
14. Rakha EA, Elsheikh SE, Aleskandarany MA, Habashi HO, Green AR, Powe DG, et al. Triple-negative breast cancer: distinguishing between basal and nonbasal subtypes. Clin Cancer Res. 2009;15(7):2302-10.
15. Munirah MA, Siti-Aishah MA, Reena MZ, Sharifah NA, Rohaizak M, Norlia A, et al. Identification of different subtypes of breast cancer using tissue microarray. Rom J Morphol Embryol. 2011;52(2):669-77.
16. Pal SK, Miller MJ, Agarwal N, Chang SM, Chavez-MacGregor M, Cohen E, et al. Clinical Cancer Advances 2019: Annual Report on Progress Against Cancer From the American Society of Clinical Oncology. J Clin Oncol. 2019;37(10):834-49.
17. Fitzpatrick DJ, Lai CS, Parkyn RF, Walters D, Humeniuk V, Walsh DC. Time to breast cancer relapse predicted by primary tumour characteristics, not lymph node involvement. World J Surg. 2014;38(7):1668-75.
18. Mateo AM, Pezzi TA, Sundermeyer M, Kelley CA, Klimberg VS, Pezzi CM. Atypical medullary carcinoma of the breast has similar prognostic factors and survival to typical medullary breast carcinoma: 3,976 cases from the National Cancer Data Base. J Surg Oncol. 2016;114(5):533-6.
19. Ng CH, Pathy NB, Taib NA, Ho GF, Mun KS, Rhodes A, et al. Do clinical features and survival of single hormone receptor positive breast cancers differ from double hormone receptor positive breast cancers? Asian Pac J Cancer Prev. 2014;15(18):7959-64.
20. Ulas A, Kos T, Avci N, Cubukcu E, Olmez OF, Bulut N, et al. Patients with HER2-positive early breast cancer receiving adjuvant trastuzumab: clinicopathological features, efficacy, and factors affecting survival. Asian Pac J Cancer Prev. 2015;16(4):1643-9.
21. He KW, Sun JJ, Liu ZB, Zhuo PY, Ma QH, Liu ZY, et al. Prognostic significance of lymphatic vessel invasion diagnosed by D2-40 in Chinese invasive breast cancers. Medicine (Baltimore). 2017;96(44):e8490.
22. Ejlertsen B, Jensen MB, Rank F, Rasmussen BB, Christiansen P, Kroman N, et al. Population-based study of peritumoral lymphovascular invasion and outcome among patients with operable breast cancer. J Natl Cancer Inst. 2009;101(10):729-35.
23. Chen L, Linden HM, Anderson BO, Li CI. Trends in 5-year survival rates among breast cancer patients by hormone receptor status and stage. Breast Cancer Res Treat. 2014;147(3):609-16.
24. Gujam FJ, McMillan DC, Mohammed ZM, Edwards J, Going JJ. The relationship between tumour budding, the tumour microenvironment and survival in patients with invasive ductal breast cancer. Br J Cancer. 2015;113(7):1066-74.
25. Lamouille S, Xu J, Derynck R. Molecular mechanisms of epithelial-mesenchymal transition. Nat Rev Mol Cell Biol. 2014;15(3):178-96.
26. Balkwill FR, Capasso M, Hagemann T. The tumor microenvironment at a glance. J Cell Sci. 2012;125(Pt 23):5591-6.

27. Hanahan D, Weinberg RA. Hallmarks of cancer: the next generation. Cell. 2011;144(5):646-74.
28. Curtis C, Shah SP, Chin SF, Turashvili G, Rueda OM, Dunning MJ, et al. The genomic and transcriptomic architecture of 2,000 breast tumours reveals novel subgroups. Nature. 2012;486(7403):346-52.
29. Abd El-Rehim DM, Ball G, Pinder SE, Rakha E, Paish C, Robertson JF, et al. High-throughput protein expression analysis using tissue microarray technology of a large well-characterised series identifies biologically distinct classes of breast cancer confirming recent cDNA expression analyses. Int J Cancer. 2005;116(3):340-50.
30. Jezequel P, Frenel JS, Campion L, Guerin-Charbonnel C, Gouraud W, Ricolleau G, et al. bc-GenExMiner 3.0: new mining module computes breast cancer gene expression correlation analyses. Database (Oxford). 2013;2013:bas060.
31. Gyorffy B, Lanczky A, Eklund AC, Denkert C, Budczies J, Li Q, et al. An online survival analysis tool to rapidly assess the effect of 22,277 genes on breast cancer prognosis using microarray data of 1,809 patients. Breast Cancer Res Treat. 2010;123(3):725-31.
32. Galea MH, Blamey RW, Elston CE, Ellis IO. The Nottingham Prognostic Index in primary breast cancer. Breast Cancer Res Treat. 1992;22(3):207-19.
33. McCarty KS, Jr., Miller LS, Cox EB, Konrath J, McCarty KS, Sr. Estrogen receptor analyses. Correlation of biochemical and immunohistochemical methods using monoclonal antireceptor antibodies. Arch Pathol Lab Med. 1985;109(8):716-21.
34. Abel Y, Rederstorff M. Gene expression knockdown by transfection of siRNAs into mammalian cells. Methods Mol Biol. 2015;1296:199-202.
35. Sontheimer EJ. Assembly and function of RNA silencing complexes. Nat Rev Mol Cell Biol. 2005;6(2):127-38.
36. Dennis JW, Granovsky M, Warren CE. Glycoprotein glycosylation and cancer progression. Biochim Biophys Acta. 1999;1473(1):21-34.
37. Spiro RG. Glycoproteins: their biochemistry, biology and role in human disease. N Engl J Med. 1969;281(19):1043-56 concl.
38. Gnoth MJ, Buetehorn U, Muenster U, Schwarz T, Sandmann S. In vitro and in vivo P-glycoprotein transport characteristics of rivaroxaban. J Pharmacol Exp Ther. 2011;338(1):372-80.
39. Flower DR. Beyond the superfamily: the lipocalin receptors. Biochim Biophys Acta. 2000;1482(1-2):327-36.
40. Flower DR. The lipocalin protein family: structure and function. Biochem J. 1996;318 (Pt 1):1-14.
41. Flower DR. Multiple molecular recognition properties of the lipocalin protein family. J Mol Recognit. 1995;8(3):185-95.
42. Flower DR, North AC, Attwood TK. Mouse oncogene protein 24p3 is a member of the lipocalin protein family. Biochem Biophys Res Commun. 1991;180(1):69-74.
43. Flower DR, North AC, Sansom CE. The lipocalin protein family: structural and sequence overview. Biochim Biophys Acta. 2000;1482(1-2):9-24.
44. Chakraborty S, Kaur S, Guha S, Batra SK. The multifaceted roles of neutrophil gelatinase associated lipocalin (NGAL) in inflammation and cancer. Biochim Biophys Acta. 2012;1826(1):129-69.
45. Guo BX, Wang QQ, Li JH, Gan ZS, Zhang XF, Wang YZ, et al. Lipocalin 2 regulates intestine bacterial survival by interplaying with siderophore in a weaned piglet model of Escherichia coli infection. Oncotarget. 2017;8(39):65386-96.
46. Nairz M, Theurl I, Schroll A, Theurl M, Fritsche G, Lindner E, et al. Absence of functional Hfe protects mice from invasive Salmonella enterica serovar Typhimurium infection via induction of lipocalin-2. Blood. 2009;114(17):3642-51.
47. Bahmani P, Halabian R, Rouhbakhsh M, Roushandeh AM, Masroori N, Ebrahimi M, et al. Neutrophil gelatinase-associated lipocalin induces the expression of heme oxygenase-1 and superoxide dismutase 1, 2. Cell Stress Chaperones. 2010;15(4):395-403.
48. Roudkenar MH, Halabian R, Bahmani P, Roushandeh AM, Kuwahara Y, Fukumoto M. Neutrophil gelatinase-associated lipocalin: a new antioxidant that exerts its cytoprotective effect independent on Heme Oxygenase-1. Free Radic Res. 2011;45(7):810-9.
49. Roudkenar MH, Halabian R, Ghasemipour Z, Roushandeh AM, Rouhbakhsh M, Nekogoftar M, et al. Neutrophil gelatinase-associated lipocalin acts as a protective factor against H(2)O(2) toxicity. Arch Med Res. 2008;39(6):560-6.
50. Roudkenar MH, Halabian R, Roushandeh AM, Nourani MR, Masroori N, Ebrahimi M, et al. Lipocalin 2 regulation by thermal stresses: protective role of Lcn2/NGAL against cold and heat stresses. Exp Cell Res. 2009;315(18):3140-51.
51. Roudkenar MH, Kuwahara Y, Baba T, Roushandeh AM, Ebishima S, Abe S, et al. Oxidative stress induced lipocalin 2 gene expression: addressing its expression under the harmful conditions. J Radiat Res. 2007;48(1):39-44.
52. Kjeldsen L, Cowland JB, Borregaard N. Human neutrophil gelatinase-associated lipocalin and homologous proteins in rat and mouse. Biochim Biophys Acta. 2000;1482(1-2):272-83.
53. Ding G, Wang J, Feng C, Jiang H, Xu J, Ding Q. Lipocalin 2 over-expression facilitates progress of castration-resistant prostate cancer via improving androgen receptor transcriptional activity. Oncotarget.

2016;7(39):64309-17.
54. Miyamoto T, Kashima H, Yamada Y, Kobara H, Asaka R, Ando H, et al. Lipocalin 2 Enhances Migration and Resistance against Cisplatin in Endometrial Carcinoma Cells. PLoS One. 2016;11(5):e0155220.
55. Yamada Y, Miyamoto T, Kashima H, Kobara H, Asaka R, Ando H, et al. Lipocalin 2 attenuates iron-related oxidative stress and prolongs the survival of ovarian clear cell carcinoma cells by up-regulating the CD44 variant. Free Radic Res. 2016;50(4):414-25.
56. Aoyama T, Kuwahara-Arai K, Uchiyama A, Kon K, Okubo H, Yamashina S, et al. Spleen-derived lipocalin-2 in the portal vein regulates Kupffer cells activation and attenuates the development of liver fibrosis in mice. Lab Invest. 2017;97(8):890-902.
57. Kang Z, Qiao N, Tan Z, Tang Z, Li Y. Expression patterns and changes of the LCN2 gene in the testes of induced cryptorchidism and busulfan-treated mice. Syst Biol Reprod Med. 2017;63(6):364-9.
58. Naude PJ, Eisel UL, Comijs HC, Groenewold NA, De Deyn PP, Bosker FJ, et al. Neutrophil gelatinase-associated lipocalin: a novel inflammatory marker associated with late-life depression. J Psychosom Res. 2013;75(5):444-50.
59. Rebalka IA, Monaco CMF, Varah NE, Berger T, D'Souza D M, Zhou S, et al. Loss of the adipokine lipocalin-2 impairs satellite cell activation and skeletal muscle regeneration. Am J Physiol Cell Physiol. 2018;315(5):C714-C21.
60. Smith ER, Zurakowski D, Saad A, Scott RM, Moses MA. Urinary biomarkers predict brain tumor presence and response to therapy. Clin Cancer Res. 2008;14(8):2378-86.
61. Viau A, El Karoui K, Laouari D, Burtin M, Nguyen C, Mori K, et al. Lipocalin 2 is essential for chronic kidney disease progression in mice and humans. J Clin Invest. 2010;120(11):4065-76.
62. Hu C, Yang K, Li M, Huang W, Zhang F, Wang H. Lipocalin 2: a potential therapeutic target for breast cancer metastasis. Onco Targets Ther. 2018;11:8099-106.
63. Bauer M, Eickhoff JC, Gould MN, Mundhenke C, Maass N, Friedl A. Neutrophil gelatinase-associated lipocalin (NGAL) is a predictor of poor prognosis in human primary breast cancer. Breast Cancer Res Treat. 2008;108(3):389-97.
64. Stoesz SP, Gould MN. Overexpression of neu-related lipocalin (NRL) in neu-initiated but not ras or chemically initiated rat mammary carcinomas. Oncogene. 1995;11(11):2233-41.
65. Arlinghaus R, Leng X. Requirement of lipocalin 2 for chronic myeloid leukemia. Leuk Lymphoma. 2008;49(4):600-3.
66. Leng X, Lin H, Ding T, Wang Y, Wu Y, Klumpp S, et al. Lipocalin 2 is required for BCR-ABL-induced tumorigenesis. Oncogene. 2008;27(47):6110-9.
67. Tong Z, Chakraborty S, Sung B, Koolwal P, Kaur S, Aggarwal BB, et al. Epidermal growth factor down-regulates the expression of neutrophil gelatinase-associated lipocalin (NGAL) through E-cadherin in pancreatic cancer cells. Cancer. 2011;117(11):2408-18.
68. Lambert AW, Pattabiraman DR, Weinberg RA. Emerging Biological Principles of Metastasis. Cell. 2017;168(4):670-91.
69. Moustakas A, de Herreros AG. Epithelial-mesenchymal transition in cancer. Mol Oncol. 2017;11(7):715-7.
70. Tong Z, Wu X, Ovcharenko D, Zhu J, Chen CS, Kehrer JP. Neutrophil gelatinase-associated lipocalin as a survival factor. Biochem J. 2005;391(Pt 2):441-8.
71. Kurozumi S, Alsaeed S, Orah N, Miligy IM, Joseph C, Aljohani A, et al. Clinicopathological significance of lipocalin 2 nuclear expression in invasive breast cancer. Breast Cancer Res Treat. 2019.
72. Fang WK, Xu LY, Lu XF, Liao LD, Cai WJ, Shen ZY, et al. A novel alternative spliced variant of neutrophil gelatinase-associated lipocalin receptor in oesophageal carcinoma cells. Biochem J. 2007;403(2):297-303.
73. Mannelqvist M, Stefansson IM, Wik E, Kusonmano K, Raeder MB, Oyan AM, et al. Lipocalin 2 expression is associated with aggressive features of endometrial cancer. BMC Cancer. 2012;12:169.
74. Zhang H, Xu L, Xiao D, Xie J, Zeng H, Wang Z, et al. Upregulation of neutrophil gelatinase-associated lipocalin in oesophageal squamous cell carcinoma: significant correlation with cell differentiation and tumour invasion. J Clin Pathol. 2007;60(5):555-61.
75. Tschesche H, Zolzer V, Triebel S, Bartsch S. The human neutrophil lipocalin supports the allosteric activation of matrix metalloproteinases. Eur J Biochem. 2001;268(7):1918-28.
76. Cakirca G, Turgut FH. Serum Matrix Metalloproteinase-9, Tissue Inhibitor of Metalloproteinase-1 and Matrix Metalloproteinase-9/ Neutrophil Gelatinase-associated Lipocalin Complex Levels in Patients With Early-stage Diabetic Nephropathy. Iran J Kidney Dis. 2018;12(5):299-304.
77. Cabedo Martinez AI, Weinhaupl K, Lee WK, Wolff NA, Storch B, Zerko S, et al. Biochemical and Structural Characterization of the Interaction between the Siderocalin NGAL/LCN2 (Neutrophil Gelatinase-associated Lipocalin/Lipocalin 2) and the N-terminal Domain of Its Endocytic Receptor SLC22A17. J Biol Chem. 2016;291(6):2917-30.
78. Devireddy LR, Gazin C, Zhu X, Green MR. A cell-surface receptor for lipocalin 24p3 selectively mediates apoptosis and iron uptake. Cell. 2005;123(7):1293-305.
79. Dizin E, Hasler U, Nlandu-Khodo S, Fila M, Roth I, Ernandez T, et al. Albuminuria induces a proinflammatory and profibrotic response in cortical collecting ducts via the 24p3 receptor. Am J Physiol Renal

Physiol. 2013;305(7):F1053-63.
80. Giltnane JM, Moeder CB, Camp RL, Rimm DL. Quantitative multiplexed analysis of ErbB family coexpression for primary breast cancer prognosis in a large retrospective cohort. Cancer. 2009;115(11):2400-9.
81. Felipe Lima J, Nofech-Mozes S, Bayani J, Bartlett JM. EMT in Breast Carcinoma-A Review. J Clin Med. 2016;5(7).
82. Leng X, Wu Y, Arlinghaus RB. Relationships of lipocalin 2 with breast tumorigenesis and metastasis. J Cell Physiol. 2011;226(2):309-14.
83. Tomao F, Papa A, Zaccarelli E, Rossi L, Caruso D, Minozzi M, et al. Triple-negative breast cancer: new perspectives for targeted therapies. Onco Targets Ther. 2015;8:177-93.
84. Xia L, Tan S, Zhou Y, Lin J, Wang H, Oyang L, et al. Role of the NFkappaB-signaling pathway in cancer. Onco Targets Ther. 2018;11:2063-73.
85. Aleskandarany MA, Sonbul S, Surridge R, Mukherjee A, Caldas C, Diez-Rodriguez M, et al. Rho-GTPase activating-protein 18: a biomarker associated with good prognosis in invasive breast cancer. Br J Cancer. 2017;117(8):1176-84.
86. Nagi C, Guttman M, Jaffer S, Qiao R, Keren R, Triana A, et al. N-cadherin expression in breast cancer: correlation with an aggressive histologic variant--invasive micropapillary carcinoma. Breast Cancer Res Treat. 2005;94(3):225-35.
87. Fang X, Cai Y, Liu J, Wang Z, Wu Q, Zhang Z, et al. Twist2 contributes to breast cancer progression by promoting an epithelial-mesenchymal transition and cancer stem-like cell self-renewal. Oncogene. 2011;30(47):4707-20.
88. Yang J, Bielenberg DR, Rodig SJ, Doiron R, Clifton MC, Kung AL, et al. Lipocalin 2 promotes breast cancer progression. Proc Natl Acad Sci U S A. 2009;106(10):3913-8.
89. Hanai J, Mammoto T, Seth P, Mori K, Karumanchi SA, Barasch J, et al. Lipocalin 2 diminishes invasiveness and metastasis of Ras-transformed cells. J Biol Chem. 2005;280(14):13641-7.
90. Nielsen TO, Hsu FD, Jensen K, Cheang M, Karaca G, Hu Z, et al. Immunohistochemical and clinical characterization of the basal-like subtype of invasive breast carcinoma. Clin Cancer Res. 2004;10(16):5367-74.
91. Kurozumi S, Yamaguchi Y, Matsumoto H, Inoue K, Kurosumi M, Oyama T, et al. Comparing protein and mRNA expressions of the human epidermal growth factor receptor family in estrogen receptor-positive breast cancer. Med Mol Morphol. 2019;52(2):90-8.
92. Green AR, Soria D, Stephen J, Powe DG, Nolan CC, Kunkler I, et al. Nottingham Prognostic Index Plus: Validation of a clinical decision making tool in breast cancer in an independent series. J Pathol Clin Res. 2016;2(1):32-40.
93. Martin M, Holmes FA, Ejlertsen B, Delaloge S, Moy B, Iwata H, et al. Neratinib after trastuzumab-based adjuvant therapy in HER2-positive breast cancer (ExteNET): 5-year analysis of a randomised, double-blind, placebo-controlled, phase 3 trial. Lancet Oncol. 2017;18(12):1688-700.
94. Baselga J, Cortes J, Kim SB, Im SA, Hegg R, Im YH, et al. Pertuzumab plus trastuzumab plus docetaxel for metastatic breast cancer. N Engl J Med. 2012;366(2):109-19.
95. Geyer CE, Forster J, Lindquist D, Chan S, Romieu CG, Pienkowski T, et al. Lapatinib plus capecitabine for HER2-positive advanced breast cancer. N Engl J Med. 2006;355(26):2733-43.
96. Wenners AS, Mehta K, Loibl S, Park H, Mueller B, Arnold N, et al. Neutrophil gelatinase-associated lipocalin (NGAL) predicts response to neoadjuvant chemotherapy and clinical outcome in primary human breast cancer. PLoS One. 2012;7(10):e45826.
97. Rodvold JJ, Mahadevan NR, Zanetti M. Lipocalin 2 in cancer: when good immunity goes bad. Cancer Lett. 2012;316(2):132-8.
98. Leng X, Ding T, Lin H, Wang Y, Hu L, Hu J, et al. Inhibition of lipocalin 2 impairs breast tumorigenesis and metastasis. Cancer Res. 2009;69(22):8579-84.
99. Lim R, Ahmed N, Borregaard N, Riley C, Wafai R, Thompson EW, et al. Neutrophil gelatinase-associated lipocalin (NGAL) an early-screening biomarker for ovarian cancer: NGAL is associated with epidermal growth factor-induced epithelio-mesenchymal transition. Int J Cancer. 2007;120(11):2426-34.
100. Liu MF, Jin T, Shen JH, Shen ZY, Zheng ZC, Zhang ZL, et al. NGAL and NGALR are frequently overexpressed in human gliomas and are associated with clinical prognosis. J Neurooncol. 2011;104(1):119-27.
101. Du ZP, Lv Z, Wu BL, Wu ZY, Shen JH, Wu JY, et al. Neutrophil gelatinase-associated lipocalin and its receptor: independent prognostic factors of oesophageal squamous cell carcinoma. J Clin Pathol. 2011;64(1):69-74.
102. Drew BG, Hamidi H, Zhou Z, Villanueva CJ, Krum SA, Calkin AC, et al. Estrogen receptor (ER)alpha-regulated lipocalin 2 expression in adipose tissue links obesity with breast cancer progression. J Biol Chem. 2015;290(9):5566-81.
103. Liu Y, Beyer A, Aebersold R. On the Dependency of Cellular Protein Levels on mRNA Abundance. Cell. 2016;165(3):535-50.
104. Hageman RS, Leduc MS, Korstanje R, Paigen B, Churchill GA. A Bayesian framework for inference of the genotype-phenotype map for segregating populations. Genetics. 2011;187(4):1163-70.
105. Ahn HJ, Jung SJ, Kim TH, Oh MK, Yoon HK. Differences in Clinical Outcomes between Luminal A and B Type Breast Cancers according to the St. Gallen Consensus 2013. J Breast Cancer. 2015;18(2):149-59.

106. Massague J. TGFbeta in Cancer. Cell. 2008;134(2):215-30.
107. Rakha EA, Boyce RW, Abd El-Rehim D, Kurien T, Green AR, Paish EC, et al. Expression of mucins (MUC1, MUC2, MUC3, MUC4, MUC5AC and MUC6) and their prognostic significance in human breast cancer. Mod Pathol. 2005;18(10):1295-304.
108. Shariat SF, Khoddami SM, Saboorian H, Koeneman KS, Sagalowsky AI, Cadeddu JA, et al. Lymphovascular invasion is a pathological feature of biologically aggressive disease in patients treated with radical prostatectomy. J Urol. 2004;171(3):1122-7.
109. Miyamoto T, Asaka R, Suzuki A, Takatsu A, Kashima H, Shiozawa T. Immunohistochemical detection of a specific receptor for lipocalin2 (solute carrier family 22 member 17, SLC22A17) and its prognostic significance in endometrial carcinoma. Exp Mol Pathol. 2011;91(2):563-8.
110. Abergel RJ, Clifton MC, Pizarro JC, Warner JA, Shuh DK, Strong RK, et al. The siderocalin/enterobactin interaction: a link between mammalian immunity and bacterial iron transport. J Am Chem Soc. 2008;130(34):11524-34.
111. Sheng Z, Wang SZ, Green MR. Transcription and signalling pathways involved in BCR-ABL-mediated misregulation of 24p3 and 24p3R. EMBO J. 2009;28(7):866-76.
112. Jung M, Weigert A, Mertens C, Rehwald C, Brune B. Iron Handling in Tumor-Associated Macrophages-Is There a New Role for Lipocalin-2? Front Immunol. 2017;8:1171.
113. Zang X, Allison JP. The B7 family and cancer therapy: costimulation and coinhibition. Clin Cancer Res. 2007;13(18 Pt 1):5271-9.
114. Sun X, Vale M, Leung E, Kanwar JR, Gupta R, Krissansen GW. Mouse B7-H3 induces antitumor immunity. Gene Ther. 2003;10(20):1728-34.
115. Zang X, Sullivan PS, Soslow RA, Waitz R, Reuter VE, Wilton A, et al. Tumor associated endothelial expression of B7-H3 predicts survival in ovarian carcinomas. Mod Pathol. 2010;23(8):1104-12.
116. Sun Y, Wang Y, Zhao J, Gu M, Giscombe R, Lefvert AK, et al. B7-H3 and B7-H4 expression in non-small-cell lung cancer. Lung Cancer. 2006;53(2):143-51.
117. Wu CP, Jiang JT, Tan M, Zhu YB, Ji M, Xu KF, et al. Relationship between co-stimulatory molecule B7-H3 expression and gastric carcinoma histology and prognosis. World J Gastroenterol. 2006;12(3):457-9.
118. Roth TJ, Sheinin Y, Lohse CM, Kuntz SM, Frigola X, Inman BA, et al. B7-H3 ligand expression by prostate cancer: a novel marker of prognosis and potential target for therapy. Cancer Res. 2007;67(16):7893-900.
119. Yamato I, Sho M, Nomi T, Akahori T, Shimada K, Hotta K, et al. Clinical importance of B7-H3 expression in human pancreatic cancer. Br J Cancer. 2009;101(10):1709-16.
120. Sun J, Chen LJ, Zhang GB, Jiang JT, Zhu M, Tan Y, et al. Clinical significance and regulation of the costimulatory molecule B7-H3 in human colorectal carcinoma. Cancer Immunol Immunother. 2010;59(8):1163-71.
121. Suh WK, Gajewska BU, Okada H, Gronski MA, Bertram EM, Dawicki W, et al. The B7 family member B7-H3 preferentially down-regulates T helper type 1-mediated immune responses. Nat Immunol. 2003;4(9):899-906.
122. Leitner J, Klauser C, Pickl WF, Stockl J, Majdic O, Bardet AF, et al. B7-H3 is a potent inhibitor of human T-cell activation: No evidence for B7-H3 and TREML2 interaction. Eur J Immunol. 2009;39(7):1754-64.
123. Prasad DV, Nguyen T, Li Z, Yang Y, Duong J, Wang Y, et al. Murine B7-H3 is a negative regulator of T cells. J Immunol. 2004;173(4):2500-6.
124. Lee YH, Martin-Orozco N, Zheng P, Li J, Zhang P, Tan H, et al. Inhibition of the B7-H3 immune checkpoint limits tumor growth by enhancing cytotoxic lymphocyte function. Cell Res. 2017;27(8):1034-45.
125. Chapoval AI, Ni J, Lau JS, Wilcox RA, Flies DB, Liu D, et al. B7-H3: a costimulatory molecule for T cell activation and IFN-gamma production. Nat Immunol. 2001;2(3):269-74.
126. Carvajal-Hausdorf D, Altan M, Velcheti V, Gettinger SN, Herbst RS, Rimm DL, et al. Expression and clinical significance of PD-L1, B7-H3, B7-H4 and TILs in human small cell lung Cancer (SCLC). J Immunother Cancer. 2019;7(1):65.
127. Wang L, Zhang Q, Chen W, Shan B, Ding Y, Zhang G, et al. B7-H3 is overexpressed in patients suffering osteosarcoma and associated with tumor aggressiveness and metastasis. PLoS One. 2013;8(8):e70689.
128. Sauerbrei W, Taube SE, McShane LM, Cavenagh MM, Altman DG. Reporting Recommendations for Tumor Marker Prognostic Studies (REMARK): An Abridged Explanation and Elaboration. J Natl Cancer Inst. 2018;110(8):803-11.
129. Wang L, Kang FB, Shan BE. B7-H3-mediated tumor immunology: Friend or foe? Int J Cancer. 2014;134(12):2764-71.
130. Marmarelis ME, Aggarwal C. Combination Immunotherapy in Non-small Cell Lung Cancer. Curr Oncol Rep. 2018;20(7):55.
131. Crispen PL, Sheinin Y, Roth TJ, Lohse CM, Kuntz SM, Frigola X, et al. Tumor cell and tumor vasculature expression of B7-H3 predict survival in clear cell renal cell carcinoma. Clin Cancer Res. 2008;14(16):5150-7.
132. Picarda E, Ohaegbulam KC, Zang X. Molecular Pathways: Targeting B7-H3 (CD276) for Human Cancer Immunotherapy. Clin Cancer Res. 2016;22(14):3425-31.
133. Steinberger P, Majdic O, Derdak SV, Pfistershammer K, Kirchberger S, Klauser C, et al. Molecular characterization of human 4Ig-B7-H3, a member of the B7 family with four Ig-like domains. J Immunol.

2004;172(4):2352-9.
134. Arigami T, Narita N, Mizuno R, Nguyen L, Ye X, Chung A, et al. B7-h3 ligand expression by primary breast cancer and associated with regional nodal metastasis. Ann Surg. 2010;252(6):1044-51.
135. Liu Z, Pei MM, Liu JX, Shi F, Zhang Y, Zhao DF, et al. The expressions and significance of B7-H3 and CTLA-4 in the clinical stages of non-small-cell lung cancer. Int J Clin Exp Pathol. 2019;12(8):3032-41.
136. Li Y, Yang X, Wu Y, Zhao K, Ye Z, Zhu J, et al. B7-H3 promotes gastric cancer cell migration and invasion. Oncotarget. 2017;8(42):71725-35.
137. Nunes-Xavier CE, Karlsen KF, Tekle C, Pedersen C, Oyjord T, Hongisto V, et al. Decreased expression of B7-H3 reduces the glycolytic capacity and sensitizes breast cancer cells to AKT/mTOR inhibitors. Oncotarget. 2016;7(6):6891-901.
138. Seliger B, Quandt D. The expression, function, and clinical relevance of B7 family members in cancer. Cancer Immunol Immunother. 2012;61(8):1327-41.
139. Maasho K, Masilamani M, Valas R, Basu S, Coligan JE, Borrego F. The inhibitory leukocyte-associated Ig-like receptor-1 (LAIR-1) is expressed at high levels by human naive T cells and inhibits TCR mediated activation. Mol Immunol. 2005;42(12):1521-30.
140. Meyaard L. LAIR and collagens in immune regulation. Immunol Lett. 2010;128(1):26-8.
141. Wang Y, Zhang X, Miao F, Cao Y, Xue J, Cao Q, et al. Clinical significance of leukocyte-associated immunoglobulin-like receptor-1 expression in human cervical cancer. Exp Ther Med. 2016;12(6):3699-705.
142. Yuan Y. Modelling the spatial heterogeneity and molecular correlates of lymphocytic infiltration in triple-negative breast cancer. J R Soc Interface. 2015;12(103).
143. Hadrup S, Donia M, Thor Straten P. Effector CD4 and CD8 T cells and their role in the tumor microenvironment. Cancer Microenviron. 2013;6(2):123-33.
144. Yu X, Zhang Z, Wang Z, Wu P, Qiu F, Huang J. Prognostic and predictive value of tumor-infiltrating lymphocytes in breast cancer: a systematic review and meta-analysis. Clin Transl Oncol. 2016;18(5):497-506.
145. Lebbink RJ, de Ruiter T, Adelmeijer J, Brenkman AB, van Helvoort JM, Koch M, et al. Collagens are functional, high affinity ligands for the inhibitory immune receptor LAIR-1. J Exp Med. 2006;203(6):1419-25.
146. Joseph C, Al-Izzi S, Alsaleem M, Kurozumi S, Toss MS, Arshad M, et al. Retinoid X receptor gamma (RXRG) is an independent prognostic biomarker in ER-positive invasive breast cancer. Br J Cancer. 2019;121(9):776-85.
147. Mahmoud SM, Paish EC, Powe DG, Macmillan RD, Grainge MJ, Lee AH, et al. Tumor-infiltrating CD8+ lymphocytes predict clinical outcome in breast cancer. J Clin Oncol. 2011;29(15):1949-55.
148. Mahmoud SM, Paish EC, Powe DG, Macmillan RD, Lee AH, Ellis IO, et al. An evaluation of the clinical significance of FOXP3+ infiltrating cells in human breast cancer. Breast Cancer Res Treat. 2011;127(1):99-108.
149. Singh M, Bhatia P, Shandilya JK, Rawat A, Varma N, Sachdeva MS, et al. Low Expression of Leucocyte Associated Immunoglobulin Like Receptor-1 (LAIR-1/CD305) in a Cohort of Pediatric Acute Lymphoblastic Leukemia Cases. Asian Pac J Cancer Prev. 2018;19(11):3131-5.
150. Xue J, Zhang X, Zhao H, Fu Q, Cao Y, Wang Y, et al. Leukocyte-associated immunoglobulin-like receptor-1 is expressed on human megakaryocytes and negatively regulates the maturation of primary megakaryocytic progenitors and cell line. Biochem Biophys Res Commun. 2011;405(1):128-33.
151. Zhang Y, Ding Y, Huang Y, Zhang C, Boquan J, Ran Z. Expression of leukocyte-associated immunoglobulin-like receptor-1 (LAIR-1) on osteoclasts and its potential role in rheumatoid arthritis. Clinics (Sao Paulo). 2013;68(4):475-81.
152. Poggi A, Catellani S, Bruzzone A, Caligaris-Cappio F, Gobbi M, Zocchi MR. Lack of the leukocyte-associated Ig-like receptor-1 expression in high-risk chronic lymphocytic leukaemia results in the absence of a negative signal regulating kinase activation and cell division. Leukemia. 2008;22(5):980-8.
153. Aaltonen K, Amini RM, Heikkila P, Aittomaki K, Tamminen A, Nevanlinna H, et al. High cyclin B1 expression is associated with poor survival in breast cancer. Br J Cancer. 2009;100(7):1055-60.
154. Shen M, Feng Y, Gao C, Tao D, Hu J, Reed E, et al. Detection of cyclin b1 expression in g(1)-phase cancer cell lines and cancer tissues by postsorting Western blot analysis. Cancer Res. 2004;64(5):1607-10.
155. Eccles SA. The epidermal growth factor receptor/Erb-B/HER family in normal and malignant breast biology. Int J Dev Biol. 2011;55(7-9):685-96.
156. Merlo A, Casalini P, Carcangiu ML, Malventano C, Triulzi T, Menard S, et al. FOXP3 expression and overall survival in breast cancer. J Clin Oncol. 2009;27(11):1746-52.
157. Ni C, Yang L, Xu Q, Yuan H, Wang W, Xia W, et al. CD68- and CD163-positive tumor infiltrating macrophages in non-metastatic breast cancer: a retrospective study and meta-analysis. J Cancer. 2019;10(19):4463-72.
158. Sousa S, Brion R, Lintunen M, Kronqvist P, Sandholm J, Monkkonen J, et al. Human breast cancer cells educate macrophages toward the M2 activation status. Breast Cancer Res. 2015;17:101.
159. Mahmoud SM, Lee AH, Paish EC, Macmillan RD, Ellis IO, Green AR. Tumour-infiltrating macrophages and clinical outcome in breast cancer. J Clin Pathol. 2012;65(2):159-63.